MODELING RHEOLOGICAL PROPERTIES OF SOME MOLASSES-TAHIN BLENDS

Dlshad Abdalla Mohammed

MSc THESIS

Chemical Engineering Department

Supervisor: Prof. Dr. Fethi KAMIŞLI

July-2018

T.C.
FIRAT UNIVERSITY
THE INSTITUTE OF NATURAL AND APPLIED SCIENCES

MODELING RHEOLOGICAL PROPERTIES OF SOME MOLASSES-TAHIN BLENDS

MSc THESIS

By

Dlshad Abdalla Mohammed
(151118105)

Study Field: Chemical Engineering

Program: Unit Operation and Thermodynamics

Supervisor: Prof. Dr. Fethi KAMIŞLI

Submitted Date: 23.07.2018

July-2018

T.C.
FIRAT UNIVERSITY
THE INSTITUTE OF NATURAL AND APPLIED SCIENCES

MODELING RHEOLOGICAL PROPERTIES OF SOME MOLASSES-TAHIN BLENDS

MSc THESIS

by

DlshadAbdalla Mohammed
(151118105)

Submitted Date: 23.07.2018

Examination Date: 9.08.2018

Supervisor:	**Prof. Dr. Fethi KAMIŞLI**
Jury Members:	**Prof. Dr. Dursun PEHLİVAN**
	Dr. Öğr. Üyesi Hakan YOĞURTÇU

August-2018

ACKNOWLEDGEMENTS

This work would have not been possible without assistance and guidance of number of individuals and their courage who by one way or another appreciably contributed to accomplishment of this thesis.

At the starting, I would like to precise my significant and fair gratefully to my supervisor Prof. Dr. Fethi KAMIŞLI not as it were for his cherished direction, coordinate offer assistance, back and support but too for his parental care amid my residency in Turkey. I moreover, would like to communicate my profound appreciation to all staff of chemical designing office in Firat University for their help and their special classy treatment with me during my study.

I cheerfully thank Prof. Cevdet AKOSMAN who helped me, thanks to Prof. Nurhan ARSLAN who helped me to integrate into Turkish society and much obliged to Research Assist. Ercan AYDOĞMUŞ for giving me hands in my work, all of that made a difference me to communicate and be commonplace with other understudies and cadres of the division and feel as be at my home.

Finally, I must express my very profound gratitude to my parents and to my wife, for providing me with unfailing support and continuous encouragement throughout my years of study and through the process of researching and writing this thesis. I want to dedicate this work to my wife and both my little daughters Lana and Wara. Thank you.

Dlshad Abdalla Mohammed

TABLE OF CONTENTS

SUMMARY

The aim of this study is to determine the rheological properties of some molasses-tahin blends such as date syrup-tahin, mulberry molasses-tahin, grape molasses-tahin and carob syrup-tahin (sesame paste) blends at the different ratios (20 -55 %) and different temperatures (25- 60 °C) by using a rotary viscometer (Brookfield) to develop models appropriate to the experimental data. In order to obtain the viscosities of each blend as a function of the shear strain, those samples were sheared with five different rotational speeds at an increasing order. The variation of viscosity of those blends with the strain rates (2.5-30 s^{-1}) showed that all considered ratios of the molasses-tahin blends were non-Newtonian shear thinning fluids at all temperatures.

The experimental data of apparent viscosity versus shear rate were successfully described with the Power-law model. The model parameters such as the flow behavior index (n) and the consistency coefficient (K) of the considered blends were respectively found to be ranged from 0.522 to 0.641 and from 4365.1 to 10013 mPa.s^n for the date molasses- sesame paste blends; from 0.659 to 0.699 and from 4461.1 to 10207 mPa.s^n for mulberry molasses- sesame paste blends; from 0.331 to 0.62 and from 966.88 to 4218.2 mPa.s^n for grape molasses- sesame paste blends; from 0.444 to 0.599 and from 3194.4 to 17480 mPa.s^n for the carob molasses- sesame paste blends. It was observed that apparent viscosities and consistency coefficients of blends increased with increasing molasses concentration and decreasing temperature.

Temperature sensitivity of the consistency index (K) was examined using an Arrhenius-type equation. Activation energies (Ea) of the considered blends were found to be ranged from 4378.15 to 9499 J/mol for the blends of date molasses-sesame paste; from 13216.69 to 7514 J/mol for the blends of mulberry molasses-sesame paste; from 4340.98 to 17378.08 J/mol for the blends of grape molasses-sesame paste; from 6779.04 to 13444.5 J/mol for the blends of carob molasses-sesame paste.

The relationship between concentration and consistency coefficient for each blend was described with both the exponential and power functions. While the exponential function was found to be superior in explaining the variation of Ea with concentrations of date, grape and carob molasses, power function was found to be superior in explaining the variation of Ea with concentration of mulberry molasses.

A mathematical model was determined to describe the combined impact of temperature, concentrations of the molasses and shear rate on apparent viscosity with high consistency.

Keywords: Rheology, modeling, molasses and sesame paste blends.

ÖZET

Bazı Pekmez-Tahin Karışımlarının Reolojik Özelliklerinin Modellenmesi

Bu çalışmanın amacı deneysel verilere uyan bir model geliştirmek için farklı konsantrasyon (% 20–55) ve sıcaklıklarda (25–60 °C) hurma, dut, üzüm ve keçiboynuzu pekmezleri-tahin gibi bazı pekmez-tahin karışımlarının döner viskozimetre (Brookfield) ile reolojik özelliklerinin belirlenmesidir. Kayma geriliminin fonksiyonu olarak her karışımın viskozitesini elde etmek için bu örnekler artan bir şekilde 5 farklı dönme hızında kayma gerilimine tabi tutuldu. Kayma gerilimleriyle (2.5–30 s^{-1}) karışımların viskozitelerindeki değişim, çalışılan pekmez-tahin karışımlarının bütün sıcaklıklarda Newtonien olmayan kayma incelmeli sıvılar olduğunu gösterdi.

Kayma gerilimlerine karşı görünür viskozitenin deneysel verileri üs kanunu modeli ile başarılı bir şekilde tanımlandı. Çalışılan karışımların akış davranışı indeksi (n) ve kıvamlılık katsayısı (K) gibi model parametreleri sırasıyla; hurma pekmezi-tahin karışımı için 0.522 ile 0.641 ve 4365.1 ile 10013 mPa.s^n, dut pekmezi-tahin karışımı için 0.659 ile 0.699 ve 4461.1 ile 10207 mPa.s^n, üzüm pekmezi-tahin karışımı için 0.331 ile 0.62 ve 966.88 ile 4218.2 mPa.s^n ve keçiboynuzu pekmezi-tahin karışımı için 0.444 ile 0.599 ve 3194.4 ile 17480 mPa.s^n aralıklarında bulundu. Karışımların görünür viskoziteleri ve kıvamlılık katsayıları pekmez konsantrasyonlarının artmasıyla ve sıcaklığın azalmasıyla arttığı gözlendi.

Kıvamlılık katsayılarının sıcaklık duyarlılığı Arrhenius tipi eşitlik kullanılarak incelendi. Çalışılan karışımların aktivasyon enerjisi (Ea); hurma pekmezi-tahin karışımı için 4378.15 ile 9499 J/mol, dut pekmezi-tahin karışımı için 7514 ile 13216.7 J/mol, üzüm pekmezi-tahin karışımı için 4341 ile 17378.08 J/mol ve keçiboynuzu pekmezi-tahin karışımı için 6779.04 ile 13444.5 J/mol arasında bulundu. Her bir karışım için derişim ile kıvamlılık katsayısı arasındaki ilişki hem üstel hem de üs fonksiyonları ile tanımlandı. Ea'nın hurma, üzüm ve keçiboynuzu pekmezlerinin derişimleriyle değişiminin açıklanmasında üstel fonksiyonun daha üstün olduğu bulunurken, Ea'nın dut pekmezi derişimi ile değişimin açıklanmasında üs fonksiyonun daha iyi olduğu bulundu.

Görünür viskozite üzerinde sıcaklık, bazı pekmez derişimleri ve kayma geriliminin birleşik etkisini yüksek tutarlılıkla tanımlama için bir matematiksel model belirlendi.

Anahtar kelimler: Reoloji, modelleme, pekmezle ve tahin karışımları.

LIST OF FIGURES

Page No

LIST OF TABLES

Page No

SYMBOLS

$\boldsymbol{\mu}$: Newtonian viscosity
$\dot{\gamma}$: Shear rate
$\boldsymbol{\tau_0}$: yield stress
μp_l : plastic viscosity
K : consistency coefficient
n : flow behavior index
μa : apparent viscosity, for power-law fluids
μ_{a0} : initial apparent viscosity
$\mu_{a\infty}$: equilibrium apparent viscosity
m : the order of the structure breakdown reaction. Equation (3.6)
k : the rate constant. Equation (3.6)
t : time of measurement. Equation (3.6)
μ_0 : experimental constants. Equation (3.7)
kt : experimental constants. Equation (3.8)
Ea : activation energy (J/mol),
R : universal gas law constant
T : absolute temperature (K).
Kc1 : experimental constants. Equation (3.9)
Kc2 : experimental constants. Equation (3.10)
b_1 : experimental constants. Equation (3.9)
b_2 : experimental constants. Equation (3.10)
K ($\dot{\gamma}$, T, C): experimental constants. Equation (3.11 and 3.12)
$\bar{n}$: average value for flow behavior index. Equation (3.11)
b : experimental constants. Equation (3.11 and 3.12)
A1 : experimental constants. Equation (3.13)
A2 : experimental constants. Equation (4.14)
d1 : experimental constants. Equation (3.13)
d2 : experimental constants. Equation (3.14)
C : total soluble solid content. Equation (3.13 and 3.14)
Ω :angular velocity (rad/s)

1. INTRODUCTION

Molasses-Sesame paste blends is one of a traditional food product in East Asian and Middle Eastern countries. It is mainly consumed for breakfast. Because of it is high-energy content, it has a wide usage specifically in cold weather conditions, such as winter. The constituents of molasses - sesame paste have risen high nutrition value. Usually in markets, molasses and sesame paste are available for sale separately; thus, the blending process is carried out by the consumers. The ratio of molasses to sesame paste is determined according to the consumers taste and preference.

Molasses are commonly produced from grape, mulberry, fig, juniper, watermelon, apple, plum, carob, sugar beet and sugar cane. But in recent years, in addition to those, apricot and date have been used for the production of molasses by concentration of juices up to 70–80% soluble dry matter content with an extended shelf-life (Batu, 2005; Yoğurtçu & Kamışlı, 2006; Akbulut et. al., 2008 ; Karaman & Kayacier,. 2011 ; Özkal & Süren, 2017). Molasses processing operations vary according to origin of fruits used in production of Molasses. (Yoğurtçu & Kamışlı, 2006; Akbulut & Bilgiçli,2010; Karaman & Kayacier,2011).

Sesame paste, known as tahin in Turkey and Arabic countries and ardeh in Iran, is a traditional food in the Middle East, which is produced by grinding the dehulled and heated sesame seeds (Seyed et al.,2007; Gharehyakheh & Tavakolipour, 2014). Sesame paste is also a tradition food in East Asian and Middle Eastern countries, it has used in ingredients of many other dishes such as halawah, chickpeas, desserts, and some types of bakery (Alpaslan & Hayta,2002; Arslan et al.,2005; Akbulut & Özcan,2008; Akbulut et al.,2012).

In addition, the molasses is consumed as an ingredient in the formulation of some food items such as ice cream products, beverages, confectionery, bakery products (Habibi et al., 2006).

Knowledge of rheological behavior is important for optimization of process design, quality control, consumer acceptance of a product and sensory assessment (Arslan et al., 2005; Işıklı & Karababa, 2005; Özkal & Süren, 2017). Consumer acceptance of molasses and sesame paste blends usually depends on the capacity of spreading on other material like bread. Therefore, the spreading of the blends is directly related with viscosity (Alpaslan & Hayta, 2002; Arslan et al., 2005).

When the legitimate consistency, soundness and surface tension are the main concerns in expansion, generation and upkeep of the item, the solid rheological information is needed (Abu - Jdayil, 2003; Arslan et al., 2005).

Rheological characterization of food pastes has been widely investigated by focusing at either individual samples or blend samples. Rheological properties of individual samples can be listed as sesame paste (Altay & Ak, 2005 ; Çiftçi et al., 2008; Özkal & Süren, 2017), sunflower tahini (Muresan et al., 2014), fenugreek paste (Işikli & Karababa, 2005), tomato paste (Valencia et al.,2002; Bayod et al.,2008), ginger paste (Ahmed, 2004), molasses (pekmez) (Kaya & Belibağlı, 2002; Sengül et al., 2005; Yoğurtçu & Kamışlı, 2006; Sengül et al., 2007; Akbulut et al., 2008; Mohamed & Hassan, 2016). On the other hand, rheological properties of blend samples can be listed as grape pekmez/ tahin blends (Alpaslan & Hayta, 2002; Arslan et al., 2005); corn starch/grape pekmez blends (Goksel et al., 2013), sesame paste/date syrup blends (Habibi et al., 2006; Razavi et al., 2008), honey/sesame paste blends (Gharehyakheh & Tavakolipour, 2013; Gharehyakheh1 et al., 2014) and poppy seed paste/grape pekmez blends (Özkal & Süren,2017).

The flow behavior, texture and sensory properties of new blends need to be determined for processing of those blends. Temperature and concentration are important factors in determining the rheological behavior of the blends. The use of different types of molasses in blending process is an essential component in the formation of a new product accepted by consumers. Some organizations such as military and police organizations required a specific blend ratio. However, much work has been done to improve the quality of food production in terms of edibility taste and texture. It can be obviously seen in the literature that the researchers have focused on blending at different concentrations of sesame paste/grape molasses and sesame paste/dates molasses at different temperature degrees in a hope to improve edibility taste, spread ability on bread and sensory properties etc. Thus, further investigation is required to determine rheological properties of the blends of sesame paste with another type of molasses such as dates, mulberry, grapes and carob juice.

Subsequently, the major objective of this study is to determine rheological behavior of mixtures of sesame paste with different types of molasses such as dates, mulberry, grapes and carob juice.

2. OVERVIEW AND LITERATURE SURVEY

2.1. Molasses

Molasses is a concentrated form of dates, mulberry, grapes and carob juice. It is produced by boiled juice to evaporate water without any food additives or sugar. The product can be looked up on natural food, which contains natural sugars with minerals. The goal of concentration or pasteurization is to extend shelf life of dates, mulberry, grapes and carob juices with boiling to lessen water content (Batu, 2005; Yoğurtçu & Kamışlı, 2006; Akbulut et al., 2008; Karaman & Kayacier, 2011; Özkal & Süren, 2017). This process will lead to producing a molasses. Thus, operations for molasses processing vary according to the source of the fruit used in the production of molasses. Some information about the preparation the raw materials such as dates, mulberry, grapes and carob used in production of molasses will be given in the next few paragraphs. The basic operations in molasses productions from the different sources are shown in Figures 2.1 - 2.4. As seen in the figures the process shows small variations according to the type of fruit. The first step in the process for production of molasses from any fruit is to wash the fruit.

2.1.1. Preparation of Date Syrup

As illustrated in Figure 2.1 the shredded samples of the date are heated in suitable amount of water for 20 minutes and mixing. The slurry is filtered. Then, the residue pulp is washed again with hot water (80-85 °C) for 10 minutes to make up the pulp/water ratio as 0.5, 0.4 and 0.3 and then it is filtered again. After that, the collected raw juice is concentrated by using the rotary evaporator apparatus at 70 °C under vacuum. Finally, the produced date syrup is packed and stored at room temperature (20-30 °C) (Ramadan, 1998). Obviously, there are differences between dates and other fruits in producing their juices, other fruit juices are got by pressing (e.g. citrus, berries, grapes), but soluble solids in dates are too concentrated to squeeze (Ramadan, 1998).

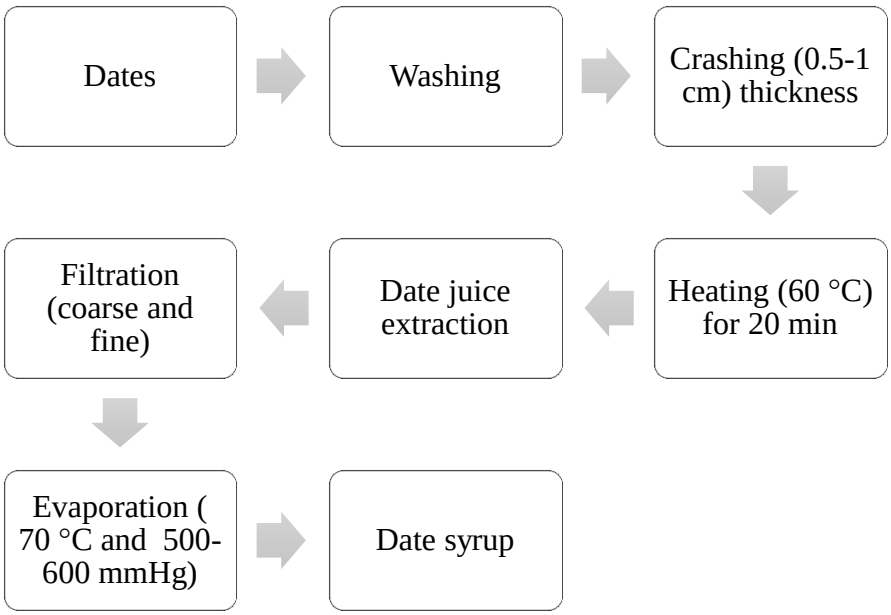

Figure 2.1 Operations for the production of date molasses

2.1.2. Fresh Mulberry

Fresh mulberry is used as a raw material for the production of mulberry molasses. As can be seen in Figure 2.2, firstly, mulberry placed ships are boiled after washing and then some water is added into it the ratio water to mulberry 0.3-0.4 liter/kg. After that, the mixture is heated about boiling temperature with mixing for about an hour. After that, the mixture is cooled down to about 40-50 ° C. Then, the cold mixture is filtered to obtain clear juice under the pressure. Juice of mulberry is concentrated in open containers by evaporate water, which results in a finished product having 65-72 ° Brix. The final product called mulberry molasses is packaged and stored at room temperature (Basiri, 2016; Sengül et al., 2005).

2.1.3. Fresh Grapes

In the production of grape molasses, (Figure 2.3), the primary step is to wash and smash by utilizing a pneumatic or mechanical press to obtain the grape juice. The obtained grape juice is treated with calcareous soil called molasses earth that contains high amounts of calcium carbonate (ca. 90%).

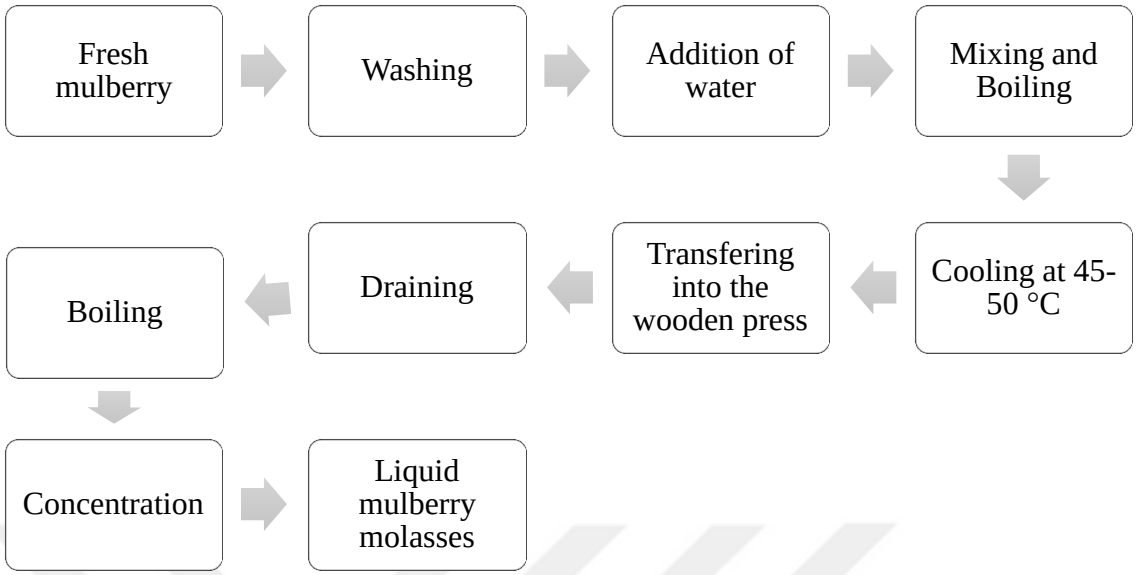

Figure 2.2 Operations for the production of mulberry molasses

After keeping the earthed juice at the rest for some time, the juice is clarified by sedimentation of calcium tartrat and calcium malate that naturally exist in the form of tartaric and malic acids in the grape juice. Hence, after being decreased acidity, the clear up syrup was boiled in open vessels and seldom in vacuum to take out liquid molasses (Batu, 2005; Hatamikia et al., 2013).

The concentration of grape juice contains a high proportion of mineral, especially calcium and iron. Grape molasses is usually recommended in anemia treatment due to the high iron content (Ozturk & Oner, 1999).

2.1.4. Carob Molasses

As mentioned previously molasses have been produced using various techniques considering species of fruits used in production. In order to obtain carob molasses, the fruits (carob) are smashed into the powdered by using wooden mortar, then added water 1 liter/ kg in an open container during 3 days. After that, the mixture is filtered to obtain carob juice that is concentrated up to 72° Brix in an open vessel with boiling. The final product is known as carob molasses and its color varies between light brown to dark brown depending on the concentration process, (Sengül et al., 2007; Tounsi et al., 2017).

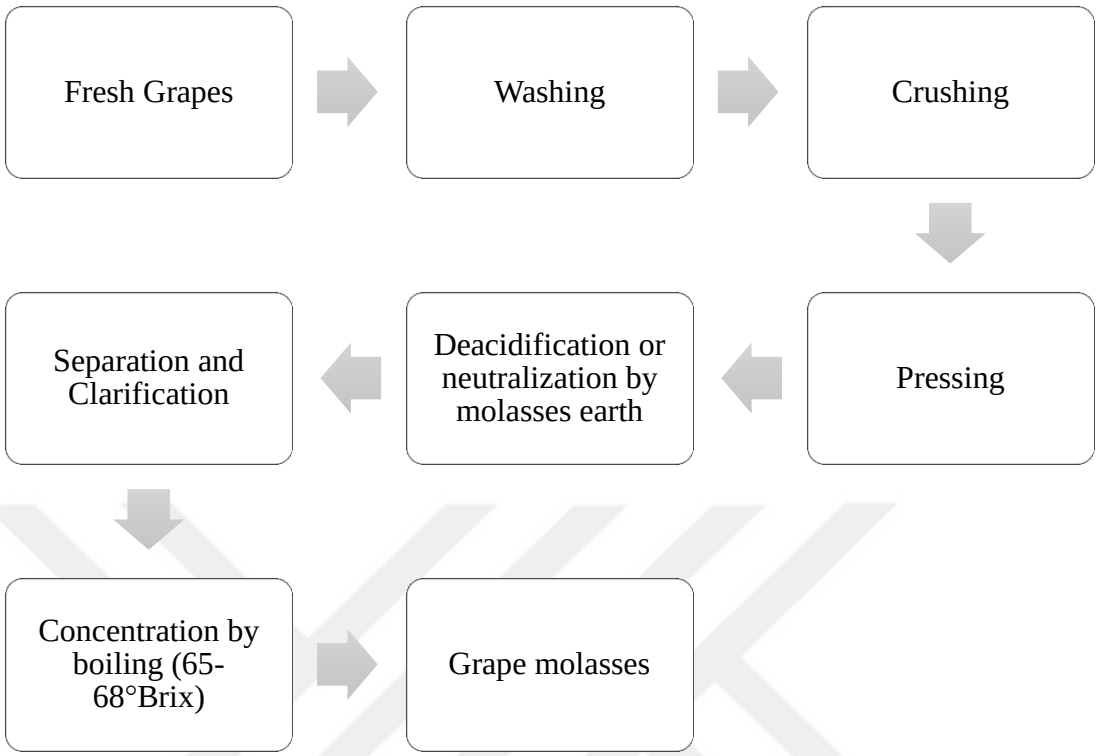

Figure 2.3 Operations for the production of grape molasses

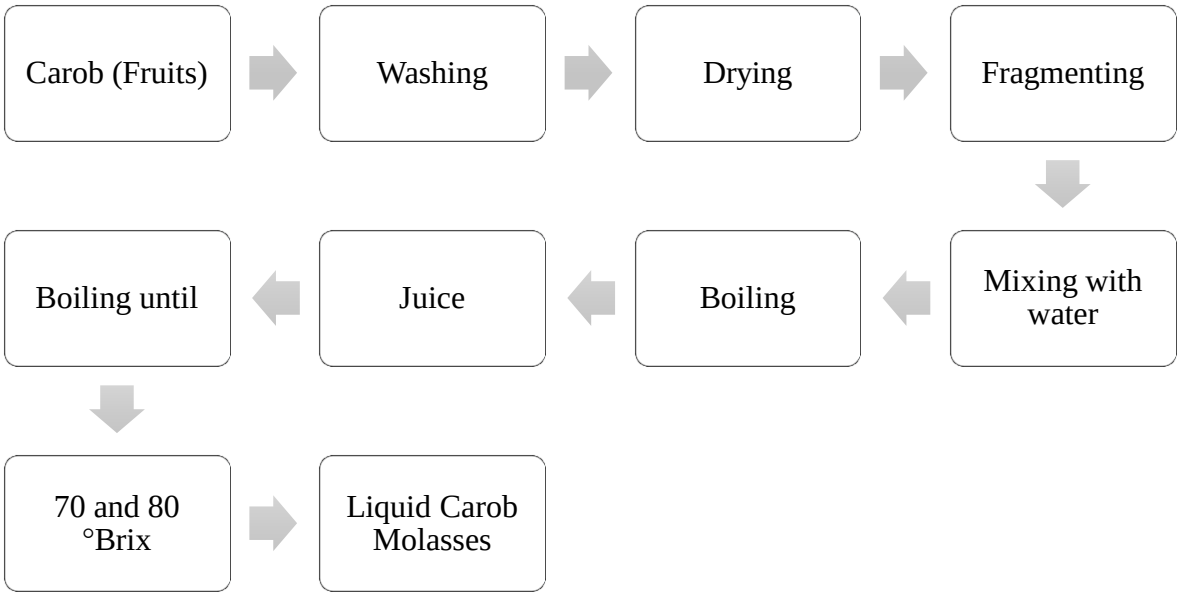

Figure 2.4 Operations for the production of carob molasses

2.2. Sesame Paste

Sesame paste is a final pure product that produced from crushed seeds of sesame (*Sesamum indicum L.*), which are dehulled and heated without adding or removing any of its components (Alpaslan & Hayta, 2002; Arslan et al., 2005; Gharehyakheh, 2014; Gharehyakheh & Tavakolipour, 2013; Habibi et al. 2006; Razavi et al., 2008). Sesame paste has a high stability and resistance to oxidation at room temperature because of the presence of sesamin and sesaminol that are natural antioxidants (Gharehyakheh & Tavakolipour, 2013; Morris, 2002). It has a significant antioxidant activity due to the main component of sesame oil. The cancer prevention factors, sesamin and sesamolin, are compelling chemicals to smother the arrangement of free radicals hence act as anticarcinogenic materials. Moreover, sesame oil is advantageous for decreasing cholesterol because of its high polyunsaturated fat content (Arslan et al., 2005; Morris, 2002). Besides this, sesame oil can prevent oxidative rancidity due to cancer avoidance factors (Arslan et al., 2005; Jannat et al., 2010).

A typical process of sesame paste production is illustrated in Figure 2.5. The sesame seeds are wetted and then left for 8-10 hours for removing rind process. After the rinds are detached, the seeds are washed for removing any remaining undesirable particles such as stone and dirt. The seeds are centrifuged to remove water, then grilled. The grilled seeds are grinded for obtaining last product, sesame paste. 90 % sesamin, original antioxidant, is discovered after grilling (Arslan et al., 2005; J. Bradley Morris, 2002).

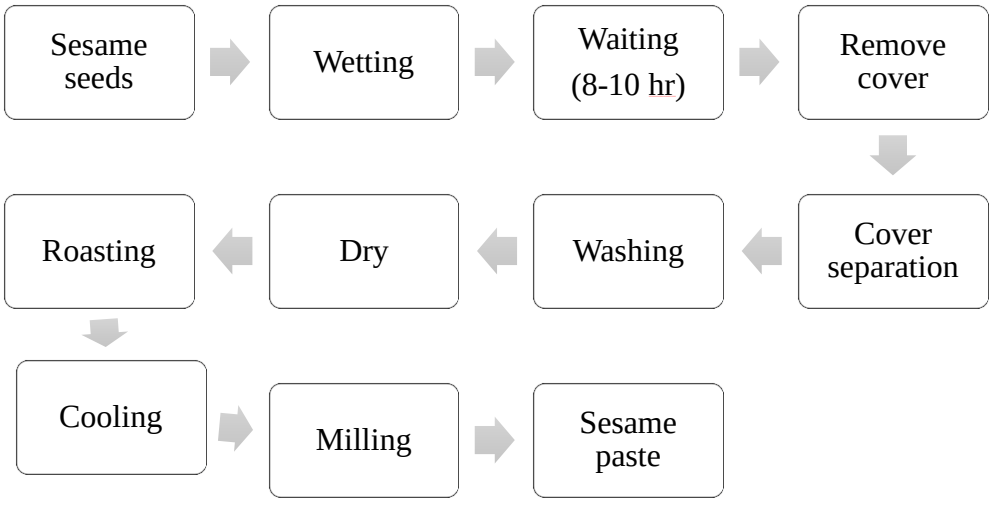

Figure 2.5 Operation for sesame paste production

2.3. Molasses/Sesame paste mixtures

Various food products exist in state emulsion such as the mixed salad dressings, sauces, mayonnaise, butter, cream and refreshments. In food system, there are two common types of emulsion, water in oil or oil in water. Blends of molasses and sesame pastes can be regarded as a typical case of an oil-in-water type emulsion (Alpaslan & Hayta, 2002; Arslan et al., 2005). The two non-miscible liquids; molasses and sesame paste form a two-stage system, molasses has water phase (continue stage) and sesame paste has oil phase (dispersed phase). Oil particles are suspended within the water through the assistance of mechanical development of the emulsion (Alpaslan and Hayta, 2002 ; Arslan et al., 2005 ; Seyed et al., 2007).

Emulsion stability depends on oil and water interface. Proteins are amphiphilic molecules that are mostly used to stabilize emulsions in food products. Proteins have a key role to facilitate droplet breakup through homogenization and to stabilize the droplets against coalescence through emulsification and storage. The ability of a protein emulsifier is determined by its ability to reduce tension between the surfaces (Day et al.,2009). In the case of molasses and sesame paste blend, protein and lipids usually interact and thus the protein reduces the tension between surfaces of protein and lipids, which causes a stable emulsion to form (Alpaslan & Hayta, 2002; Arslan et al., 2005).

Sesame paste possesses a high protein and dietary fiber content. When strengthened with high mineral and vitamin being contained in molasses might offer a promising nutritious and healthy substitute to consumers (Alpaslan and Hayta, 2002; Arslan et al., 2005; Çiftçi & Kahyaoglu, 2008).

3. RHEOLOGY AND FLUID FLOW MODELS

3.1. Rheology

Rheology can be defined as a research of deformation and flow of matter. It is applied to various industrial fields such as mining, geology, cosmetics, and polymers. The biological nature of foods offers an excellent circumstance toward rheological study of fluid foods. An accurate study of the rheological measurement is crucial to tackle the optimization problems in the areas of product development efforts, to design process for processing foods and to improve quality of food product (Heldman & Singh, 1981; Rao, 1999; Vinet & Zhedanov, 2010).

3.2. Importance in the Food Industry

The rheological information is very important in many areas of the food industry assessment such as process design equipments, food texture estimation, shelf life analysis, sensory evaluation and product quality control (Heldman & Singh, 1981; Vinet & Zhedanov, 2010).

3.3. Rheological Behaviors of Fluid Flows

A mathematical equation can be derived from fluid flow behavior that contains rheological information such as viscosity versus shear strain. In addition, it is crucial to specify which model parameters are influenced from the state variables such as temperature and concentration.

In classical mechanics, the difference between liquids and solids is very obvious, as their behaviors are identified using separate physical rules; Hooke's law and Newton's law of viscosity. While Hooke's law defines the solid-state behavior, Newton's law of viscosity establishes the relationship between shear stress and shear rate for Newtonian fluids. As known solid and fluid materials exhibit different behavior when a stress is applied on them. In this way, the outcome of same amount of stress produces different deformation patterns; the amount of elastic solid deformation is directly proportional to the applied stress, while a fluid deformation continues.

A basic distinction between fluid foods is either Newtonian or non-Newtonian behaviors. Fluid foods can be described as either Newtonian or non-Newtonian fluids based on their rheological behavior, whether they follow Newton's law of viscosity.

3.3.1. Newtonian Fluids

Newtonian fluids can be described as a liquid or gas that comply with Newton's law of viscosity (Eq.3.1). As mentioned in the previous section, for a perfect Newtonian liquid, the shear stress is linearly proportional to the shear rate (Figure 3.1), with preserving this relationship by a constant value (μ) that is independent of the shear rate (Gankoplis, 1993).

In this case, when plotting shear stress versus shear strain, the curve starts from the origin and the slope of curve (μ) stays constant. Let us denote the force as N, area as m^2, length as m, and final velocity as m/s.

$$\tau = \mu \cdot \dot{\gamma} \tag{3.1}$$

Here τ is the shear stress, μ is the Newtonian viscosity and $\dot{\gamma}$ is the shear rate. A common Newtonian food can be defined as compounds of low molecular weight with low concentrations. Such as water, sugar syrups, and milk (Intergovernmental Panel on Climate Change, 1999).

3.3.2. Non-Newtonian Fluids

The fluids belonging non-Newtonian types are those which do not obey Newtonian's law of viscosity and this can be observed by focusing on the relationship between shear stress with shear rate. The curve for shear stress versus shear strain is nonlinear and does not begin from origin.

Dispersions, emulsions, and polymer solutions can be counted as typical non-Newtonian materials. The viscosity is not constant, but is a function of shear rate and appears as either a time-dependent or independent. Time-independent flow behavior does not rely on duration of shear but only on shear rate while time-dependent flow behavior relies on the duration of shear.

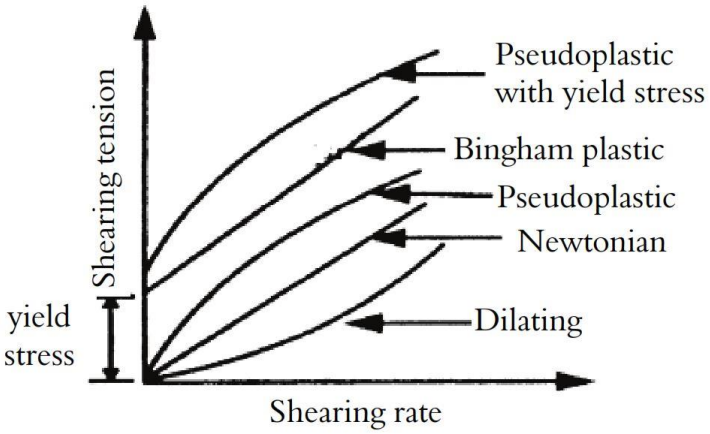

Figure 3.1 Rheological behavior of main kinds of liquid

3.3.2.1. Time Independent Fluids

Bingham Plastics

The behavior of this type of fluid is the closest to the Newtonian behavior and the relationship between shear stress and shear rate is linear, only difference is that the curve of this type of fluid does not begin from the origin (see Figure 3.1) (Vinet & Zhedanov, 2010). The relationship between shear stress and shear rate is given as follows:

$$\tau = \mu_{pl}\,\dot{\gamma} + \tau_0 \qquad (3.2)$$

where τ_0 is the yield stress and μ_{pl} is the plastic viscosity. Yield stress (τ_0) is required to stat flow. Underneath the yield stress, no flow occurs and the material exhibits solid like characteristics due to the stored energy (Vinet & Zhedanov, 2010).

Power-law Fluids

The behavior of this sort of liquid has a place in non-Newtonian behavior; they can be characterized by an Ostwald de Waele (or Power-law model) equation. It is demonstrated that Power-law model has been utilized broadly to clarify flow behavior of non-Newtonian fluids, in both hypothetical examination and observational calculations (Fung, 1982; Vinet & Zhedanov, 2011)

$$\tau = K \cdot \dot{\gamma}^{n} \quad (3.3)$$

where, K (Pa. s^n) is consistency coefficient, n is flow behavior index, dimensionless. The consistency coefficient is very important to identify the viscous nature of a liquid.

Apparent viscosity can be well defined by the ratio of shear stress to shear rate; this ratio is not a constant but relies on the shear rate. In other words, the apparent viscosity represents the non-Newtonian viscosity (Van Wazer & Lyons, 1966**)**. The apparent viscosity (μa) for Power-law fluids (Vinet & Zhedanov, 2010) is given as:

$$\mu_a = f(\dot{\gamma}) = \left(\frac{K.\dot{\gamma}^{n}}{\dot{\gamma}}\right) = K.\dot{\gamma}^{n-1} \quad (3.4a)$$

of which the logarithmic frame is utilized to obtain its parameters such as the consistency coefficient and flow behavior index when exploratory information is accessible as,

$$\ln\mu_a = \ln K + (n-1)\ln\dot{\gamma} \quad (3.4b)$$

Flow behavior index, n, is effect on power law fluids that is classified into two types such as shear thinning fluid and shear thickening fluid.

Shear Thinning (or pseudo plastic) Fluids

This type of non-Newtonian fluids is more encountered than other types. In this type of fluid, the plotted curve for the shear stress versus shear rate is concave upward and it begins at the origin (Figure 3.1). An increase in shear stress gives less than equal increments in the shear rate. Apparent viscosity decreases with increasing shear rate in shear thinning fluids whilst it is constant with Newtonian fluids. If Eq. (3.3) is assigned to this sort of behavior, it will be seen that the flow behavior index is less than unity (n <1) (Heldman & Singh, 1981; Rao, 1999; Vinet & Zhedanov, 2010). Orange juice concentrate, banana puree, many salad dressings and applesauce exhibit shear thinning fluid behaviors (or pseudo plastic).

Shear Thickening (or Dilatant) Fluids

In Dilatant (or shear thickening) behavior, the plotted curve for the shear stresses versus shear rates in this sort of liquid is concave descending and it moreover starts at the origin point (see Figure 3.1). Apparent viscosity is the slope of the related curve and depends upon the shear rate. This sort of flow is watched with gelatinized starch dispersion and corn flour-sugar arrangements (Rao, 1999). Model equation of Power law (Eq.3.3) is often proper with the flow behavior index more than unity (n >1).

Herschel - Bulkley Fluids

Herschel- Bulkley (or Pseudoplastic) model can be counted as a common relation to characterize the behavior of non-Newtonian liquids.

$$\tau = K.\dot{\gamma}^{n} + \boldsymbol{\tau_0} \qquad (3.5)$$

It is more general equation since it reduces to the power law fluid ($n \neq 1$) and to Newtonian fluid ($n = 1$) as extraordinary cases ($\tau_0 = 0$). Moreover, it is suitable for the Bingham Plastic fluid where the yield stress is required (Vinet & Zhedanov, 2011).

3.3.2.2. Time-Dependent Fluids

The reversible or irreversible changes take place according to increase or decrease of apparent viscosity with time at a constant shear rate. Time dependent fluids can be examined by dividing into two subtitles namely thixotropic and rheopectic fluids.

Thixotropic Fluids

Thixotropic fluids are known as shear thinning behavior, dependent on time (see Figure 3.2). The majority of these fluids have a heterogeneous system consist of an excellent dispersed phase. When at rest, particles and molecules in the food are linked together by weak forces. During shear the hydrodynamic forces are sufficiently high to break the

interparticle linkages, resulting in a reduction in the size of structural units. Hence, a lower resistance during the fluid flow is seen at amid shear rates.

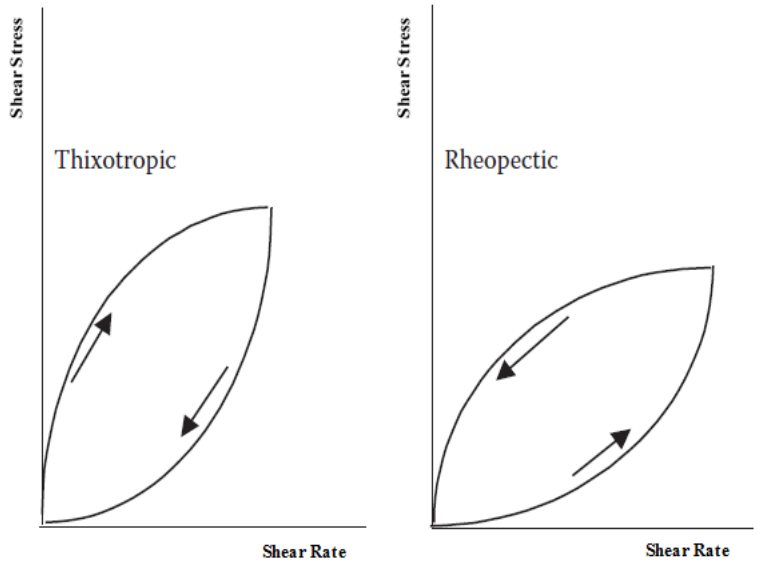

Figure 3.2 Time-dependent fluids

This sort of stream behavior is likely seen with nourishments, for instance serving of mixed salad dressing and delicate cheeses where the structural changes take put within the nourishment until stability is satisfied (Rao, 1999). The event of thixotropy suggests that the flow history needs to be considered if the liquid behavior is foreseen (**S**ingh, 2001).

Sesame paste was considered to show the thixotropic behavior by Abu - Jdayil (2003). The auxiliary breakdown of sesame oil at a consistent shear rate was expressed by,

$$\left(\frac{\mu_a-\mu_{a\infty}}{\mu_{a^0}-\mu_{a\infty}}\right)^{1-m} = (m-1)kt + 1 \qquad (3.6)$$

where, initial apparent viscosity is μ_{a0}, equilibrium apparent viscosity is $\mu_{a\infty}$, the structure breakdown response is m, rate constant is k and time of estimation is t.

Rheopectic Fluids

Rheopexy fluids are known as shear thickening behavior, dependent on time (see Figure 3.2). The viscosity of these foods at a constant shear rate increases with time (Vinet & Zhedanov, 2010).

3.4. Effective Variables on Viscosity

The viscosity of a fluid depends on many factors such as temperature, concentration, shear rate time of shearing and pressure. Because of the changes in these variables, liquids are subjected to high affectability. In turn, these variables affect viscosity because of the resulting structural changes in the fluid. Although the effect of pressure is ignored for most practical purposes, the effect of temperature and concentration are obvious on the fluid behaviors (Singh, 2001).

Effect of Temperature

Temperature usually has an inverse relationship with viscosity. During preparing and storing of liquid nourishments, a massive range of temperatures are encountered. The role of temperature on viscosity is clarified by Arrhenius type equation (Rao, 1999; Singh, 2001) that is given as:

$$\mu_a = \mu_0 . e^{\left[\frac{Ea}{R.T}\right]} \quad (3.7)$$

$$K = Kt . e^{\left[\frac{Ea}{R.T}\right]} \quad (3.8)$$

where, μ_0 and Kt constants, Ea is the activation energy, R is the universal gas constant and T is the absolute temperature

Effect of Concentration

Concentration of a solute has, as a rule feature, a nonlinear relationship with viscosity at a constant temperature (Vinet & Zhedanov, 2010). It is essential to distinguish the components that play a crucial role on the rheological behavior. Hence, the impact of concentration on viscosity is expressed by either exponential or power functions (Rao, 1999) as follows:

$$K = Kc1 . e^{b1.C} \quad (3.9)$$

$$K = Kc2 . C^{b2} \quad (3.10)$$

where, Kc1, Kc2, $b_1$and b_2 are empirical constants.

The Combined Effect of Temperature and Concentration

The viscosity of a fluid food increase with a decrease in temperature and an increase in concentration. The combination factor of temperature and concentration are well described with shear rate. In other word the combined effects of temperature, concentration and shear rate on the apparent viscosity is expressed with the exponential and power function as follow:

$$\mu_a = f(\dot{\gamma}, c, T) = K(\dot{\gamma}, c, T) \exp\left[\frac{Ea}{R}.\left(\frac{1}{T}\right) + b.C\right].\dot{\gamma}^{\bar{n}-1} \quad (3.11)$$

or:

$$\mu_a = f(c, T) = K(c, T) \exp\left(\frac{Ea}{R.T}\right).C^b.\dot{\gamma}^{\bar{n}-1} \quad (3.12)$$

where, K (T, C, $\dot{\gamma}$) is empirical constant, and $\bar{n}$ is a moderate value for stream behavior index (Vinet & Zhedanov, 2010).

3.5. Impact of Concentration on Activation Energy

The soluble solid content of food is a significant function for activation energy at a certain temperature. The exponential or power functions are utilized to express concentration effect on activation energy.

$$Ea = A1.e^{d1.C} \quad (3.13)$$

$$Ea = A2.C^{d2} \quad (3.14)$$

where, A1, A2, d1, d2 are empirical constants and C is solid content in the mixture (Kaya and Belibağlı, 2002).

4. MATERIALS AND METHODS

4.1. Materials

The composition of sesame paste (tahin) bought from Merter Helva San. ve Tic. A.Ş., Istanbul was 60.2 % total fat, 9.7 % carbohydrate, and 26 % protein. °Brix values for date, mulberry, grape and carob were 73. 68.75, 60.56 and 77.5 respectively.

Brix level of each commercial molasses, soluble solid content, was determined by using a refractometer (METTLER TOLEDO RE50, Switzerland) in the local sugar beet processing plant (Elazığ Şeker Fabrikası).

Table 4.1 The composition of molasses used in the experiments

Types / Composition	Dates Molasses	Mulberry Molasses	Grapes Molasses	Carob Molasses
Total carbohydrate (%)	77	73	64.1	66.95
Protein (%)	0. 1	2.4	1.9	2
°Brix	73	68.75	60.56	77.35

To accurate viscosity estimation, samples ought to be free from entrapped air (air bubbles); for this reason, the homogeneous blends of molasses and sesame paste are rested at room temperature for 5 hours.

4.1.1. Preparation of Same Molasses/Sesame Paste Blends

After making sure the samples free from entrapped air or air bubbles, the molasses-sesame paste blends such as blends of date syrup- sesame paste, mulberry molasses-sesame paste, grape molasses-sesame paste and carob syrup-sesame paste (tahin) at the different weight ratios (20 %, 30 %, 30 % and 55 %) (wt./wt.) were sheared under different shear strains to measure viscosities of those blends. In order to prepare a homogenous blend, the mixtures were blended consistently with a spatula. The blends were rested for 5 hours before subjecting to the rheological measurements.

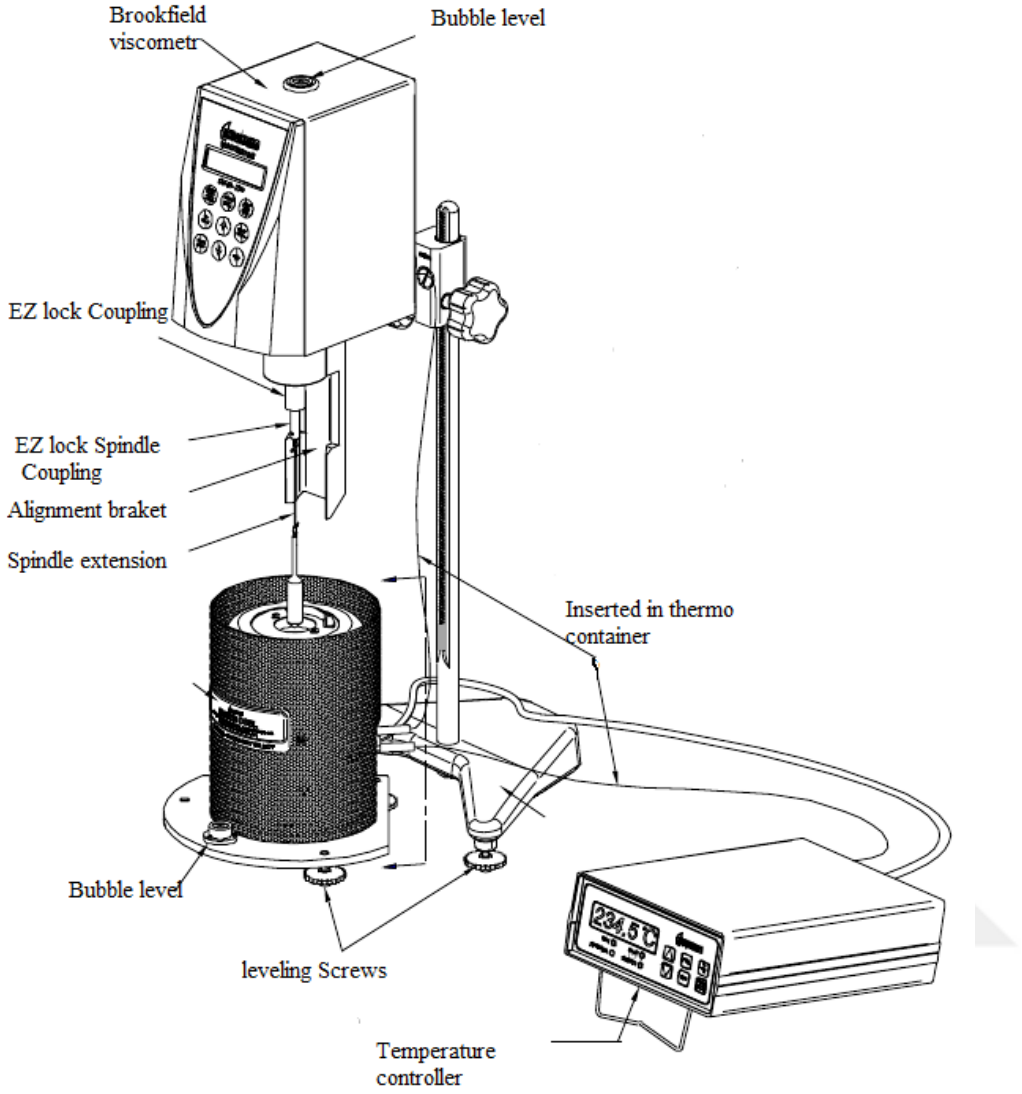

Figure 4.1 Brookfield rotational viscometer

The viscosity for each blend was measured at various temperatures (25, 30, 40, 50 and 60 °C) by using a rotary Viscometer (Brookfield). In order to obtain the viscosities of each blend as a function of the shear strain, those specimens were sheared with a few distinctive rotational speeds at a rising arrange.

4.2. Rheological Analysis

4.2.1. Measuring of Rheological Behavior

Brookfield rotational viscometer (Model DV-II, Brookfield Engineering Laboratories) was utilized to measure viscosities of the blends by using spindle 28 and the sample cup with 12 ml sample volume was at different temperature and concentration.

For obtaining the rheograms for each blend, the shear stress and viscosity were directly read from the viscometer for each shear rate in ranges of 2.5 to 30 rpm.

The rheological measurements of some ratios of the molasses-sesame paste mixtures with changing molasses contents of 20 %, 30 %, 40 % and 55 % (wt./wt.) were studied at different temperatures of 25, 30, 40, 50 and 60 °C. For all experiment, data collection for each specimen was finished after 5 revolutions at a set rotational speed. At that point for each progressive revolution, one point of viscosity and shear stress information on the set rotational speeds was recorded up to 5 values.

4.2.2. Statistical Analysis

Rheological properties and flow behavior of some ratios of the molasses-sesame paste mixes were evaluated by applying the linear regression method via Microsoft Excel software. The utilized equations and coefficient of determination (R^2) were detailed. Analysis of variance (ANOVA) test was approved to recognize any noteworthy contrast, among theoretical parameters; n and K beneath the temperature impact and molasses concentration impact ($\alpha = 0.05$). Factors of temperature, concentration, and shear rate were combined into a single logarithmic model by utilizing multiple linear regression system with using lines function in Microsoft Excel Software.

5. RESULTS AND DISCUSSION

5.1. Determination of Flow Behavior

In order to evaluate the rheological behavior of some molasses/sesame paste blends at different concentrations of molasses and temperatures, the blends were prepared by adding molasses into the sesame paste in ratios of 20-55% (wt. /wt.). During the measurement of viscosity of each blend, the temperatures were varied from 25 °C to 60 °C for each concentration and each shear rate. Five different rotational speeds were set to measure viscosity and shear stress for each blend.

By considering the relationship between shear stress and shear rate at each temperature and concentrations, all experimental results indicated that the blends are Power-law type shear thinning non-Newtonian fluids. Figures 5.1 to 5.16 illustrated the variation of measured shear stress with the shear rate of the considered blends at different temperatures and concentrations of molasses. The measured apparent viscosities of the blends versus shear rates are depicted in Figures 5.17 – 5.32. As can be seen in the figures the apparent viscosities decrease with increasing shear rates, which means the blends in question exhibit shear thinning behavior.

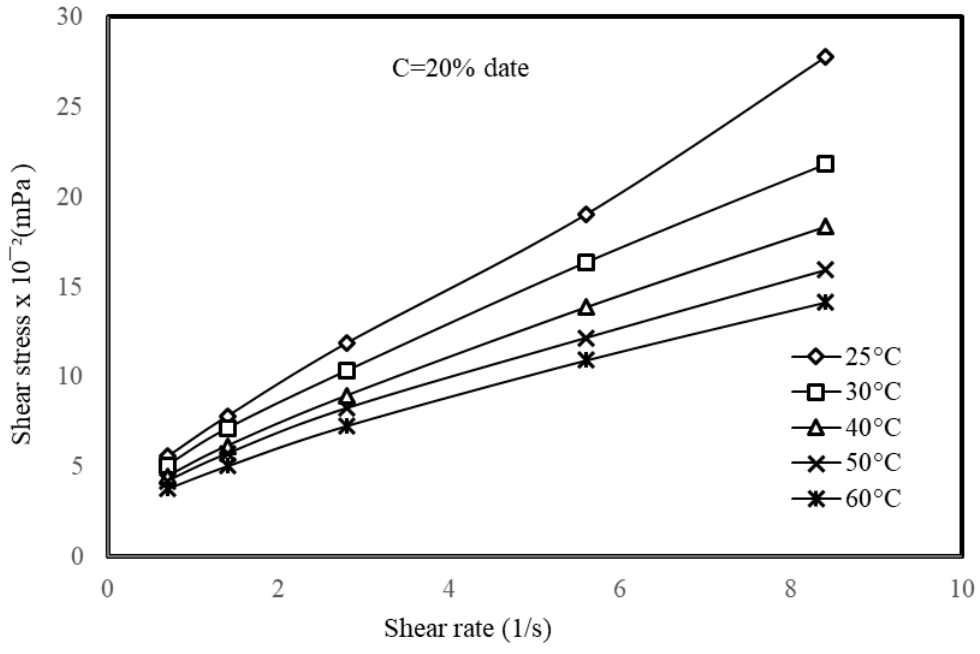

Figure 5.1 Change of shear stress with shear rate at various temperatures for a 20 % date molasses in sesame paste

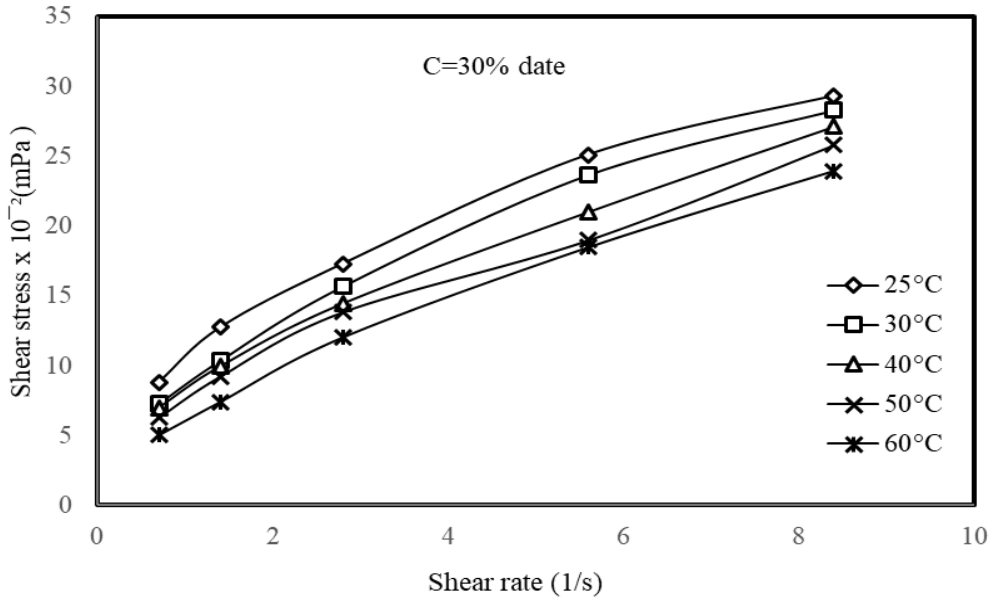

Figure 5.2 Variation of shear stress with shear rate at various temperatures for a 30 % date molasses in sesame paste

.

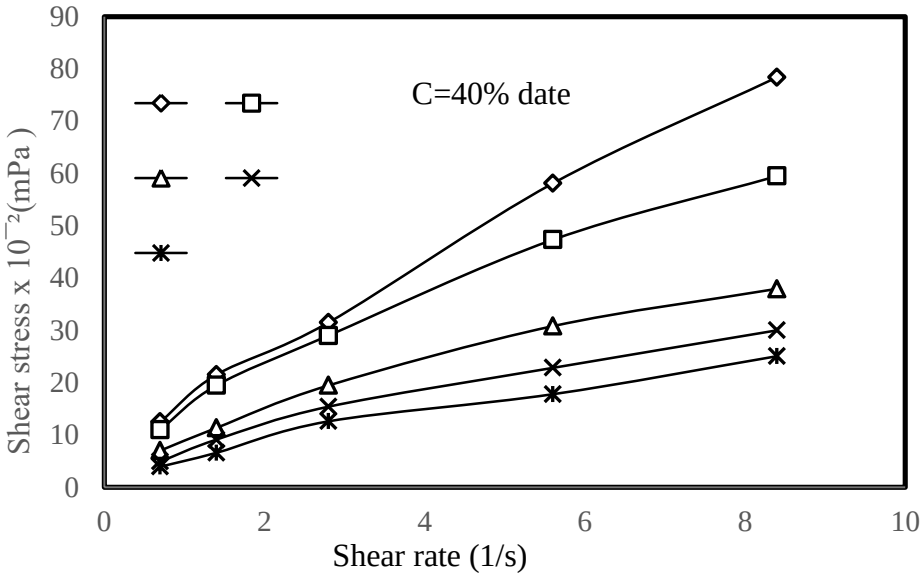

Figure 5.3 Variation of shear stress with shear rate at various temperatures for a 40 % date molasses in sesame paste

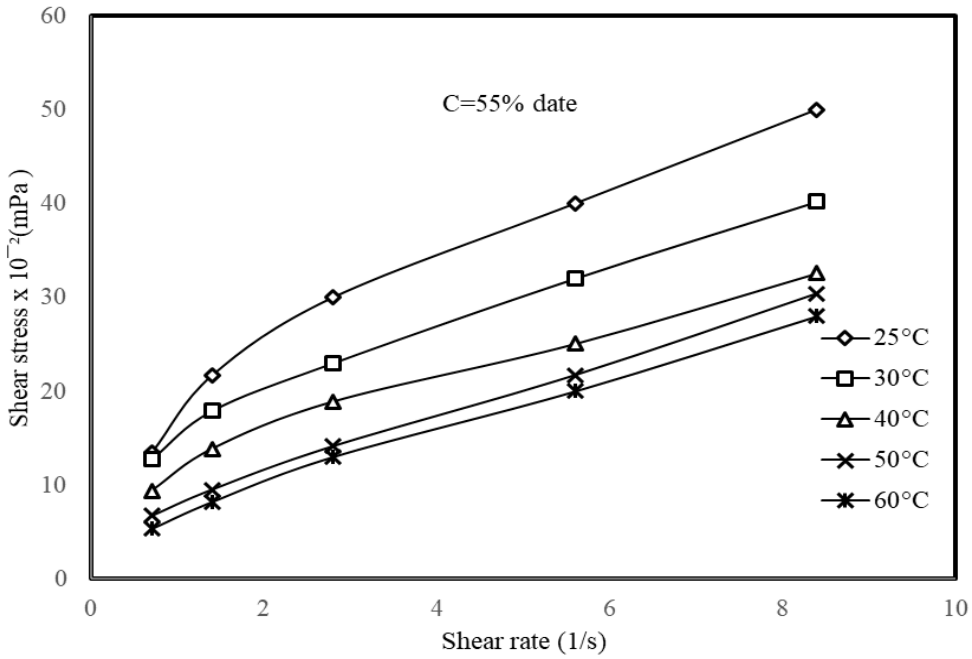

Figure 5.4 Variation of shear stress with shear rate at various temperatures for a 55 % date molasses in sesame paste

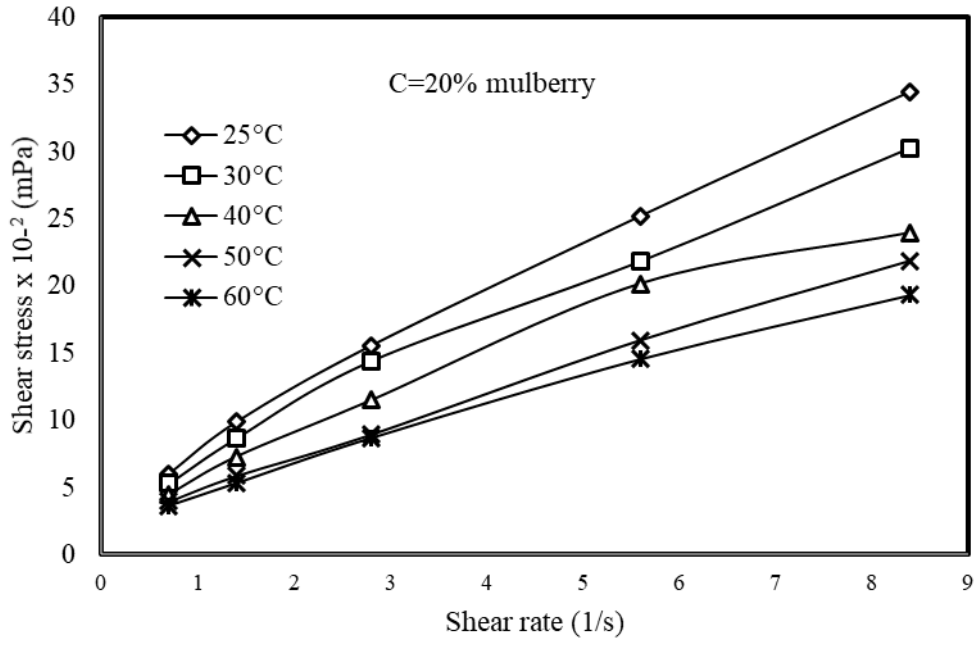

Figure 5.5 Variation of shear stress with shear rate at various temperatures for a 20 % mulberry molasses in sesame paste

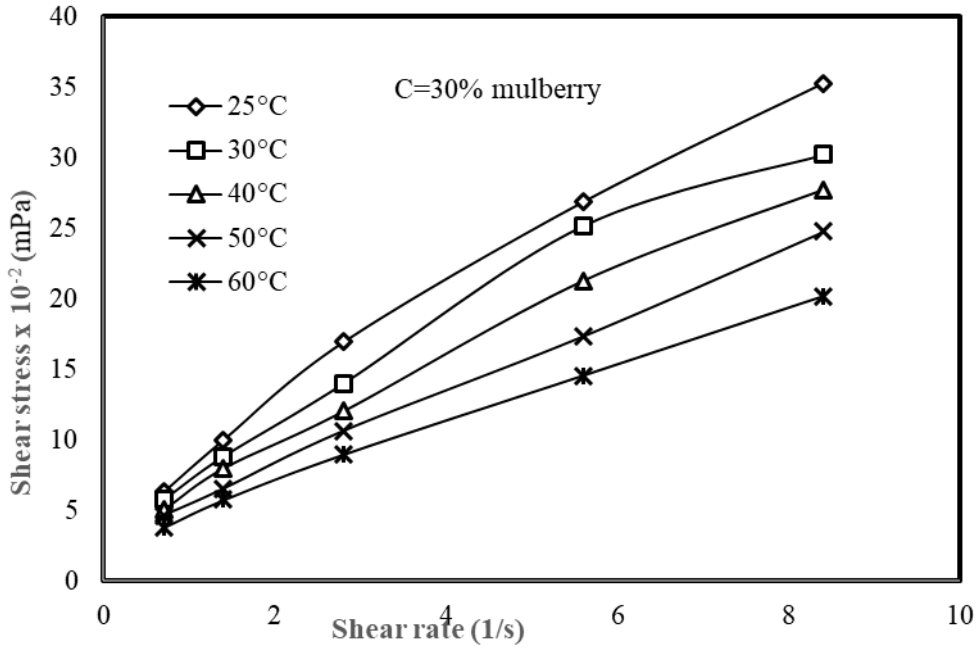

Figure 5.6 Variation of shear stress with shear rate at various temperatures for a 30 % mulberry molasses in sesame paste

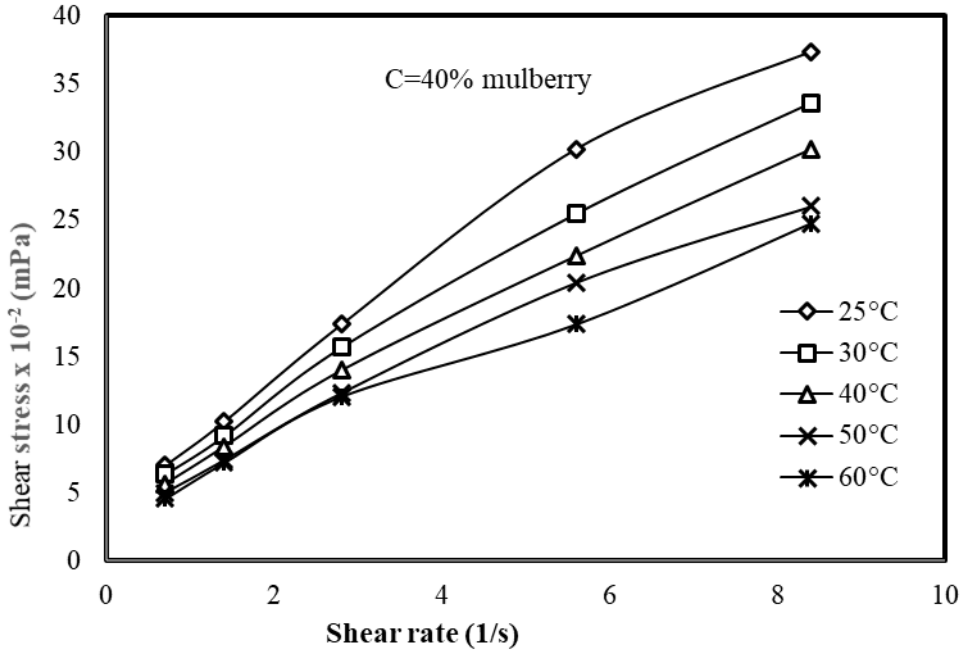

Figure 5.7 Variation of shear stress with shear rate at various temperatures for a 40 % mulberry molasses in sesame paste

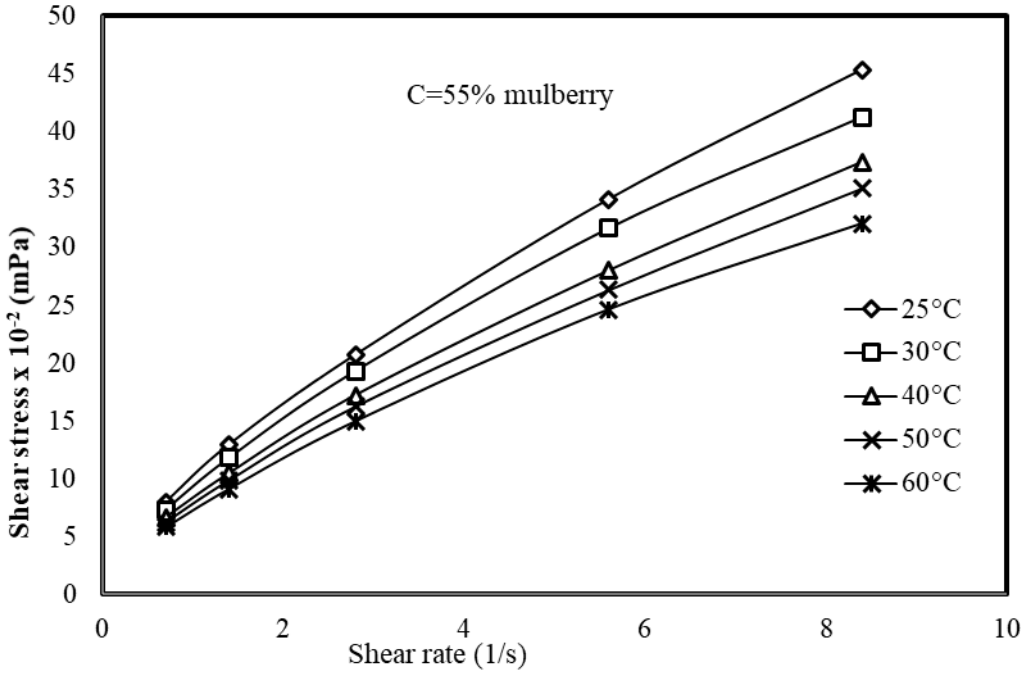

Figure 5.8 Variation of shear stress with shear rate at various temperatures for a 55 % mulberry molasses in sesame paste

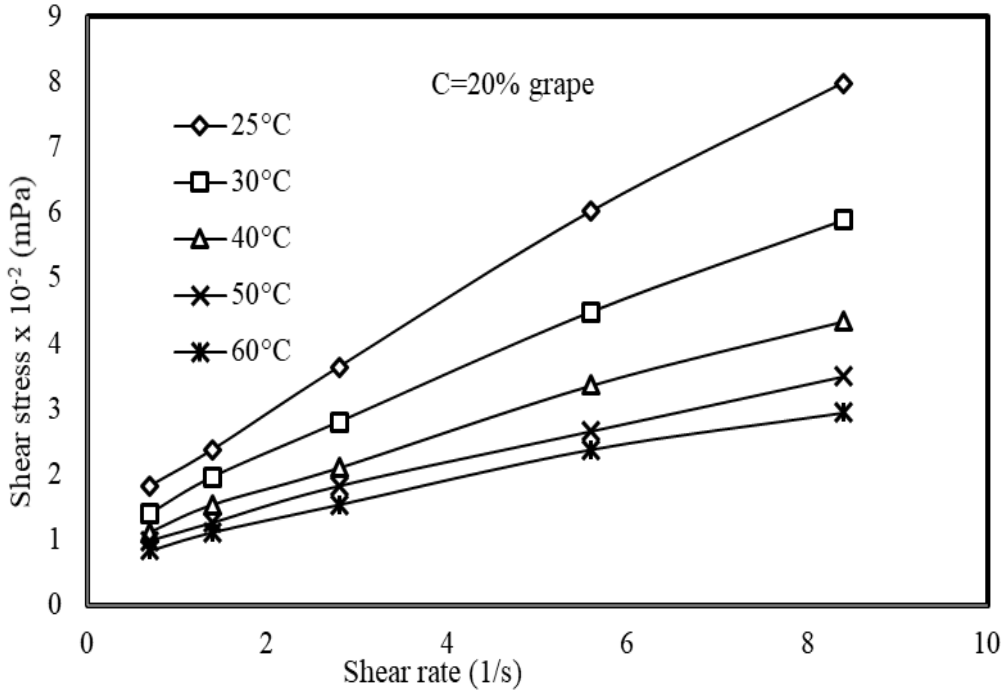

Figure 5.9 Variation of shear stress with shear rate at various temperatures for a 20 % grape molasses in sesame paste

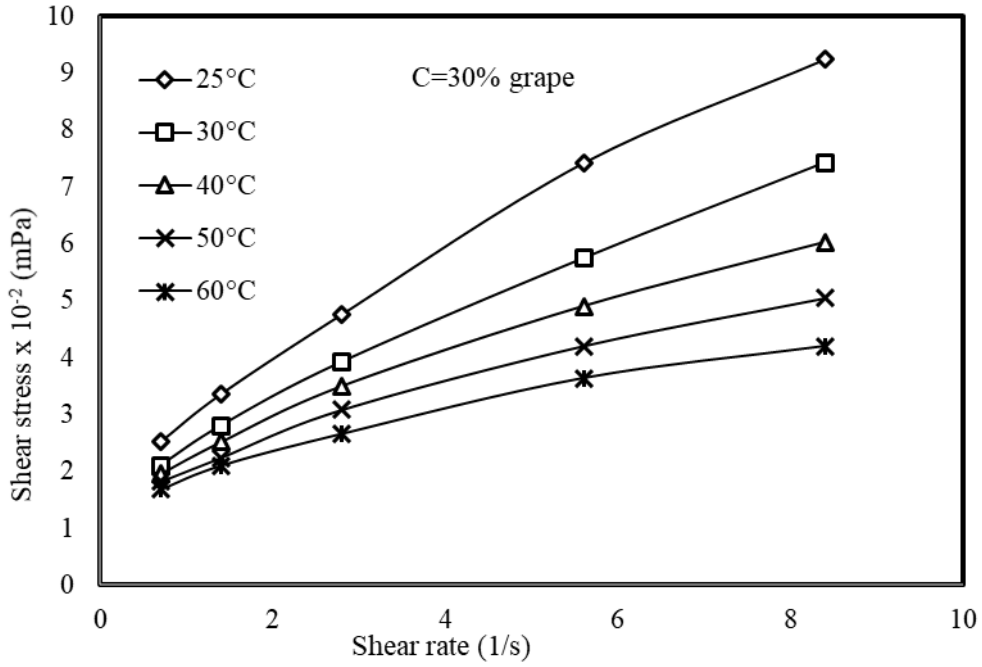

Figure 5.10 Variation of shear stress with shear rate at various temperatures for a 30 % grape molasses in sesame paste

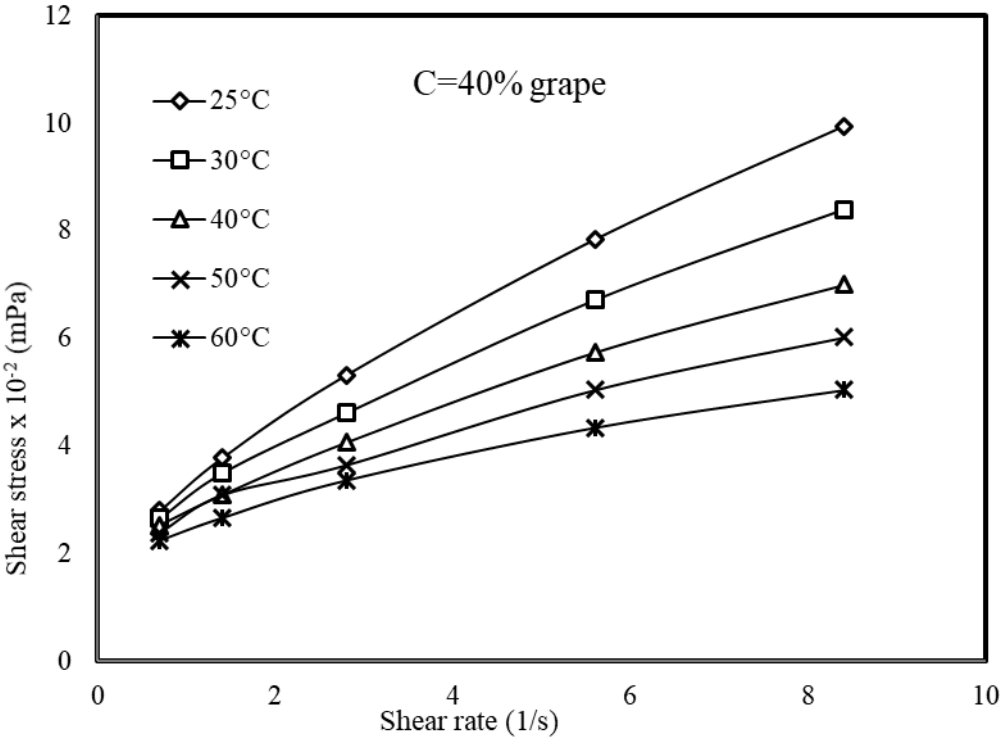

Figure 5.11 Variation of shear stress with shear rate at various temperatures for a 40 % grape molasses in sesame paste

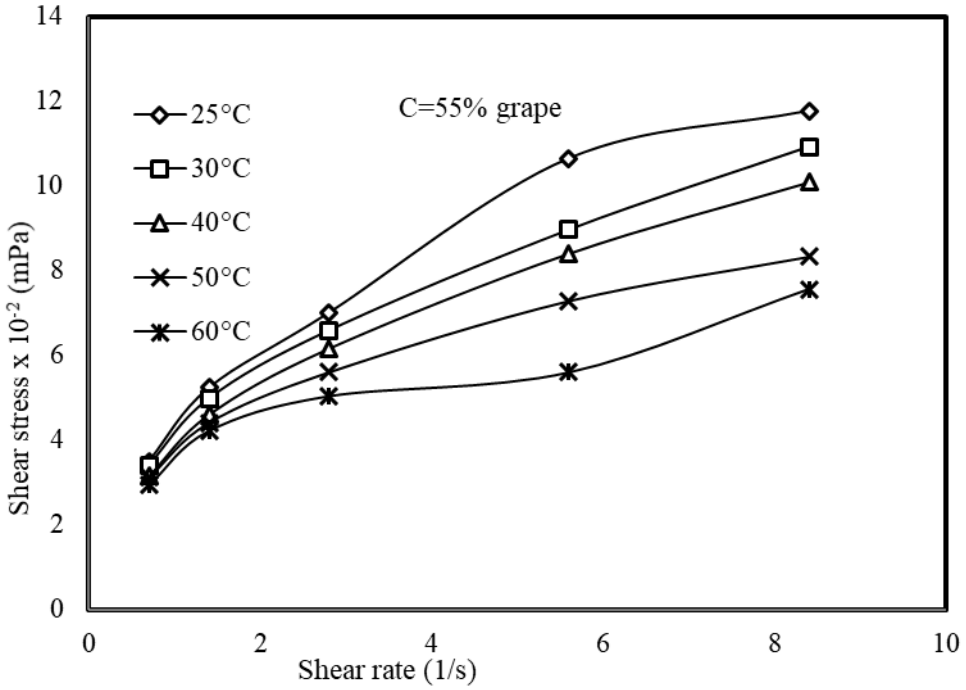

Figure 5.12 Variation of shear stress with shear rate at various temperatures for a 55 % grape molasses in sesame paste

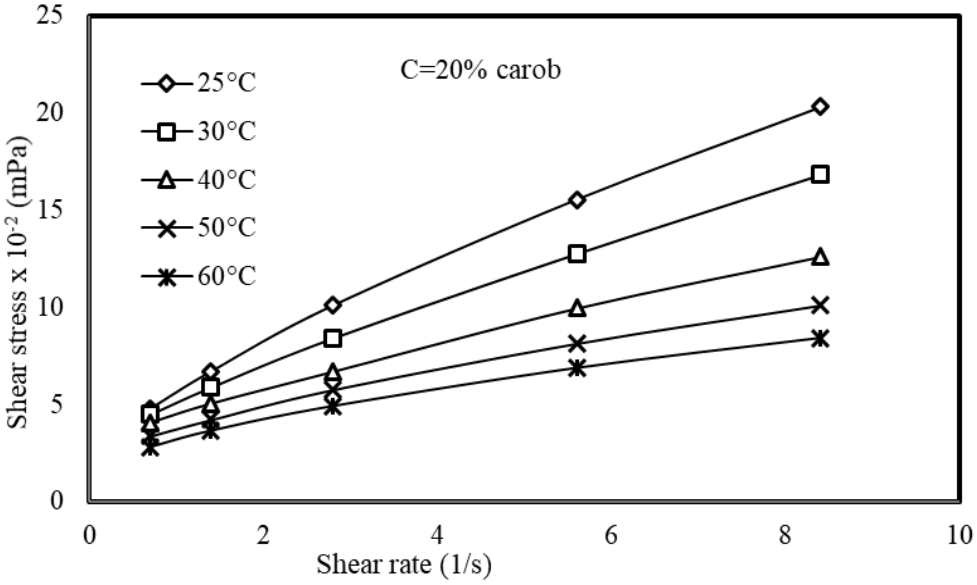

Figure 5.13 Variation of shear stress with shear rate at various temperatures for a 20 % carob molasses in sesame paste

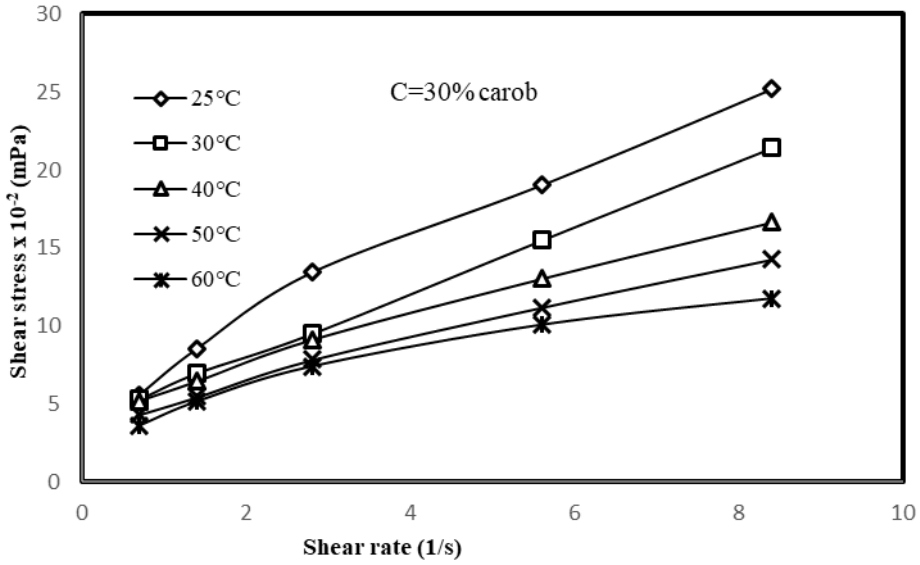

Figure 5.14 Variation of shear stress with shear rate at various temperatures for a 30 % carob molasses in sesame paste

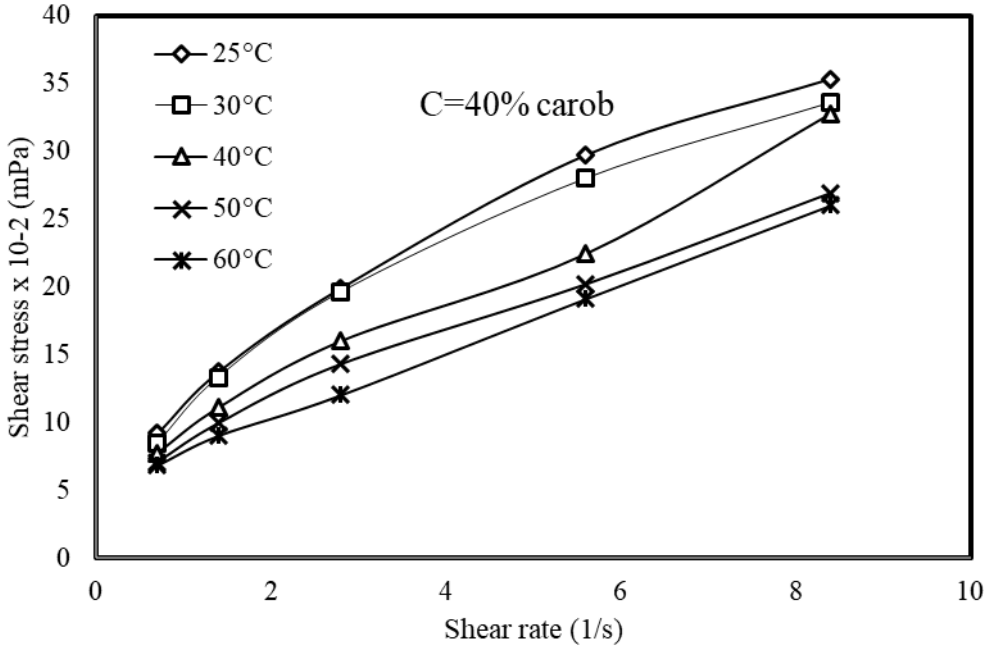

Figure 5.15 Variation of shear stress with shear rate at various temperatures for a 40 % carob molasses in sesame paste

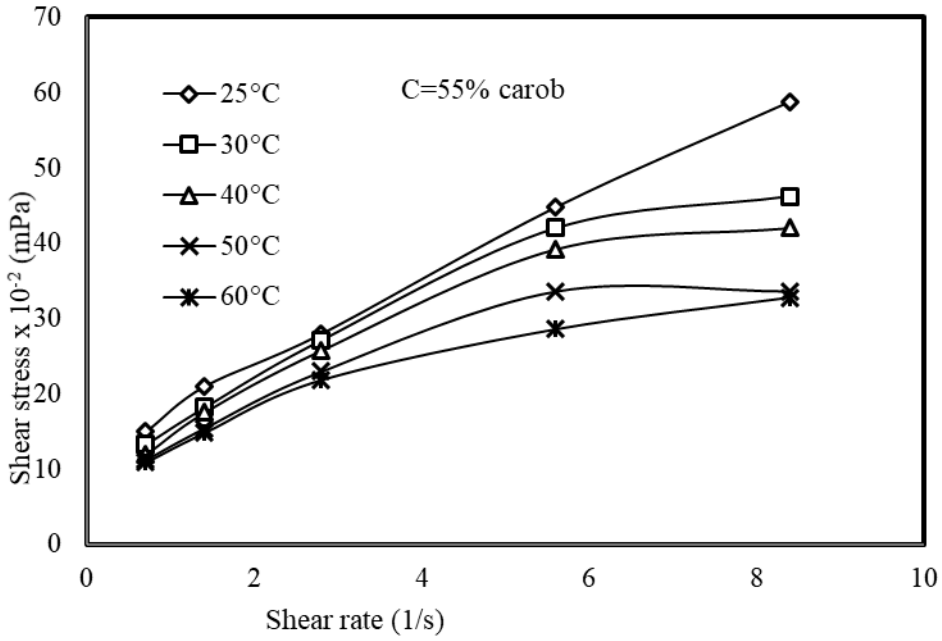

Figure 5.16 Variation of shear stress with shear rate at various temperatures for a 55 % carob molasses in sesame paste

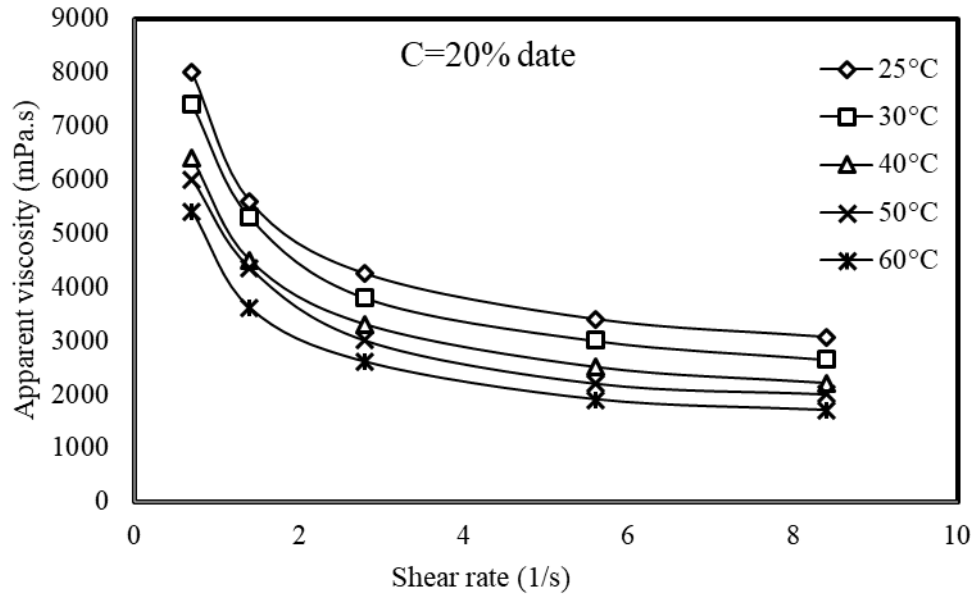

Figure 5.17 Variation of apparent viscosity with shear rates at different temperatures for a 20 % date molasses in sesame paste

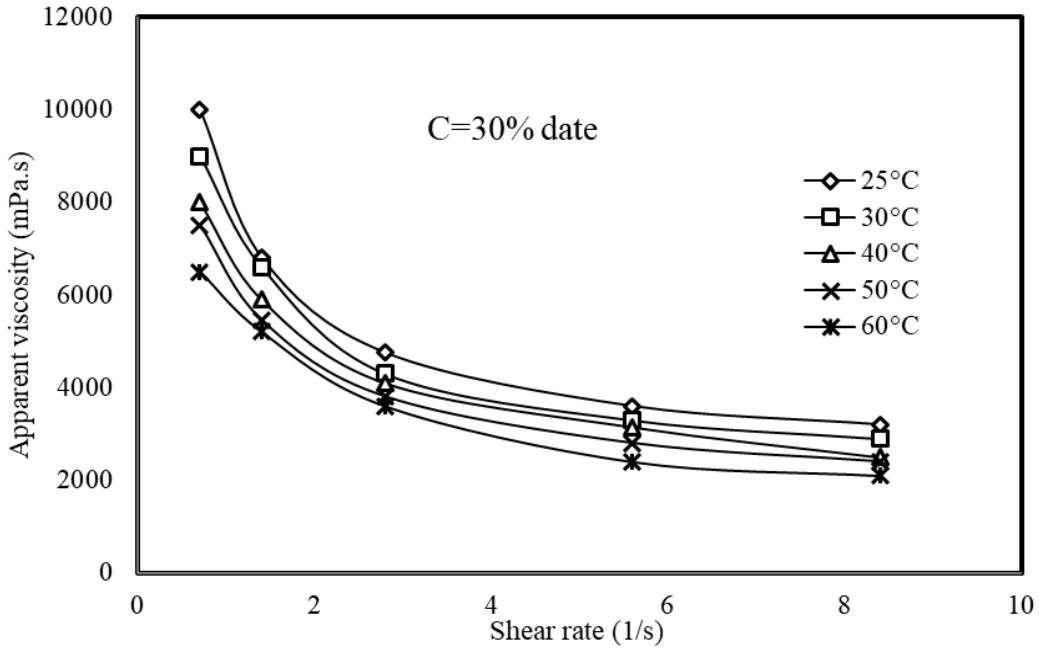

Figure 5.18 Variation of apparent viscosity with shear rates at different temperatures for a 30 % date molasses in sesame paste

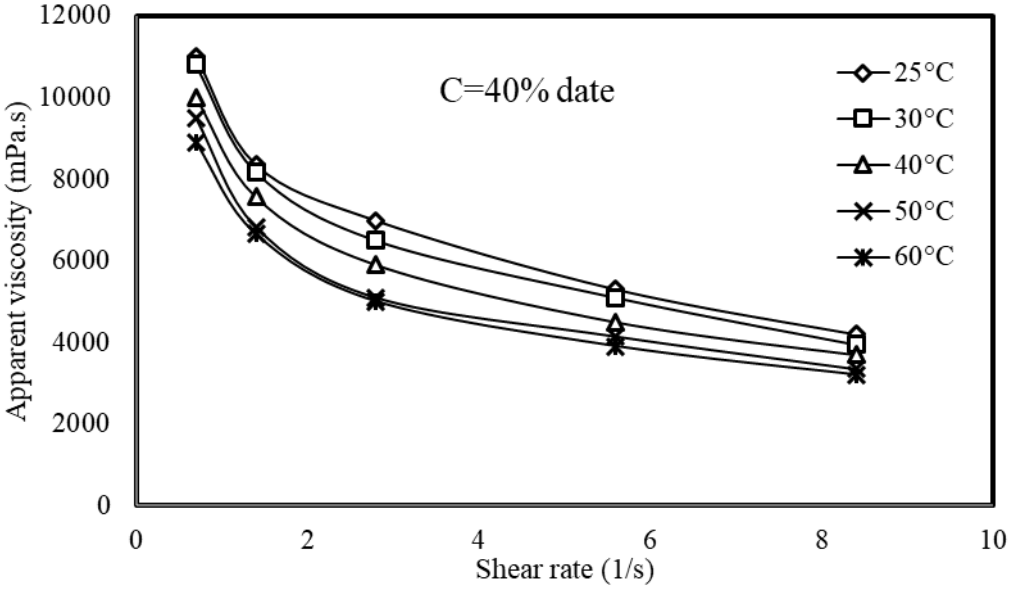

Figure 5.19 Change of apparent viscosity with shear rates at different temperatures for a 40 % date molasses in sesame paste

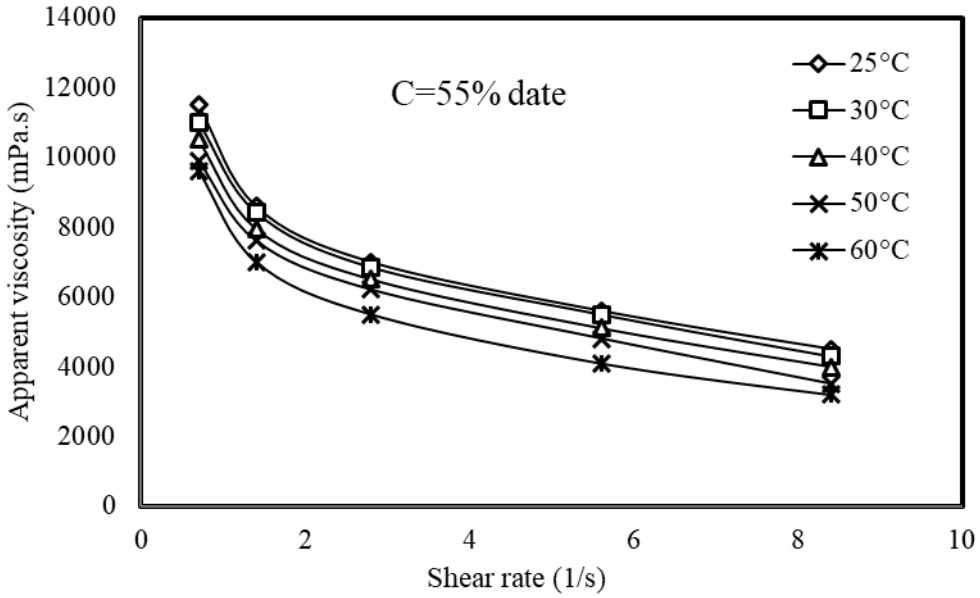

Figure 5.20 Variation of apparent viscosity with shear rates at different temperatures for a 55 % date molasses in sesame paste

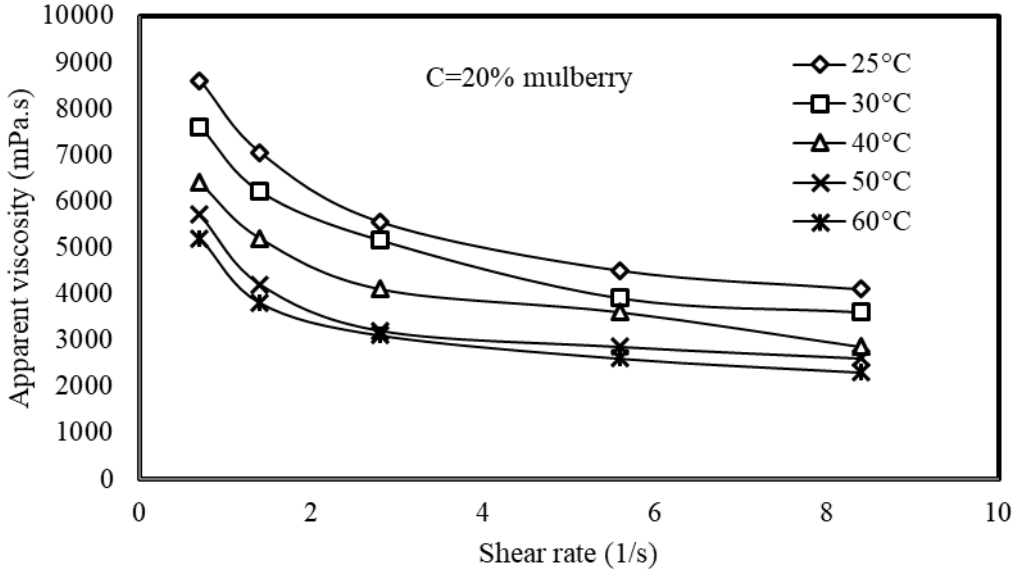

Figure 5.21 Variation of apparent viscosity with shear rates at different temperatures for a 20 % mulberry molasses in sesame paste

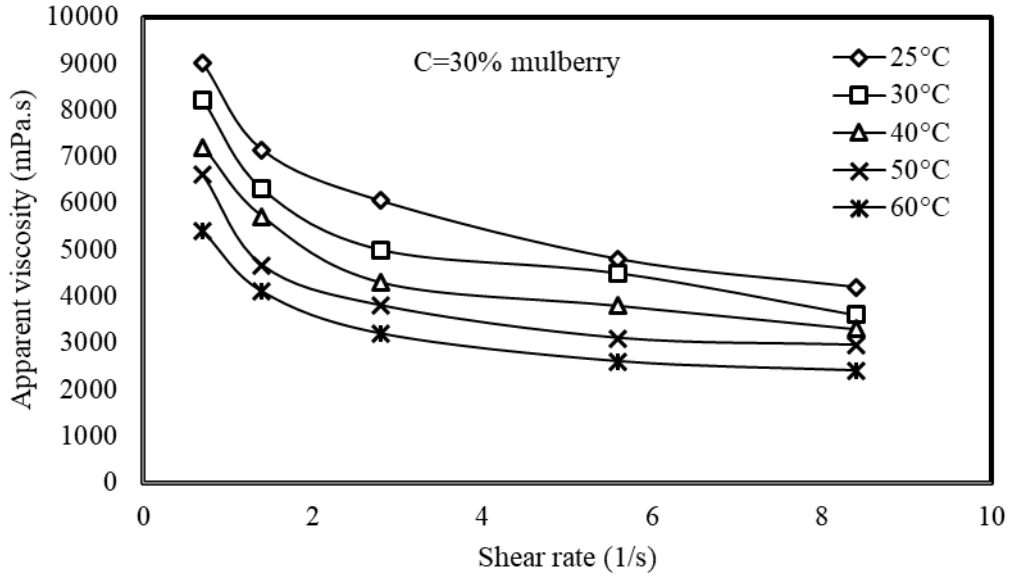

Figure 5.22 Variation of apparent viscosity with shear rates at different temperatures for a 30 % mulberry molasses in sesame paste

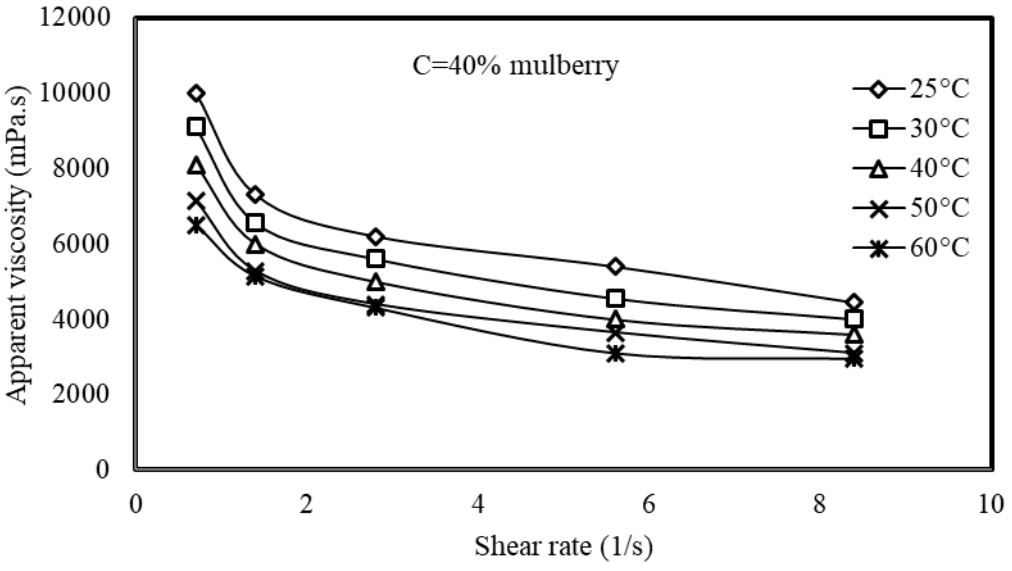

Figure 5.23 Change of apparent viscosity with shear rates at different temperatures for a 40 % mulberry molasses in sesame paste

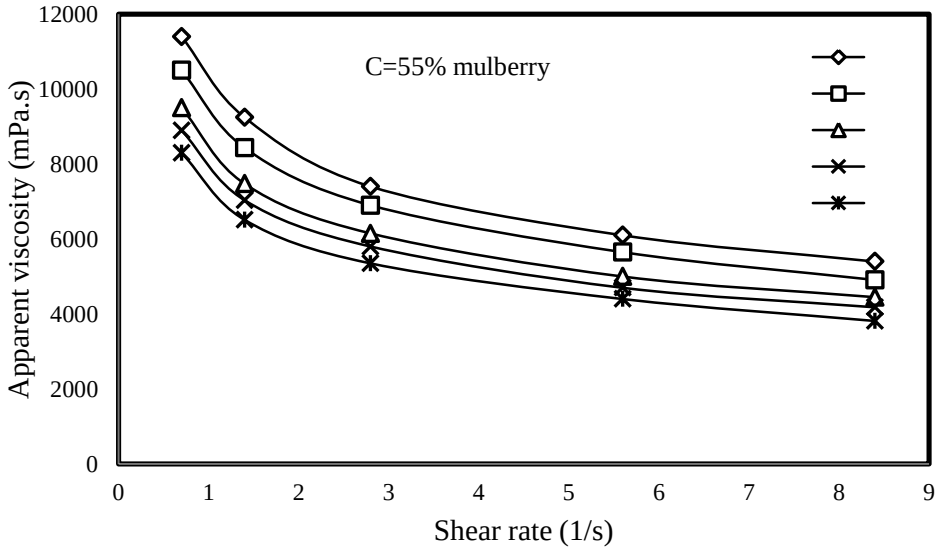

Figure 5.24 Variation of apparent viscosity with shear rates at different temperatures for a 55 % mulberry molasses in sesame paste

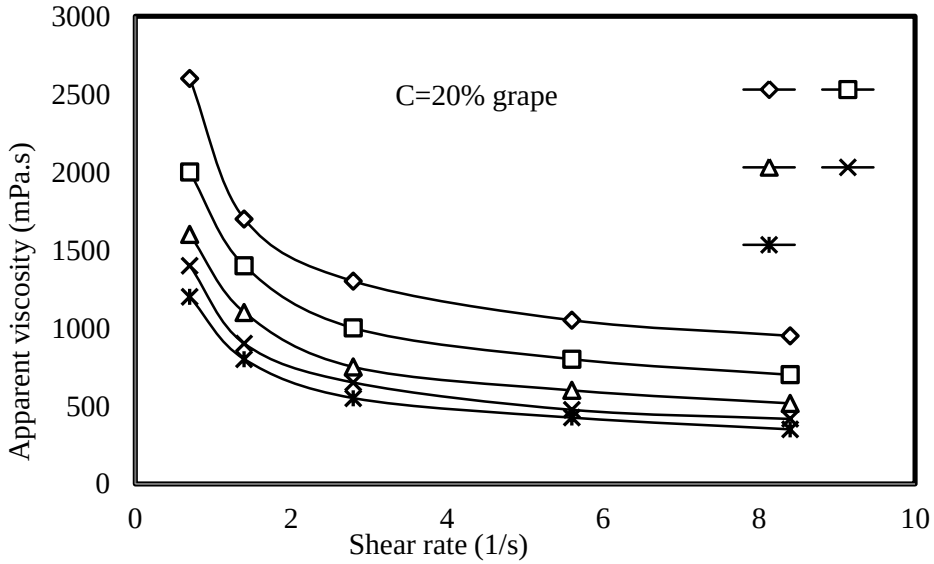

Figure 5.25 Variation of apparent viscosity with shear rates at different temperatures for a 20 % grape molasses in sesame paste

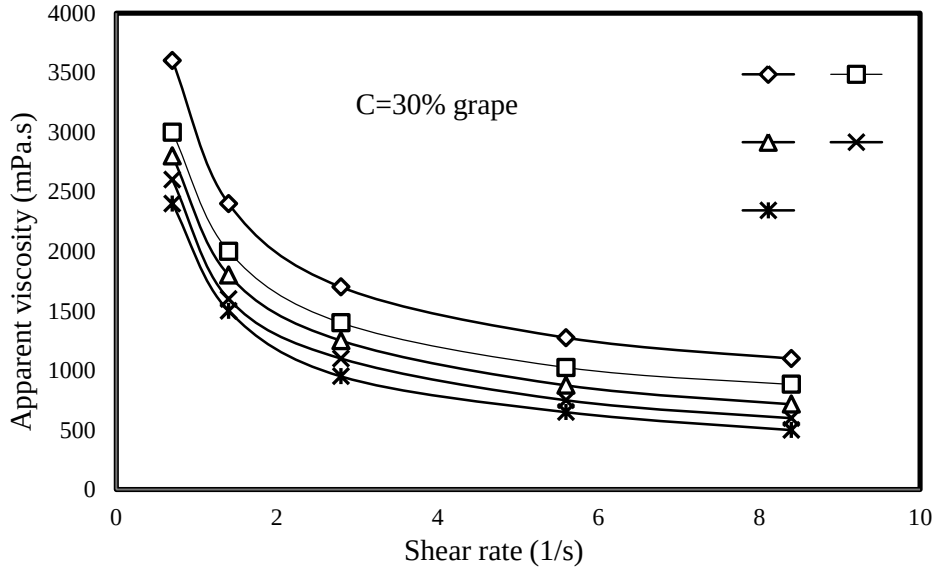

Figure 5.26 Change of apparent viscosity with shear rates at different temperatures for a 30 % grape molasses in sesame paste

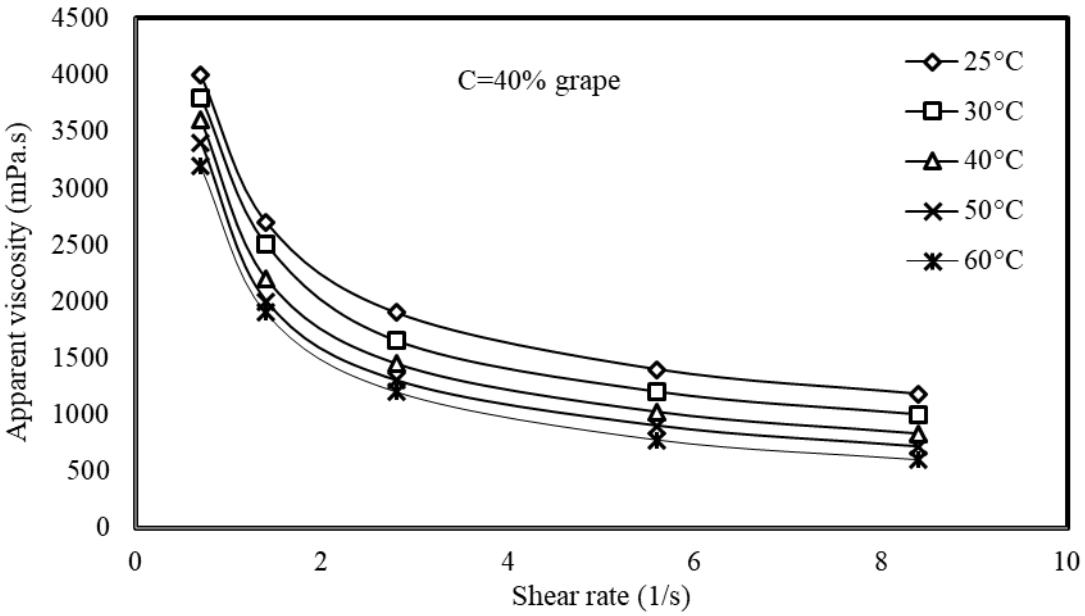

Figure 5.27 Variation of apparent viscosity with shear rates at different temperatures for a 40 % grape molasses in sesame paste

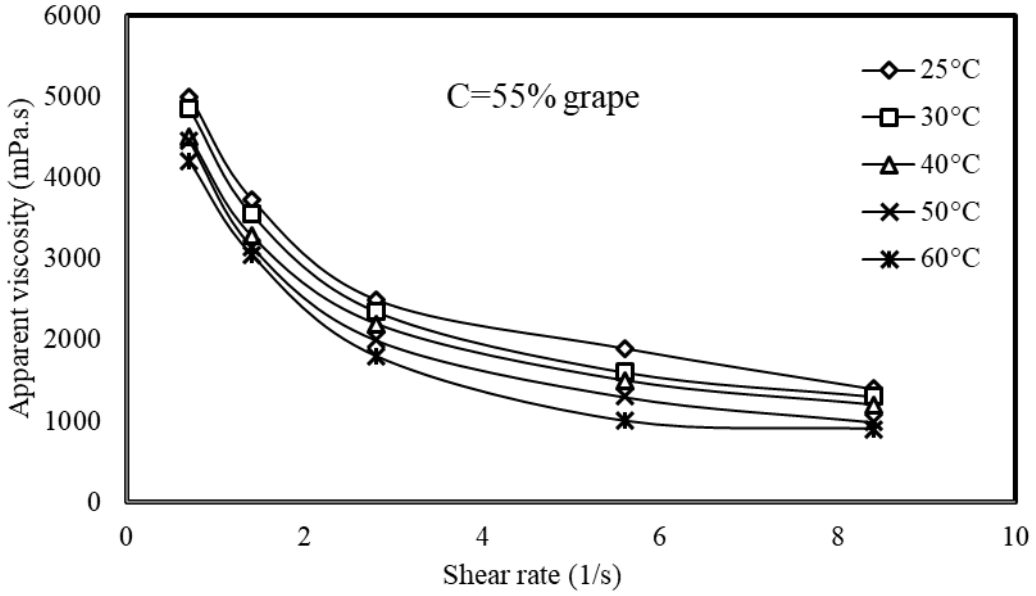

Figure 5.28 Variation of apparent viscosity with shear rates at different temperatures for a 55 % grape molasses in sesame paste

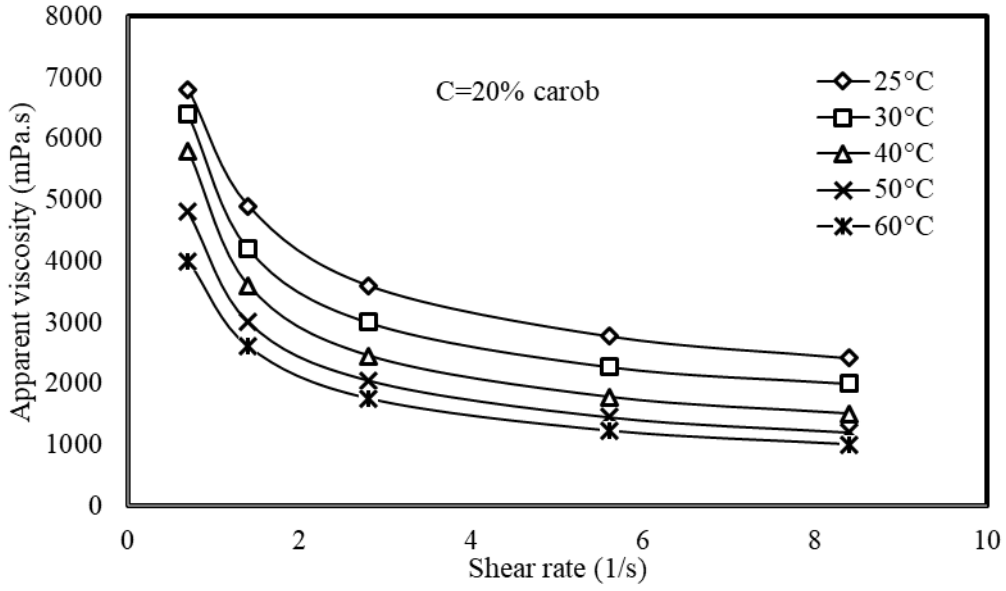

Figure 5.29 Variation of apparent viscosity with shear rates at different temperatures for a 20 % carob molasses in sesame paste

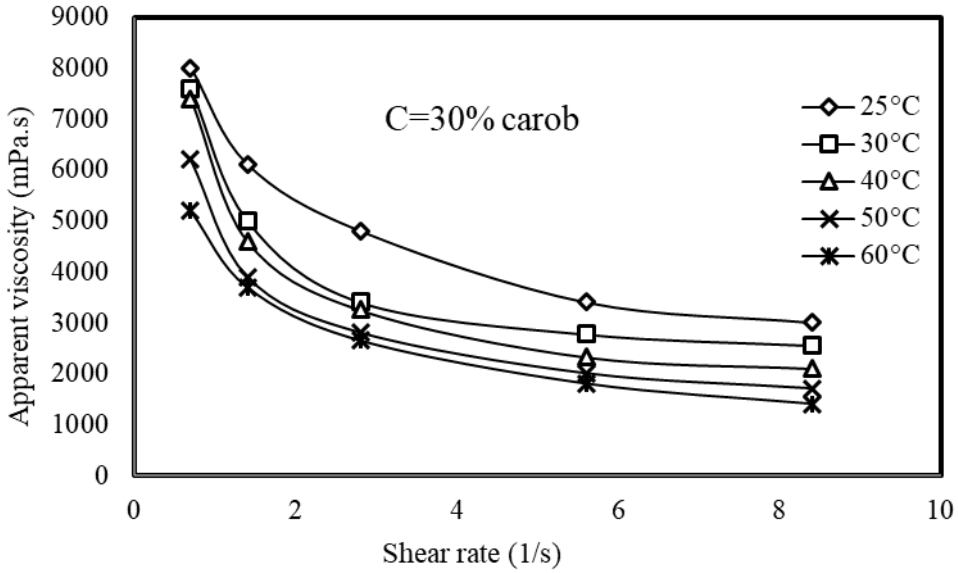

Figure 5.30 Variation of apparent viscosity with shear rates at different temperatures for a 30 % carob molasses in sesame paste

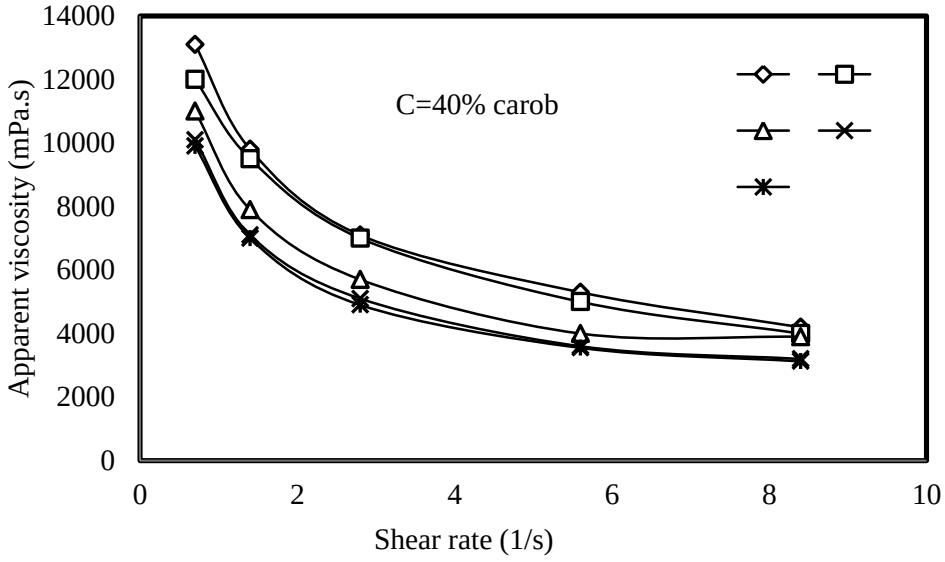

Figure 5.31 Change of apparent viscosity with shear rates at different temperatures for a 40 % carob molasses in sesame paste

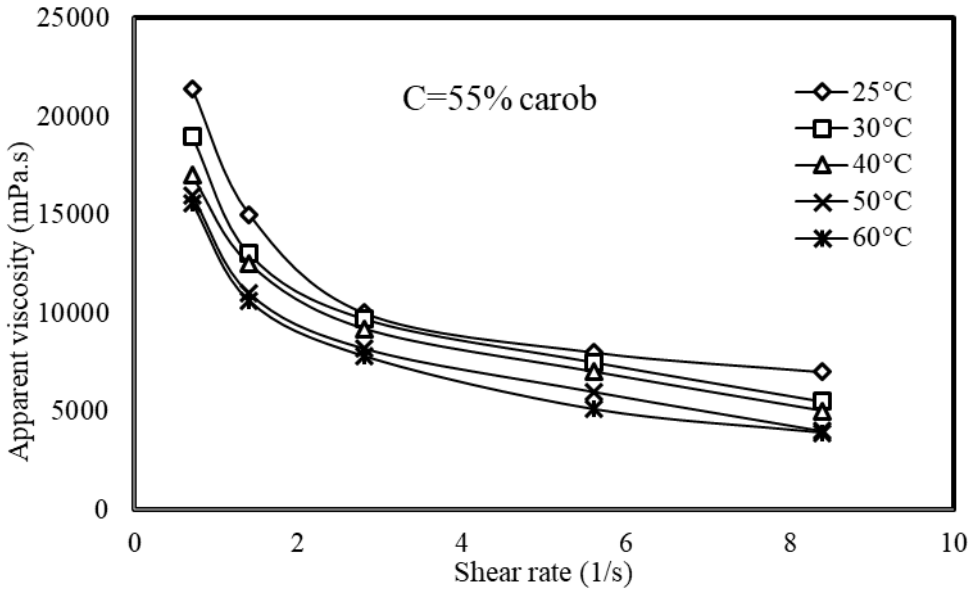

Figure 5.32 Variation of apparent viscosity with shear rates at different temperatures for a 55 % carob molasses in sesame paste

The model parameters such as the consistency coefficient and the flow behavior index can be determined by regression analysis based on the achieved results. According to the experimental finding, viscosities as a function of shear rates were finely fitted with Eq. (3.4b) to determine the model parameters; where the slope of regression line represents a flow behavior index, n, and the intercept of the graph shows the consistency coefficient, K. Table 5.1 to 5.4 includes the values of n, K and the coefficient of determination, R^2 for the considered blends at the specified concentrations and temperatures. In fact, the values of each type of blend given in Table 5.1 to 5.4 were obtained from each curve equation in Figure 5.17 – 5.32 at the specified concentrations and temperatures. The equation for each curve in the figures were found to be in a power function since the equation for the best fitting curve to the experimental data were found to be in a general form of $y = ax^b$.

The corrections were applied to the shear rate of the experimental data. Power-law approximation method was implemented for the corrections of Newtonian shear rates. The average correction has been calculated for the consistency coefficient, and flow behavior index, were found to be near 7 % for date, 9 % for mulberry, 4.6 % for grape and 5.4 % for carob of data. The correction values also consistent with the error in the theoretical percentage might produce from the use of the Newtonian approximation instead of power-law approximation.

Table 5.1 Parameters of power-law for the date blends at the various temperatures and concentrations

	date											
	20 %			30 %			40 %			55 %		
T(˚C)	n	K(mPa.s^n)	R^2	n	K(mPa.s^n)	R^2	n	K(mPa.s^n)	R^2	n	K(mPa.s^n)	R^2
25	0.617	6626.9	0.9855	0.538	8113.3	0.9897	0.629	9719.3	0.9878	0.639	10013	0.9927
30	0.585	6166.3	0.9914	0.532	7505.5	0.9901	0.612	9468.6	0.9908	0.641	9704	0.9888
40	0.569	5315	0.9948	0.536	6798.7	0.9976	0.607	8712.6	0.9984	0.629	9231.4	0.9892
50	0.544	5013.1	0.9924	0.535	6308.8	0.9982	0.594	8014.5	0.9939	0.606	8813.1	0.9753
60	0.532	4365.1	0.991	0.522	5744.7	0.9903	0.595	7664.6	0.9988	0.573	8269.7	0.9942

Table 5.2 Parameters of power-law for the mulberry blends at the various temperatures and concentrations

	mulberry											
	20 %			30 %			40 %			55 %		
T(˚C)	n	K(mPa.s^n)	R^2	n	K(mPa.s^n)	R^2	n	K(mPa.s^n)	R^2	n	K(mPa.s^n)	R^2
25	0.659	7714	0.9977	0.698	8057.4	0.9972	0.699	8597.7	0.9755	0.69	10207	0.9953
30	0.691	6868.1	0.9942	0.69	7165.5	0.979	0.683	7769.1	0.9846	0.682	9401	0.9844
40	0.690	5753.2	0.9837	0.69	6311.9	0.9862	0.68	6981.9	0.9917	0.676	8418.7	0.9732
50	0.689	4809.9	0.9648	0.679	5513.6	0.9689	0.679	6168.7	0.99	0.674	7905.6	0.987
60	0.683	4461.1	0.9886	0.671	4657.2	0.9906	0.67	5792	0.987	0.661	7351.5	0.9959

Table 5.3 Parameters of power-law for the grape blends at the different temperatures and concentrations

	grape											
	20 %			30 %			40 %			55 %		
T(˚C)	n	K(mPa.s^n)	R^2	n	K(mPa.s^n)	R^2	n	K(mPa.s^n)	R^2	n	K(mPa.s^n)	R^2
25	0.604	2084.5	0.9715	0.525	2906.5	0.9927	0.512	3254.4	0.9964	0.496	4218.2	0.9931
30	0.579	1647.4	0.9886	0.508	2421.8	0.9945	0.462	3033.4	0.9953	0.46	4100.6	0.9982
40	0.546	1300.1	0.9869	0.456	2232.7	0.9976	0.62	2782.3	0.9943	0.461	3809.7	0.9984
50	0.515	1113.7	0.9899	0.418	2033.9	0.9971	0.382	2582	0.9942	0.389	3709.5	0.9976
60	0.511	966.88	0.9928	0.374	1876.5	0.9985	0.331	2446.5	0.9986	0.336	3496.6	0.986

Table 5.4 Parameters of power-law for the carob blends at the various temperatures and concentrations

	carob											
	20 %			30 %			40 %			55 %		
T(˚C)	n	K(mPa.s^n)	R^2	n	K(mPa.s^n)	R^2	n	K(mPa.s^n)	R^2	n	K(mPa.s^n)	R^2
25	0.583	5714.8	0.9963	0.599	7001.6	0.9964	0.547	11290	0.9982	0.546	17480	0.9853
30	0.534	5123.2	0.9881	0.558	6007.1	0.9667	0.556	10671	0.9933	0.527	15808	0.9905
40	0.460	4515.9	0.991	0.492	5769.1	0.9847	0.562	9176.6	0.9838	0.528	14660	0.9876
50	0.447	3762.7	0.9949	0.485	4894.4	0.9926	0.529	8390.3	0.9964	0.475	13479	0.9813
60	0.444	3194.4	0.9981	0.476	4397	0.9978	0.528	8213.7	0.9963	0.451	12990	0.996

$$\%\text{Error} = 1 - \left[\frac{\text{shear rate of newtonian}}{\text{shear rate of power}}\right] \quad (5.1)$$

Newton shear rates and non-Newton shear rate were computed by following equations.

$$\dot{\gamma}_{\text{Ь}} = 2.\Omega.\left[\frac{\alpha^2}{\alpha^2-1}\right] \quad (5.2)$$

$$\dot{\gamma}_{\text{Ь}} = \left(\frac{2\Omega}{\text{n}}\right)\left[\frac{\alpha^{\frac{2}{\text{n}}}}{\alpha^{\frac{2}{\text{n}}}-1}\right] \quad (5.3)$$

The obtained model parameters namely flow behavior index and consistency coefficient in the range of the determination coefficient (R^2) indicate that the Power- law model seems to be convenient to describe the flow behavior of mixtures. The ranges of these model parameters for date, mulberry, grape, and carob molasses are shown in Tables 5.1, 5.2, 5.3, and 5.4 respectively. For the date molasses range correlation coefficient (R^2) between 0.9753 – 0 .9988, for the flow behavior index (n) is in 0.522 – 0.641 and for the consistency coefficient (K) is in 4365.1 – 10013 mPa.s^n. For the mulberry molasses range correlation coefficient (R^2) between 0.9977 – 0.9648), for the flow behavior index is in 0.659 – 0.699 and for the consistency coefficient is 4461.1 – 10207 mPa.s^n. For the grape molasses range correlation coefficient (R^2) between 0.9986 – 0.9715, for the flow behavior index is in 0.331 – 0.62 and for the consistency coefficient is in 966.88 – 4218.2 mPa.s^n. For the carob molasses range correlation coefficient (R^2) between 0.9986 – 0.9667, for the flow behavior index is in 0.444 – 0.599 and for the consistency coefficient is in 3194.4 – 17480 mPa.s^n.

In all cases, it can be noticed that the determination coefficient (R^2) is higher than 0.85 and the flow behavior index are smaller than unity (n < 1) that means all blends exhibit the shear-thinning (pseudo plastic) behavior since pseudo plasticity is inversely proportional to the flow behavior index (Grigelmo et al., 1999; Arslan et al., 2005).

The major constituents of sesame paste are protein and oil whereas molasses components are mainly sugar and water. The decrease in an apparent viscosity with increasing shear rate is often explained with changing in the structure of the mixture since the uniformity level of those constituent particles increases with the hydrodynamic forces (Alparslan and Hayta, 2002; Rao, 1999). The effect of shear produced from the structural change on the oil droplet

has been stated to egg yolk stabilized mixtures by Moros et al. (2002). More specifically, shearing leads to a gradual deformation and disruption of the oil droplets, which results in less resistance for fluid flow (Singh et al., 2003).

Yoğurtçu & Kamışlı, (2006) showed that the different molasses (grape, mulberry, harnup juice, and rosehip) exhibit non-Newtonian behaviors. The viscosities of those samples decrease with increasing shear rate as in pseudo plactic fluids. Also, Kaya & Belibağlı (2002) illustrated that molasses samples with the range of 52.1- 72.9 °Brix possess Newtonian fluid behaviors.

On the other hand, Abu- Jdayil, et al., (2002) and Abu-Jdayil (2003) reported that the sesame paste exhibits thixotropic behavior. By considering, thixotropic sesame paste blended with Newtonian molasses at concentrations of 20-55 %, it can be said that the time reliance of sesame paste is likely compensated by molasses at the taken a toll of losing its Newtonian behavior. Subsequently, the detected shear thinning behavior of the mixes shows up to be a center property between both unmistakable stream behaviors (Newtonian molasses and non-Newtonian sesame paste). This explanation was backed by the empirical estimations of the apparent viscosity of molasses/sesame paste mixes at a consistent shear rate, which is uncovered no discernible alteration with time.

According to the studies of Alparslan & Hayta (2002), Arslan et al., (2005); Habibi et al., (2006) and Razavi et al., (2008), the molasses/sesame paste blends display non-Newtonian, shear thinning behavior

Alparslan & Hayta (2002) reported that all blends of sesame paste/molasses mixtures having a molasses concentration range of 2- 6% (wt./wt.) at the temperature variances of 30-75 °C exhibit pseudo plastic behavior.

Arslan et al., (2005) reported that sesame paste/molasses blends having sesame paste concentrations (20-32%) and the temperature variations of (35-65 °C) display non-Newtonian, shear thinning behavior.

The date syrup /sesame paste blends, date molasses having variety solid contents of 60 and 65 °Brix, at the temperature ranges of 25-55 °C exhibit pseudo plastic behavior (Habibi et al., 2006).

Razavi et al., (2007) studied on the flow behavior of the sesame paste/date syrup mixtures at reduced fat of three different concentrations that are xanthan gum (0.0 1, 0.015, and 0.02 %

wt.), guar gum (0.1, 0.15 and 0.2 % wt.), and starch (0.75, 1.25, and 1.75 % wt.) All blends displayed non-Newtonian, pseudo-plastic behavior.

In the present study for all considered blends the flow behavior indices were found to be less than unity ($n < 1$), which indicate that all blends are shear thinning (pseudo plastic) fluids. The flow behavior indices of the blends such as molasses of date-, mulberry-, grape- and carob-sesame paste are in ranges of 0.52–0.64, 0.659–0.699, 0.33–0.62 and 0.444–0.599, respectively.

5.2. Temperature Effect on Flow Behavior

In order to examine the effect of temperature on the rheological behavior of a few molasses/sesame paste mixes, temperature was varied from 25 °C to 60 °C. For the specified tests the increase in temperature resulted in decreased viscosity values (Figures 5.17 to 5.32). The noticeable decrease in viscosity of each specimen was observed with increasing temperature from 25 °C to 60 °C (see Figures 5.17 to 5.32). This property can be clarified by considering the intermolecular forces and the intermolecular spaces. When temperature of a liquid increase, the molecules in the liquid move away from one another and thus intermolecular space increases. As a result, the intermolecular forces decrease with increasing temperature. Moreover, thermal and thus kinetic energy of molecules increases with increasing temperature. Therefore, when the fluid is exposed to the shearing, molecules move over one another much more easily and the chain entanglement are also lined up much more easily at high temperature due to low molecular forces and high kinetic energy of molecules. Consequently, the viscosity of a liquid decreases with increasing temperature. In other words, the intermolecular spacing are essentially influenced with variation of temperature since molecular distances increases with decreasing intermolecular forces.

According to the analysis of variance (ANOVA) ($\alpha = 0.05$), the flow behavior index and the consistency coefficient (Tables B) were strongly under the effect of temperature variance. As appeared in the Tables 5.1, 5.2, 5.3, and 5.4, the relation between the values of both n and K change with temperature inversely.

In addition, an Arrhenius-type equation Eq. (3.8) interprets well the relation between the temperature and the consistency coefficient. According to the experimental finding,

consistency coefficient as a function of temperature were finely followed with Eq. (3.8) to determine the model parameters; where the slope of regression lines from Figure 5.33 to 5.36 represents an activation energy, Ea/R, and the intercept of the graph shows the constants Kt. Table 5.5 to 5.8 includes the values of Kt, Ea and the determination coefficient, R^2 for the considered blends at the specified concentrations and temperatures.

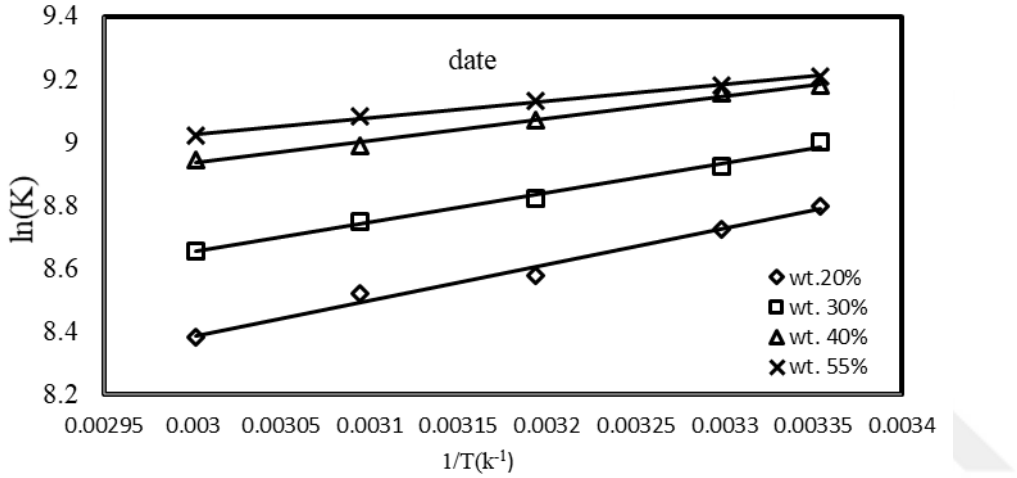

Figure 5.33 Temperature effect on consistency coefficient for the various date molasses concentrations

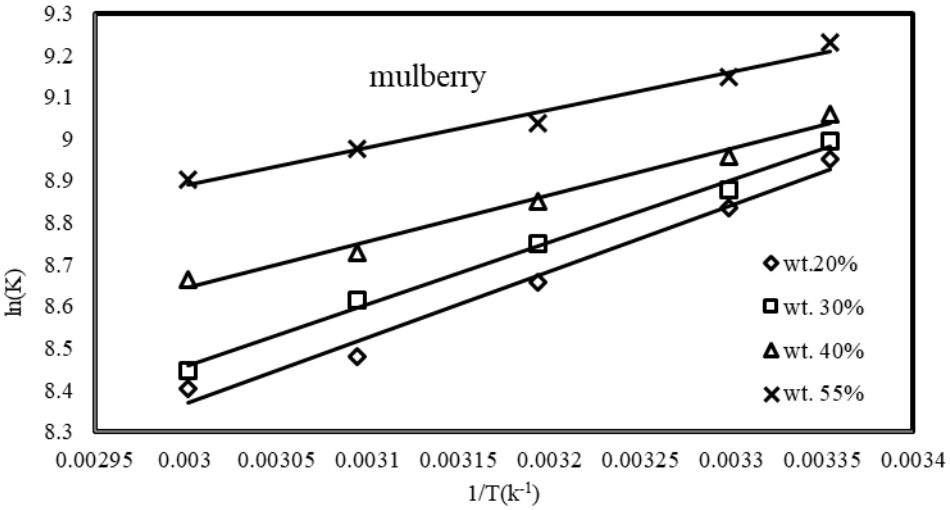

Figure 5.34 Temperature effect on consistency coefficient for the various mulberry molasses concentrations

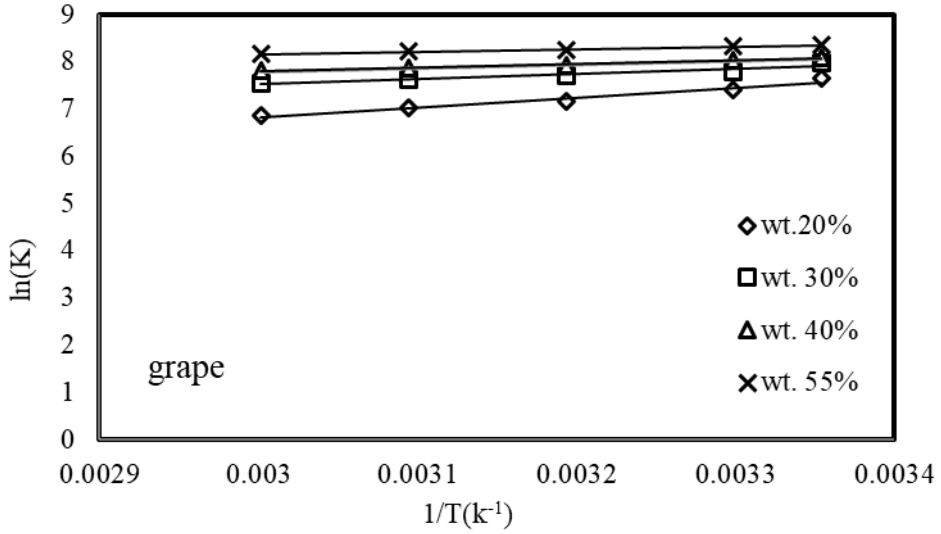

Figure 5.35 Temperature effect on consistency coefficient for the different grape molasses concentrations

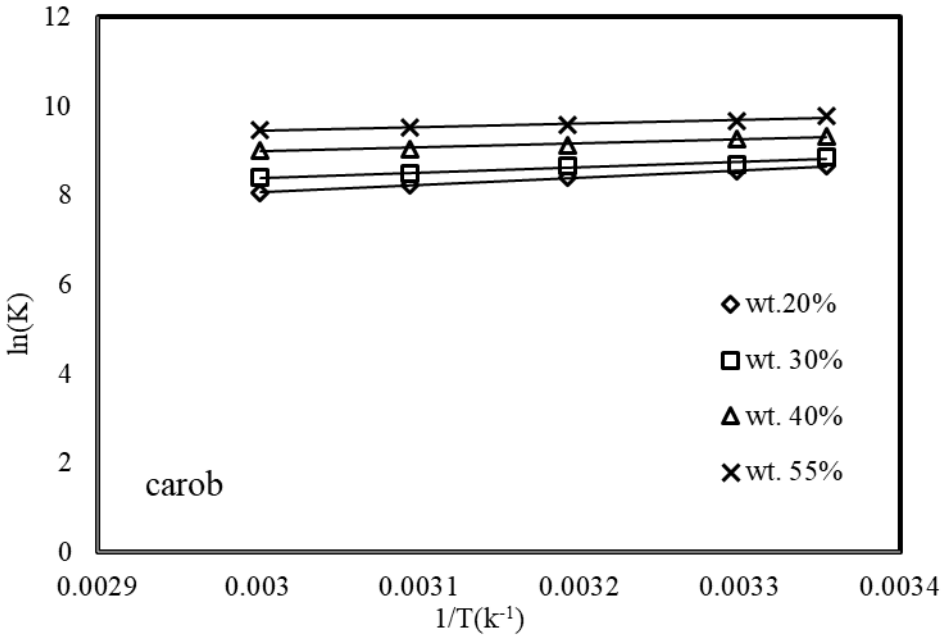

Figure 5.36 Temperature effect on consistency coefficient for the various carob molasses concentrations

Table 5.5 Finding of parameters in Eq. (3.8) for the various date molasses concentrations

C (%date)	Kt (mPa.s^n)	Ea(J/mol)	R^2
20	142.35	9499	0.9855
30	337.04	7851.1	0.9932
30	905.6	5894.7	0.9921
55	1713.68	4378.15	0.9941

Table 5.6 Finding of parameters in Eq. (3.8) for the various mulberry molasses concentrations

C (% mulberry)	Kt (mPa.s^n)	Ea(J/mol)	R^2
20	36.474	13216.68	0.9841
30	54.293	12366.11	0.9935
40	200.52	9259.827	0.9841
55	481.84	7514	0.98

Table 5.7 Finding of parameters in Eq. (3.8) for the various grape molasses concentrations

C (%grape)	Kt (mPa.sn)	Ea(J/mol)	R^2
20	1.75	17378.08	0.9646
30	62.446	9367.084	0.9287
40	219.862	6639.023	0.9865
55	729.968	4340.986	0.985

Table 5.8 Finding of parameters in Eq. (3.8) for the various carob molasses concentrations

C (% carob)	Kt (mPa.s^n)	Ea(J/mol)	R^2
20	25.186	13444.5	0.9949
30	47.39	10249.25	0.9607
40	442	7991.538	0.9494
55	1099.378	6779.038	0.9566

The activation energy (Ea) decreases on increase molasses concentration in the sesame pates. In other words, the activation energy decreases with decreasing percentage of the sesame paste in the blend.

Some researchers observed similar trends about activation energy (Ea) and the experimental constant, Kt. For instance, the activation energy decreases with increasing the grape molasses or date syrup concentration in tahin (sesame paste) whereas Kt increased in the same case (Alpaslan and Hayta, 2002; Habibi et al., 2006; Razavi et al., 2007).

The aforementioned two cases, one is the continuous phase was added to the oil phase and other one case the oil phase was added to the continuous phase. It has been concluded that increasing tahin concentration in the blend of tahin/pekmaz causes an increase in Ea and decreasing of Kt (Arslan et al., 2005). Based on the above studies, it can be said that the activation energy (Ea) is directly proportional with concentration of the oil phase and inversely proportional with the continuous phase.

5.3. Impact of Concentration on Flow Behavior

The concentration impact of molasses on rheological parameters and stream behavior was investigated with increasing concentration of molasses at constant temperatures. Concentrations of different types of molasses such as date, mulberry, grape and carob molasses varied from 20 % to 55% in order to determine effects of concentration on the consistency coefficient, flow index and the activation energy at various temperatures. It was observed that there is a linear relationship between apparent viscosities of mixtures and molasses concentrations at any temperature (Appendix A). This behavior can be seen in Figures 5.37, 5.38, 5.39 and 5.40 at the temperature of 40°C. It has similar trends for other temperatures.

Figures 5.37-5.40 illustrate the variation of the apparent viscosity as a function of shear rates at the constant temperature of 40 °C for different percentages of molasses of date, mulberry, grape and carob in the sesame paste. Figure 5.41 provides a comparison of the variations of apparent viscosity with shear rate for different blends at 40 °C. Date, Mulberry, Grape and Carob molasses exhibit non-Newtonian behavior (see Tables A.17, A.18, A.19, A. 20) that is in accord with the study of Yoğurtcu and Kamışlı (2006) since they showed that

Pekmez samples exhibit non-Newtonian behaviors. Furthermore, the apparent viscosities of molasses is inversely proportional with shear rate (Table A.7). This outcome affirms the discoveries in the recent investigations (Alparslan & Hayta, 2002; Abu- Jdayil et al., 2002; Abu-Jdayil, 2003; Arslan et al., 2005; Habibi et al., 2006).

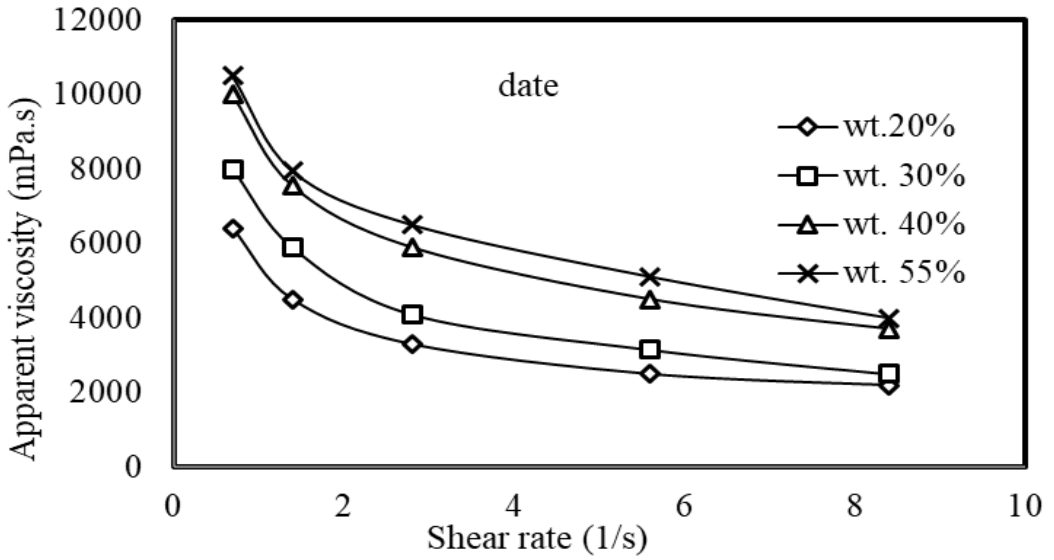

Figure 5.37 Relationships between apparent viscosities and shear rates of date molasses/sesame paste blends at 40°C

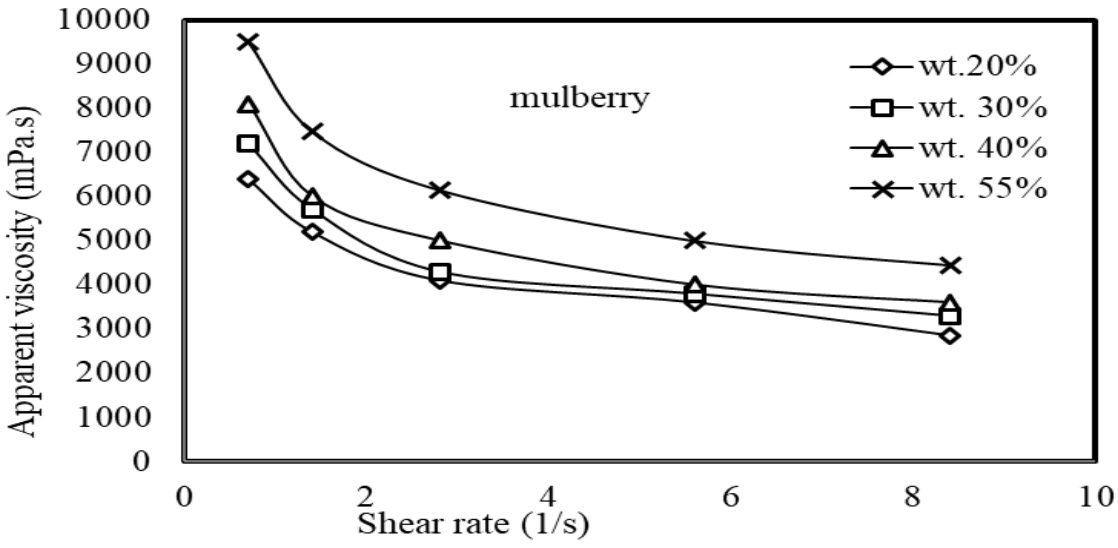

Figure 5.38 Relationships between apparent viscosities and shear rates of mulberry molasses/sesame paste blends at 40°C

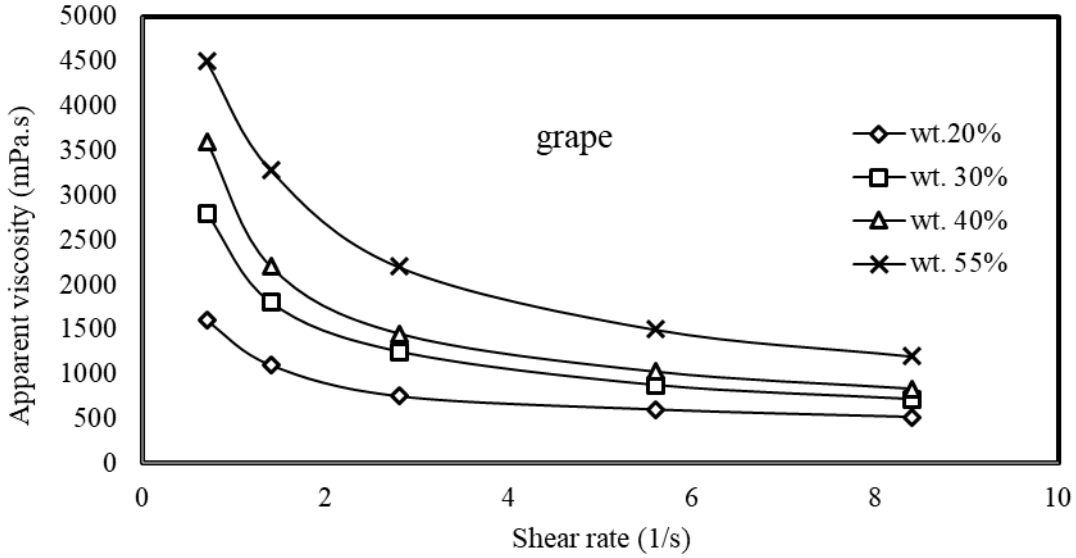

Figure 5.39 Relationships between apparent viscosities and shear rates of grape molasses/sesame paste blends at 40°C

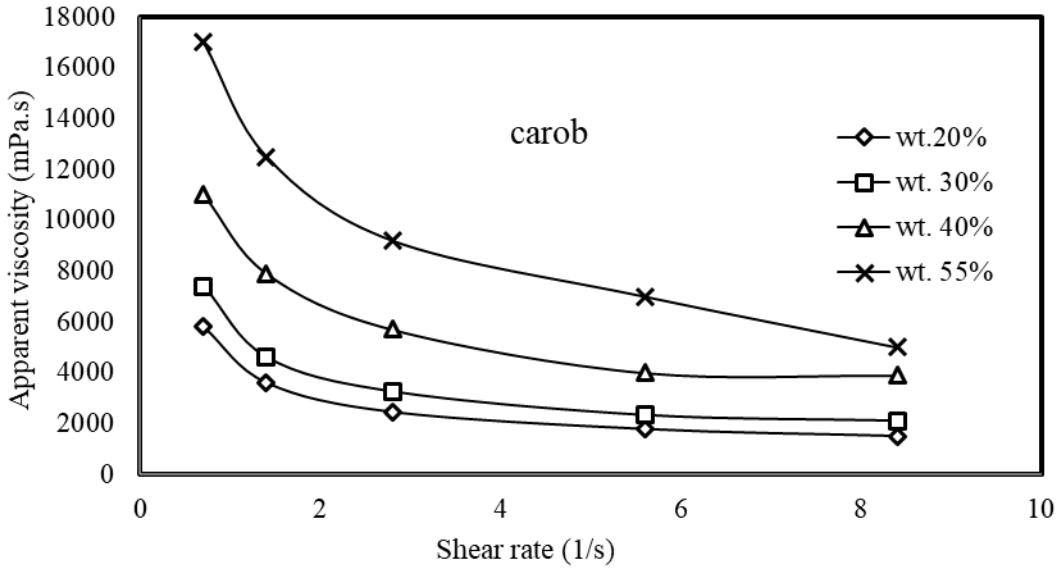

Figure 5.40 Relationships between apparent viscosities and shear rates of carob molasses/sesame paste blends at 40°C

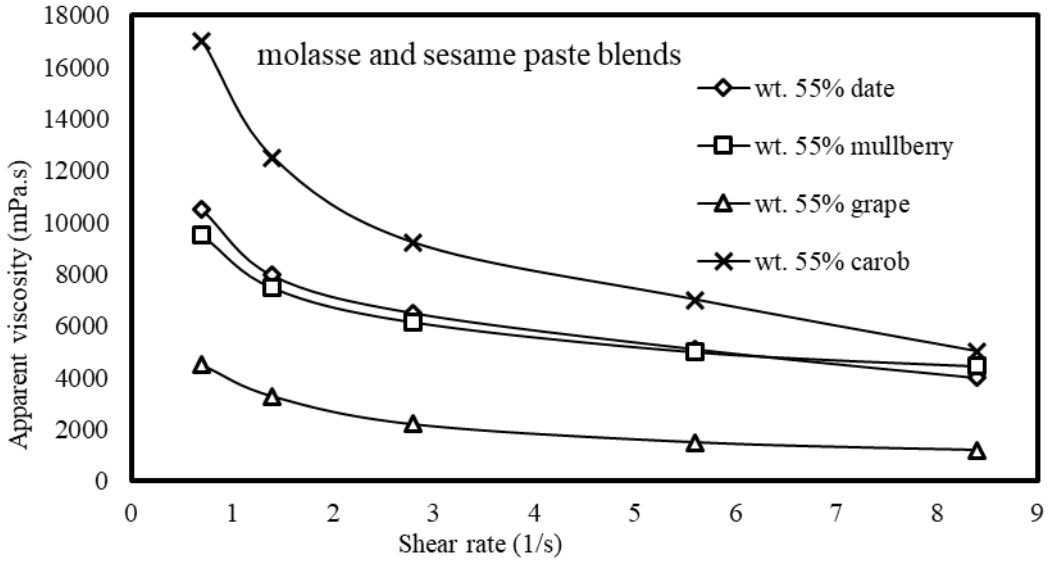

Figure 5.41 Relationships of apparent viscosity with shear rate for date, mulberry, grape and carob molasses/sesame paste blends at 40°C

By considering the rheological information of molasses and sesame paste in the past, the measurements of viscosities do not produce valuable information due to two possible reasons. A number of viscometers might not allow shear rate calculations because of their complex numerical geometries and thus, they can only generate comparative instead of absolute data of flow behavior (Steffe, 2002). The second possible reason is the variation in raw material of the product/products. In a way that very small differences in composition make process variables adequately affect the rheological behavior or treatment variables can also greatly affect the properties of rheology (Arslan et al., 2005).

A change in molasses concentrations essentially (α=0.05) influences the consistency coefficients of the mixes (see Tables B.5, B.6, B.7 and B.8) while its impact on the flow behavior (flow index) is inconsequential (see Tables B.1, B.2, B.3 and B.4). Consistency coefficient increases nonlinearly with concentration as appeared in Figures 5.42, 5.43,5.44 and 5.45. The effect of molasses concentration on consistency coefficient was portrayed by exponential and power function. Linearized forms of Eq. (3.8) and Eq. (3.9) were plotted and the comparison of parameters are given in Tables 5.8, 5.9, 5.10 and 5.11.

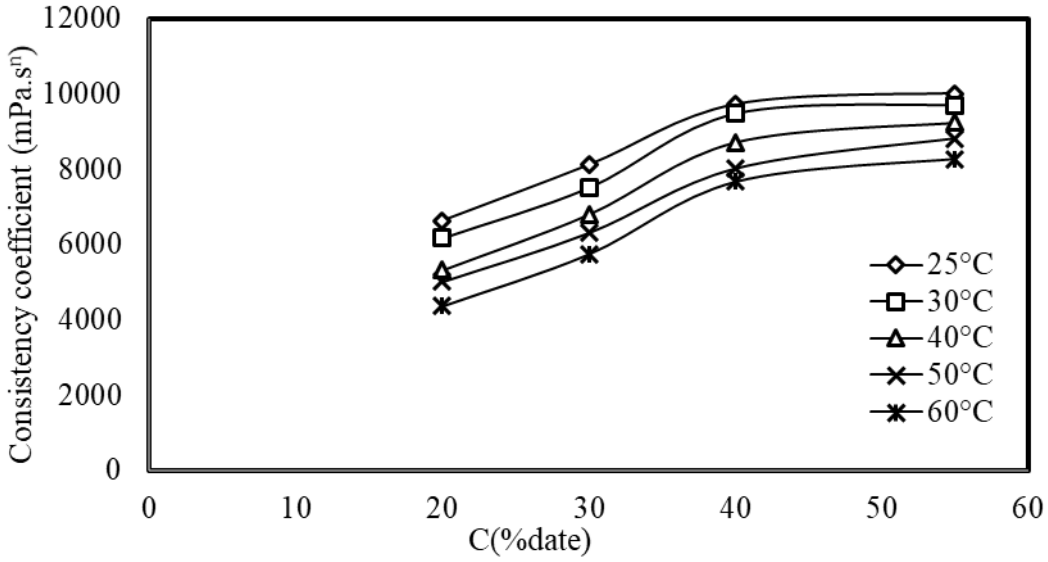

Figure 5.42 The influence of date molasses concentration on consistency coefficients at various temperatures

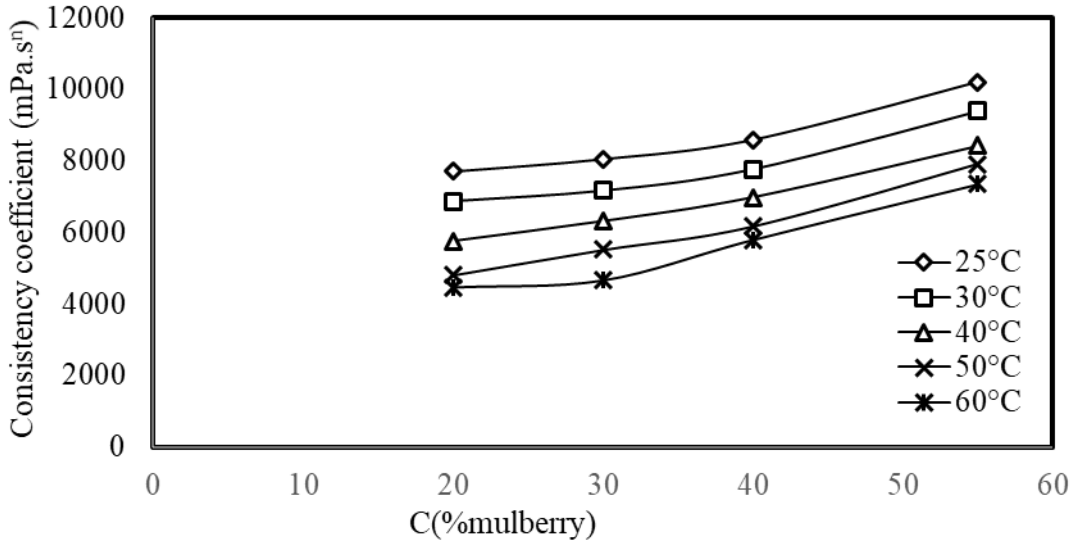

Figure 5.43 The effect of mulberry molasses concentration on consistency coefficients at various temperatures

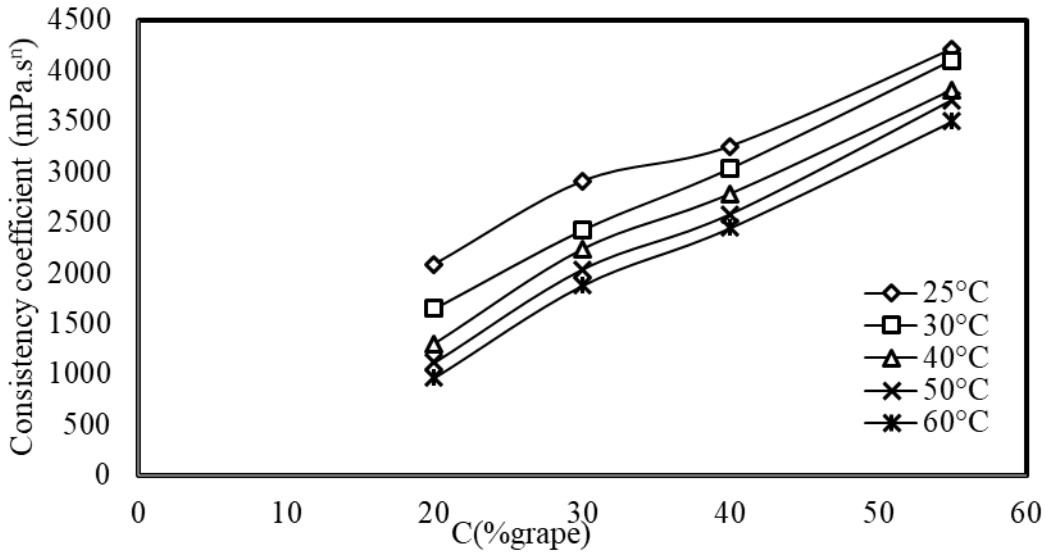

Figure 5.44 The influence of grape molasses concentration on consistency coefficients at different temperatures

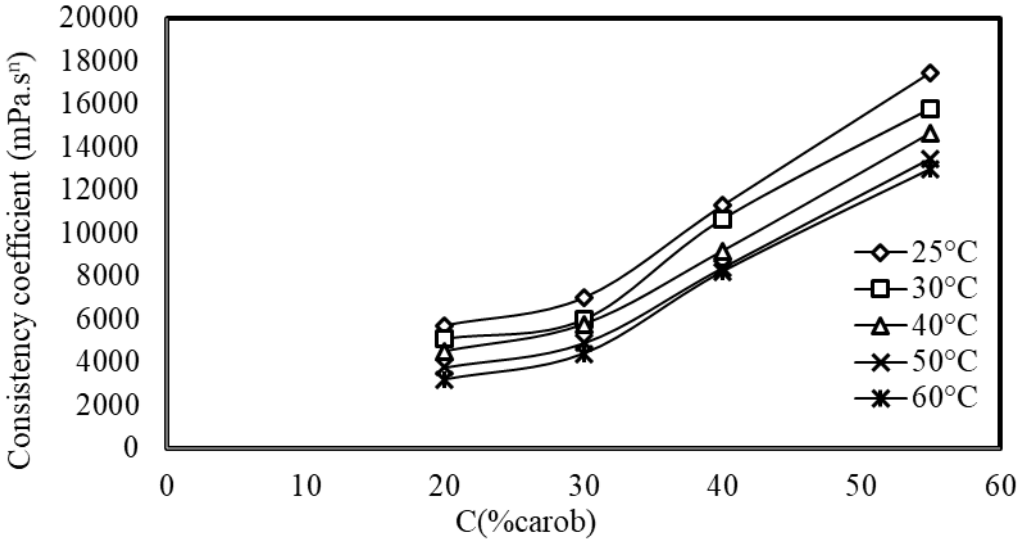

Figure 5.45 The effect of carob molasses concentration on consistency coefficients at various temperatures

Table 5.9 Finding of parameters in Eq. (3.9) and Eq. (3.10) for various concentrations of date molasses at the different temperatures

	Exponential Model Eq. (3.9)			Power Model Eq. (3.10)		
Temperature °C	b1	Kc1	R2	b2	Kc2	R^2
25	0.014	5286.3	0.9022	0.5021	1495.3	0.9679
30	0.0131	5081	0.8839	0.4726	1544	0.9578
40	0.015	4209	0.94	0.5295	1116.4	0.9913
50	0.015	3922	0.95	0.5357	1026	0.9947
60	0.016	3405	0.973	0.5631	836.43	0.9996

Table 5.10 Finding of parameters in Eq. (3.9) and Eq. (3.10) for various concentrations of mulberry molasses at the different temperatures

	Exponential Model Eq. (3.9)			Power Model Eq. (3.10)		
Temperature °C	b_1	Kc_1	R^2	b_2	Kc_2	R^2
25	0.0081	6418.2	0.9549	0.267	3354.1	0.8714
30	0.0091	5567.9	0.9534	0.3013	2678.6	0.8679
40	0.011	4580	0.995	0.369	1849.4	0.9493
50	0.0141	3604	0.9937	0.4776	1114.5	0.9528
60	0.0151	3159	0.9604	0.504	923.18	0.8922

Table 5.11 Finding of parameters in Eq. (3.9) and Eq. (3.10) for various concentrations of grape molasses at the different temperatures

	Exponential Model Eq. (3.9)			Power Model Eq. (3.10)		
Temperature °C	b_1	Kc_1	R^2	b_2	Kc_2	R^2
25	0.0192	1508.1	0.9578	0.6746	280.36	0.986
30	0.0254	1057.3	0.9734	0.8928	114.23	0.9988
40	0.0294	812.59	0.9371	1.0458	59.124	0.987
50	0.033	656.72	0.9396	1.1679	35.238	0.9873
60	0.035	557.1	0.9285	1.2524	24.066	0.9837

Table 5.12 Finding of parameters in Eq. (3.9) and Eq. (3.10) for various concentrations of carob molasses at the different temperatures

	Exponential Model Eq. (3.9)			Power Model Eq. (3.10)		
Temperature °C	b_1	Kc_1	R^2	b_2	Kc_2	R^2
25	0.0333	2823	0.9831	1.134	173.66	0.9474
30	0.0342	2455	0.9625	1.1667	139.17	0.9286
40	0.0347	2187	0.99	1.1848	118.38	0.9576
50	0.0378	1715.3	0.9854	1.2944	70.63	0.9581
60	0.042	1375.2	0.9794	1.4351	39.631	0.9653

The interrelationship coefficients of the models appeared to describe the relationship between consistency coefficient and concentration for each model successfully. For each model, the analysis of the empirical constants uncovers that the impact of molasses concentration on the consistency coefficient is more pronounced at minimum temperatures. This can be clarified by an increase in viscosity; hence, the consistency coefficients of the mix increase with increasing molasses concentration and decrease with diminishing temperature (see Figures 5.41, 5.42, 5.43, and 5.44).

Alparslan & Hayta (2002) stated that an increase in molasses concentration causes to an increase in viscosity (higher K values) and an increase in temperature causes a decrease in the consistency coefficient. The results obtained in present study agree with this observation. An increase in the viscosity of the fluid can be achieved with increasing solid contents since higher solid contents cause more internal interaction and molecular movements and thus, intermolecular forces hinder molecular movement over one another (Sopade & Filibus, 1995; Toğrul & Arslan, 2003). However, it has been reported that the increasing sugar content reduces the viscosity; this refers to the physicochemical characteristic of sugar in relation with water (Habibi et al., 2006).

5.3.1. Sensitivity of Activation Energy to Concentration (Ea)

The variation of activation energy with molasses concentration was modeled by utilizing Eq. (3.13) and Eq. (3.14). The linearized forms of the exponential function (Eq. (3.13) and power function (Eq. (3.14)) were utilized to determine the constants given in Table 5.13.

Table 5.13 Determining of parameters in Eq. (3.13) and Eq. (3.14) for various concentrations of each molasses

Exponential Model Eq.(3.13)			Power Model Eq.(3.14)			
	A1	d1	R^2	A2	d2	R^2
date	1503	-0.023	0.9942	101997	-0.776	0.9719
mulberry	19268	-0.017	0.9595	80857	-0.584	0.9175
grape	33428	-0.039	0.9624	100000	-1.361	0.9975
carob	18901	-0.02	0.9557	106737	-0.693	0.9929

As can be seen in Table 5.13, while the exponential model is more appropriate for the blends of date and mulberry molasses, the power model is more suitable for the blends of grape and carob molasses.

5.4. Combined Effects of Temperature, Concentration, and Shear Rate on Flow Behavior

A single equation which can be implemented for various parameters is a very important tool for engineering application. Thereby multiple linear regression of Eq. (3.11) with Eq. (3.12) is used to determine the combined effect of temperature, molasses concentration and shear rate on the apparent viscosity of molasses/sesame paste. The linear regression of Eq. (3.11) with Eq. (3.12) determines variable coefficients, standard error estimations tabulated in Tables C.1 to C.8.

Values of coefficients given in Tables C.1 to C.2 show that both models (Eq. (3.11) and Eq. (3.12)) are convenient for the date molasses. However, Eq. (3.12) is much more appropriate than Eq. (3.11) since Eq. (3.12) has a high quality of fit (R^2 = 0.969445), so it can be approved for a use as a single model for date molasses.

$$\mu_a = 40.74135 \exp\left[\, 960.9952 \left(\frac{1}{T}\right)\right] . C^{0.606021} . \dot{\gamma}^{-0.41826} \qquad (5.4)$$

Values of coefficients given in Tables C.3 to C.4 indicate that both models (Eq. (3.11) and Eq. (3.12)) are convenient for the mulberry molasses. However, Eq. (3.11) is much more

appropriate than Eq. (3.12) since Eq. (3.11) has a high quality of fit (R^2 = 0.974849), so it can be approved for a use as a single model for mulberry molasses.

$$\mu_a = 66.34463 \ \exp\left[1320.318\left(\frac{1}{T}\right) + 0.011674C\right].\gamma^{-0.31125} \tag{5.5}$$

Values of coefficients given in Tables C.5 to C.6 indicate that both models (Eq. (3.11) and Eq. (3.12)) are convenient for the grape molasses. However, Eq. (3.12) is much more appropriate than Eq. (3.11) since Eq. (3.12) has a high quality of fit (R^2 = 0.968149), so it can be approved for a use as a single model for grape molasses.

$$\mu_a = 0.793932 \exp\left[1533.303\ \left(\frac{1}{T}\right)\right].C^{0.888077}.\dot{\gamma}^{-0.53582} \tag{5.6}$$

Similarly, values of coefficients given in Tables C.7 to C.8 indicate that both models (Eq. (3.11) and Eq. (3.12)) are convenient for the carob molasses. However, Eq. (3.11) is much more appropriate than Eq. (3.12) since Eq. (3.11) has a high quality of fit (R^2 = 0.974528), so it can be approved for a use as a single model for carob molasses.

$$\mu_a = 21.89981 \exp\left[\ 1419.017\ \left(\frac{1}{T}\right).0.036663\ C\right].\dot{\gamma}^{-0.4837} \tag{5.7}$$

6. CONCLUSIONS AND RECOMMENDATIONS

In this thesis the flow behavior of some molasses/sesame paste mixtures at four different molasses concentrations (20-55 %) and various temperatures in range of 25-60 °C were investigated at various shear rates in ranges of 25-30 s^{-1}.

This study concludes that the apparent viscosity of the mixture of some molasses/sesame pastes gains a higher value with increasing molasses concentration and reducing temperature. The power-law model can be successfully used to express the relationship between apparent viscosity and shear rate of the mixtures. In addition, the all blends considered here exhibit non- Newtonian, shear thinning behavior.

The model parameters such as the flow behavior index and the consistency coefficient are strongly dependent on temperature. The relationship between flow behavior index and temperature are not able to formalize; however, the Arrhenius–type equation has a good interpretation of the relation between the temperature and the consistency coefficient. The impact of molasses concentration on consistency coefficient is quite large. It appears that both exponential and power functions can be utilized to describe the relationship.

Finally, in the present study four model equations were proposed to describe the combined effect of temperature, molasses concentration and shear rate on the apparent viscosity of the mixture. It was observed that the model equations are quite appropriate to define relationship among the concentration of each type of molasses (date, mulberry, grape, and carob), shear rate and temperature.

It is concluded that the obtained experimental data suggested that the model equations can be used in quality control, sensory evaluation of the product, process control applications and in designing equipment for the mixtures. Moreover, analysis can be performed considering the mixtures stability, textural attributes, sensory analysis and shelf life in order to satisfy the end users.

REFERENCES

Abu-Jdayil, B., 2003. Modelling the time-dependent rheological behavior of semisolid foodstuffs. Journal of food engineering, **57**(1), 97-102.

Ahmed, J., 2004. Rheological behaviour and colour changes of ginger paste during storage. International journal of food science & technology, **39**(3), 325-330.

Akbulut, M., Saricoban, C., & Ozcan, M. M., 2012. Determination of rheological behavior, emulsion stability, color, and sensory of sesame pastes (tahin) blended with pine honey. Food and Bioprocess Technology, **5**(5), 1832-1839.

Akbulut, M., & Bilgicli, N., 2010. Effects of different pekmez (fruit molasses) types used as a natural sugar source on the batter rheology and physical properties of cakes. Journal of food process engineering, **33**(2), 272-286.

Akbulut, M., Çoklar, H., & Özen, G., 2008. Rheological characteristics of Juniperus drupacea fruit juice (pekmez) concentrated by boiling. Food Science and Technology International, **14**(4), 321-328.

Akbulut, M., & Özcan, M. M., 2008. Some physical, chemical, and rheological properties of sweet sorghum (Sorghum Bicolor (L) Moench) Pekmez (Molasses). International Journal of Food Properties, **11**(1), 79-91.

Alpaslan, M., & Hayta, M., 2002. Rheological and sensory properties of pekmez (grape molasses)/tahin (sesame paste) blends. Journal of Food Engineering, **54**(1), 89-93.

Arslan, E., Yener, M. E., & Esin, A., 2005. Rheological characterization of tahin/pekmez (sesame paste/concentrated grape juice) blends. Journal of Food Engineering, **69**(2), 167-172.

Barnes, H. A., Hutton, J. F., & Walters, K., 1989. An introduction to rheology (Vol. 3). Elsevier.

Basiri, S., 2016. Influence of processing parameters on physicochemical properties of Iranian mulberry (Morusalba L.) molasses. Agricultural Engineering International: CIGR Journal, **18**(2), 201-208.

Batu, A., 2005. Production of liquid and white solid pekmez in Turkey. Journal of Food Quality, **28**(5-6), 417-427.

Bayod, E., Willers, E. P., & Tornberg, E., 2008. Rheological and structural characterization of tomato paste and its influence on the quality of ketchup. LWT-Food Science and Technology, **41**(7), 1289-1300.

Çiftçi, D., Kahyaoglu, T., Kapucu, S., & Kaya, S., 2008. Colloidal stability and rheological properties of sesame paste. Journal of Food Engineering, **87**(3), 428-435.

Day, L., Xu, M., Lundin, L., & Wooster, T. J., 2009. Interfacial properties of deamidated wheat protein in relation to its ability to stabilise oil-in-water emulsions. Food Hydrocolloids, **23**(8), 2158-2167.

Fung, Y. C., 1982. Rheological Techniques. Journal of Biomechanical Engineering, **104**(1), 73.

Geankoplis, C. J., 1993. Transport Processes and Unit Operations. Prentice-Hall. New Jersey, USA.

Gharehyakheh, S., Amiri, M., & Savareh, S. J., 2014. Rheological behavior of sesame paste/honey blend with different concentration of honey. European Journal of Experimental Biology, **4**(1), 53-57.

Goksel, M., Dogan, M., Toker, O. S., Ozgen, S., Sarioglu, K., & Oral, R. A., 2013. The effect of starch concentration and temperature on grape molasses: rheological and textural properties. Food and Bioprocess Technology, **6**(1), 259-271.

Habibi-Najafi, M. B., & Alaei, Z., 2006. Rheological properties of date syrup/sesame paste blend. World Journal of Dairy & Food Sciences, **1**(1), 1-5.

Hatamikia, M., Sani, A. M., & Zomorodi S., 2013. Effect of different clarifying agents on the sensory and rheological properties of grape juice concentrate. Indian Journal, **9**(3), 107-111 (Vol. 9).

Heldman, L. & S., 2006. Handbook of Food Engineering, Second Edition. Crc Press.

Işıklı, N. D., & Karababa, E., 2005. Rheological characterization of fenugreek paste (çemen). Journal of Food Engineering, **69**(2), 185-190.

Jannat, B., Oveisi, M.R., Sadeghi, N., Hajimahmoodi, M., Behzad, M., Choopankari, E., & Behfar, A.A., 2010. Effects of roasting temperature and time on healthy nutraceuticals of antioxidants and total phenolic content in Iranian sesame seeds (Sesamum indicum L.). Iranian Journal of Environmental Health Science & Engineering, **7**(1), 97.

Jin, B., & Cedrola, E. (Eds.)., 2017. Product Innovation in the Global Fashion Industry. Springer.

Karaman, S., & Kayacier, A., 2011. Effect of temperature on rheological characteristics of molasses: Modeling of apparent viscosity using Adaptive Neuro–Fuzzy Inference System (ANFIS). LWT-Food Science and Technology, **44**(8), 1717-1725.

Kaya, A., & Belibağlı, K. B., 2002. Rheology of solid gazıantep pekmez. Journal of Food Engineering, **54**(3), 221-226.

Lokumcu Altay, F., & Ak, M. M., 2005. Effects of temperature, shear rate and constituents on rheological properties of tahin (sesame paste). Journal of the Science of Food and Agriculture, **85**(1), 105-111.

Mohamed, I. O., & Hassan, E., 2016. Time-dependent and time-independent rheological characterization of date syrup. Journal of Food Research, **5**(2), 13.

Morris, J. B., 2002. Food, industrial, nutraceutical, and pharmaceutical uses of sesame genetic resources. Trends in New Crops and New Uses, 153-156.

Muresan, V., Danthine, S., Racolta, E., Muste, S., & Blecker, C., 2014. The influence of particle size distribution on sunflower tahini rheology and structure. Journal of Food Process Engineering, **37**(4), 411-426.

Özkal, S. G., & Süren, F., 2017. Rheological properties of poppy seed paste/grape pekmez blends. Journal of Food Processing and Preservation, **41**(6).

Öztürk, B. A., & Öner, M. D., 1999. Production and evaluation of yogurt with concentrated grape juice. Journal of Food Science, **64**(3), 530-532.

Ramadan, B. R., 1998, March. Preparation and evaluation of Egyptian date syrup. In First international conference on date palm. Al-Ain (pp. 8-10).

Rao, M. A., 2013. Rheology of fluid, semisolid, and solid foods: principles and applications. Springer Science & Business Media.

Razavi, S. M., Najafi, M. B. H., & Alaee, Z., 2007. The time independent rheological properties of low fat sesame paste/date syrup blends as a function of fat substitutes and temperature. Food Hydrocolloids, **21**(2), 198-202.

Razavi, S. M. A., Najafi, M. H., & Alaee, Z., 2008. Rheological characterization of low fat sesame paste blended with date syrup. International Journal of Food Properties, **11**(1), 92-101.

Sanchez, M. C., Valencia, C., Gallegos, C., Ciruelos, A., & Latorre, A., 2002. Influence of processing on the rheological properties of tomato paste. Journal of the Science of Food and Agriculture, **82**(9), 990-997.

Sengül, M., Ertugay, M. F., & Sengül, M., 2005. Rheological, physical and chemical characteristics of mulberry pekmez. Food Control, **16**(1), 73-76.

Sengül, M., Fatih Ertugay, M., Sengül, M., & Yüksel, Y., 2007. Rheological characteristics of carob pekmez. International Journal of Food Properties, **10**(1), 39-46.

Steffe, J. F., 1996. Rheological methods in food process engineering. Freeman press.

Tounsi, L., Karra, S., Kechaou, H., & Kechaou, N., 2017. Processing, physico-chemical and functional properties of carob molasses and powders. Journal of Food Measurement and Characterization, **11**(3), 1440-1448.

Van Wazer, J. R., Lyons, J.W., 1966. Viscosity and Flow Measurement. John Wiley & Sons, Inc., USA.

Vinet, L., & Zhedanov, A., 2011. A 'missing'family of classical orthogonal polynomials. Journal of Physics A: Mathematical and Theoretical, **44**(8), 085201.

Yoğurtçu, H., & Kamışlı, F., 2006. Determination of rheological properties of some pekmez samples in Turkey. Journal of Food Engineering, **77**(4), 1064-1068.

CURRICULUM VITAE

Dlshad Abdalla Mohammed was born in 1980 at Al Sulaymaneyah, Iraq. He completed bachelor's degree in Chemical Engineering at Koya University in 2006-2010. He has been working at Petroleum Refinery from 2010 until date, currently as an Operation Engineer. He has been a Master Student in Department of Chemical Engineering at Firat University. He is married with two daughters.

APPENDICES

APPENDIX A

Experimental Data

Table A.1 Experimental data of shear rate (γ), shear stress (τ) and apparent viscosity (μa) for 20 % date molasses concentrations at the different temperatures (25-60 °C)

C (%date)	T (°C)	Ω (rpm)	γ̇(1/s)	τ x 10^{-2} (mPa)	μa(mPa.s)
20%	25	2.5	0.7	5.6	8000
		5	1.4	7.84	5600
		10	2.8	11.9	4250
		20	5.6	19.04	3400
		30	8.4	27.76	3067
	30	2.5	0.7	5.1	7400
		5	1.4	7.14	5300
		10	2.8	10.36	3800
		20	5.6	16.38	3000
		30	8.4	21.84	2650
	40	2.5	0.7	4.48	6400
		5	1.4	6.16	4500
		10	2.8	8.96	3300
		20	5.6	13.86	2500
		30	8.4	18.34	2200
	50	2.5	0.7	4.2	6000
		5	1.4	5.72	4350
		10	2.8	8.26	3000
		20	5.6	12.18	2200
		30	8.4	15.96	2000
	60	2.5	0.7	3.78	5400
		5	1.4	5.04	3600
		10	2.8	7.28	2600
		20	5.6	10.92	1900
		30	8.4	14.14	1700

Table A.2 Experimental data of shear rate (γ), shear stress (τ) and apparent viscosity (μa) for 30 % date molasses concentrations at different temperatures (25-60 °C)

C (%date)	T (°C)	Ω (rpm)	γ̇(1/s)	τ x 10^{-2} (mPa)	μa(mPa.s)
30%	25	2.5	0.7	7	10000
		5	1.4	9.52	6800
		10	2.8	13.3	4750
		20	5.6	19.88	3600
		30	8.4	25.76	3200
	30	2.5	0.7	5.04	9000
		5	1.4	7.42	6600
		10	2.8	12.04	4300
		20	5.6	18.48	3300
		30	8.4	23.94	2900
	40	2.5	0.7	6.3	8000
		5	1.4	9.24	5900
		10	2.8	14	4100
		20	5.6	21	3150
		30	8.4	26.5	2500
	50	2.5	0.7	8.82	7500
		5	1.4	12.74	5450
		10	2.8	16.24	3800
		20	5.6	21.56	2800
		30	8.4	25.76	2400
	60	2.5	0.7	7.28	6500
		5	1.4	10.36	5200
		10	2.8	15.68	3600
		20	5.6	23.66	2400
		30	8.4	28.28	2100

Table A.3 Experimental data of shear rate (γ), shear stress (τ) and apparent viscosity (μa) for 40% date molasses concentrations at the different temperatures (25-60 °C)

C (%date)	T (°C)	Ω (rpm)	γ̇(1/s)	τ x 10^{-2} (mPa)	μa(mPa.s)
40%	25	2.5	0.7	11.34	11000
		5	1.4	20.02	8350
		10	2.8	30.94	6980
		20	5.6	47.32	5300
		30	8.4	59.5	4200
	30	2.5	0.7	11.2	10800
		5	1.4	19.46	8180
		10	2.8	29.54	6500
		20	5.6	58.1	5100
		30	8.4	78.4	3950
	40	2.5	0.7	7	10000
		5	1.4	11.34	7560
		10	2.8	19.46	5900
		20	5.6	30.8	4500
		30	8.4	37.94	3700
	50	2.5	0.7	4.9	9500
		5	1.4	9.1	6830
		10	2.8	15.4	5100
		20	5.6	22.82	4150
		30	8.4	30	3350
	60	2.5	0.7	3.92	8900
		5	1.4	6.58	6650
		10	2.8	12.6	5000
		20	5.6	17.78	3900
		30	8.4	25.06	3200

Table A.4 Experimental data of shear rate (γ), shear stress (τ) and apparent viscosity (μa) for 55 % date molasses concentrations at the different temperatures (25-60 °C)

C (%date)	T (°C)	Ω (rpm)	γ̇(1/s)	τ x 10^{-2} (mPa)	μa(mPa.s)
55%	25	2.5	0.7	5.32	11500
		5	1.4	8.54	8600
		10	2.8	14	7000
		20	5.6	22.96	5600
		30	8.4	30.8	4500
	30	2.5	0.7	6.72	11000
		5	1.4	9.52	8420
		10	2.8	14.14	6850
		20	5.6	21.7	5500
		30	8.4	30.38	4300
	40	2.5	0.7	9.38	10500
		5	1.4	13.86	7950
		10	2.8	18.9	6500
		20	5.6	25.06	5100
		30	8.4	32.6	3990
	50	2.5	0.7	13.44	9900
		5	1.4	21.7	7600
		10	2.8	34.3	6200
		20	5.6	58.52	4800
		30	8.4	70.7	3500
	60	2.5	0.7	12.74	9600
		5	1.4	17.92	7000
		10	2.8	30.8	5500
		20	5.6	40.74	4100
		30	8.4	40.18	3200

Table A.5 Experimental data of shear rate (γ), shear stress (τ) and apparent viscosity (μa) for 20 % mulberry molasses concentrations at the different temperatures (25-60 °C)

C (%mulberry)	T (°C)	Ω (rpm)	γ̇(1/s)	τ x 10^{-2} (mPa)	μa(mPa.s)
20%	25	2.5	0.7	6.02	8600
		5	1.4	9.87	7050
		10	2.8	15.54	5550
		20	5.6	25.2	4500
		30	8.4	34.44	4100
	30	2.5	0.7	5.32	7600
		5	1.4	8.68	6200
		10	2.8	14.42	5150
		20	5.6	21.84	3900
		30	8.4	30.24	3600
	40	2.5	0.7	4.48	6400
		5	1.4	7.28	5200
		10	2.8	11.48	4100
		20	5.6	20.16	3600
		30	8.4	23.94	2850
	50	2.5	0.7	3.99	5700
		5	1.4	5.88	4200
		10	2.8	8.96	3200
		20	5.6	15.96	2850
		30	8.4	21.84	2600
	60	2.5	0.7	3.64	5200
		5	1.4	5.32	3800
		10	2.8	8.68	3100
		20	5.6	14.56	2600
		30	8.4	19.32	2300

Table A.6 Experimental data of shear rate (γ), shear stress (τ) and apparent viscosity (μa) for 30 % mulberry molasses concentrations at the different temperatures (25-60 °C)

C (%mulberry)	T (°C)	Ω (rpm)	γ̇(1/s)	τ x 10^{-2} (mPa)	μa(mPa.s)
30%	25	2.5	0.7	6.3	9000
		5	1.4	10	7140
		10	2.8	16.94	6050
		20	5.6	26.88	4800
		30	8.4	35.28	4200
	30	2.5	0.7	5.74	8200
		5	1.4	8.82	6300
		10	2.8	14	5000
		20	5.6	25.2	4500
		30	8.4	30.24	3600
	40	2.5	0.7	5.04	7200
		5	1.4	7.99	5710
		10	2.8	12.04	4300
		20	5.6	21.28	3800
		30	8.4	27.72	3300
	50	2.5	0.7	4.62	6600
		5	1.4	6.53	4660
		10	2.8	10.64	3800
		20	5.6	17.36	3100
		30	8.4	24.78	2950
	60	2.5	0.7	3.78	5400
		5	1.4	5.74	4100
		10	2.8	8.96	3200
		20	5.6	14.56	2600
		30	8.4	20.16	2400

Table A.7 Experimental data of shear rate (γ), shear stress (τ) and apparent viscosity (μa) for 40 % mulberry molasses concentrations at the different temperatures (25-60 °C)

C (%mulberry)	T (°C)	Ω (rpm)	γ̇(1/s)	τ x 10^{-2} (mPa)	μa(mPa.s)
40%	25	2.5	0.7	7	10000
		5	1.4	10.22	7300
		10	2.8	17.36	6200
		20	5.6	30.24	5400
		30	8.4	37.38	4450
	30	2.5	0.7	6.37	9100
		5	1.4	9.17	6550
		10	2.8	15.68	5600
		20	5.6	25.48	4550
		30	8.4	33.6	4000
	40	2.5	0.7	5.67	8100
		5	1.4	8.4	6000
		10	2.8	14	5000
		20	5.6	22.4	4000
		30	8.4	30.24	3600
	50	2.5	0.7	5	7150
		5	1.4	7.39	5280
		10	2.8	12.32	4400
		20	5.6	20.44	3650
		30	8.4	26.04	3100
	60	2.5	0.7	4.55	6500
		5	1.4	7.19	5135
		10	2.8	12.04	4300
		20	5.6	17.36	3100
		30	8.4	24.78	2950

Table A.8 Experimental data of shear rate (γ), shear stress (τ) and apparent viscosity (μa) for 55 % mulberry molasses concentrations at the different temperatures (25-60 °C)

C (%mulberry)	T (°C)	Ω (rpm)	γ(1/s)	τ x 10^{-2} (mPa)	μa(mPa.s)
55%	25	2.5	0.7	7.98	11400
		5	1.4	12.94	9243
		10	2.8	20.72	7400
		20	5.6	34.16	6100
		30	8.4	45.36	5400
	30	2.5	0.7	7.35	10500
		5	1.4	11.8	8432
		10	2.8	19.32	6900
		20	5.6	31.64	5650
		30	8.4	41.25	4910
	40	2.5	0.7	6.65	9500
		5	1.4	10.46	7474
		10	2.8	17.22	6150
		20	5.6	28	5000
		30	8.4	37.38	4450
	50	2.5	0.7	6.23	8900
		5	1.4	9.85	7035
		10	2.8	16.24	5800
		20	5.6	26.32	4700
		30	8.4	35.11	4180
	60	2.5	0.7	5.81	8300
		5	1.4	9.12	6511
		10	2.8	14.98	5350
		20	5.6	24.64	4400
		30	8.4	32.05	3815

Table A.9 Experimental data of shear rate (γ), shear stress (τ) and apparent viscosity (μa) for 20 % grape molasses concentrations at the different temperatures (25-60 °C)

C (%grape)	T (°C)	Ω (rpm)	γ̇(1/s)	τ x 10^{-2} (mPa)	μa(mPa.s)
20%	25	2.5	0.7	1.82	2600
		5	1.4	2.38	1700
		10	2.8	3.64	1300
		20	5.6	6.02	1050
		30	8.4	7.98	950
	30	2.5	0.7	1.4	2000
		5	1.4	1.96	1400
		10	2.8	2.8	1000
		20	5.6	4.48	800
		30	8.4	5.88	700
	40	2.5	0.7	1.12	1600
		5	1.4	1.54	1100
		10	2.8	2.1	750
		20	5.6	3.36	600
		30	8.4	4.34	516.7
	50	2.5	0.7	0.98	1400
		5	1.4	1.26	900
		10	2.8	1.82	650
		20	5.6	2.66	475
		30	8.4	3.5	416.7
	60	2.5	0.7	0.84	1200
		5	1.4	1.12	800
		10	2.8	1.54	550
		20	5.6	2.38	425
		30	8.4	2.94	350

Table A.10 Experimental data of shear rate (γ), shear stress (τ) and apparent viscosity (μa) for 30 % grape molasses concentrations at the different temperatures (25-60 °C)

C (%grape)	T (°C)	Ω (rpm)	γ̇(1/s)	τ x 10^{-2} (mPa)	μa(mPa.s)
30%	25	2.5	0.7	2.52	3600
		5	1.4	3.36	2400
		10	2.8	4.76	1700
		20	5.6	7.42	1275
		30	8.4	9.24	1100
	30	2.5	0.7	2.1	3000
		5	1.4	2.8	2000
		10	2.8	3.92	1400
		20	5.6	5.74	1025
		30	8.4	7.42	883.3
	40	2.5	0.7	1.96	2800
		5	1.4	2.52	1800
		10	2.8	3.5	1250
		20	5.6	4.9	875
		30	8.4	6.02	716.7
	50	2.5	0.7	1.82	2600
		5	1.4	2.24	1600
		10	2.8	3.08	1100
		20	5.6	4.2	750
		30	8.4	5.04	600
	60	2.5	0.7	1.68	2400
		5	1.4	2.1	1500
		10	2.8	2.66	950
		20	5.6	3.64	650
		30	8.4	4.2	500

Table A.11 Experimental data of shear rate (γ), shear stress (τ) and apparent viscosity (μa) for 40 % grape molasses concentrations at the different temperatures (25-60 °C)

C (%grape)	T (°C)	Ω (rpm)	γ(1/s)	τ x 10^{-2} (mPa)	μa(mPa.s)
40%	25	2.5	0.7	2.8	4000
		5	1.4	3.78	2700
		10	2.8	5.32	1900
		20	5.6	7.84	1400
		30	8.4	9.94	1183
	30	2.5	0.7	2.66	3800
		5	1.4	3.5	2500
		10	2.8	4.62	1650
		20	5.6	6.72	1200
		30	8.4	8.4	1000
	40	2.5	0.7	2.52	3600
		5	1.4	3.08	2200
		10	2.8	4.06	1450
		20	5.6	5.74	1025
		30	8.4	7	833.3
	50	2.5	0.7	2.38	3400
		5	1.4	3.08	2000
		10	2.8	3.64	1300
		20	5.6	5.04	900
		30	8.4	6.02	716.7
	60	2.5	0.7	2.24	3200
		5	1.4	2.66	1900
		10	2.8	3.36	1200
		20	5.6	4.34	775
		30	8.4	5.04	600

Table A.12 Experimental data of shear rate (γ), shear stress (τ) and apparent viscosity (μa) for 55 % grape molasses concentrations at the different temperatures (25-60 °C)

C (%grape)	T (°C)	Ω (rpm)	γ̇(1/s)	τx10^{-2} (mPa)	μa(mPa.s)
55%	25	2.5	0.7	3.5	5000
		5	1.4	5.23	3735
		10	2.8	7	2500
		20	5.6	10.64	1900
		30	8.4	11.76	1400
	30	2.5	0.7	3.4	4850
		5	1.4	4.97	3550
		10	2.8	6.58	2350
		20	5.6	8.96	1600
		30	8.4	10.92	1300
	40	2.5	0.7	3.15	4500
		5	1.4	4.6	3285
		10	2.8	6.16	2200
		20	5.6	8.4	1500
		30	8.4	10.08	1200
	50	2.5	0.7	3.12	4450
		5	1.4	4.41	3150
		10	2.8	5.6	2000
		20	5.6	7.28	1300
		30	8.4	8.32	990
	60	2.5	0.7	2.94	4200
		5	1.4	4.22	3050
		10	2.8	5.04	1800
		20	5.6	5.6	1000
		30	8.4	7.56	900

Table A.13 Experimental data of shear rate (γ), shear stress (τ) and apparent viscosity (μa) for 20 % carob molasses concentrations at the different temperatures (25-60 °C)

C (%date)	T (°C)	Ω (rpm)	γ̇(1/s)	τx10^{-2} (mPa)	μa(mPa.s)
20%	25	2.5	0.7	4.76	6800
		5	1.4	6.68	4900
		10	2.8	10.08	3600
		20	5.6	15.54	2775
		30	8.4	20.3	2417
	30	2.5	0.7	4.48	6400
		5	1.4	5.88	4200
		10	2.8	8.4	3000
		20	5.6	12.74	2275
		30	8.4	16.8	2000
	40	2.5	0.7	4.06	5800
		5	1.4	5.04	3600
		10	2.8	6.68	2450
		20	5.6	9.94	1775
		30	8.4	12.6	1500
	50	2.5	0.7	3.36	4800
		5	1.4	4.2	3000
		10	2.8	5.74	2050
		20	5.6	8.12	1450
		30	8.4	10.08	1200
	60	2.5	0.7	2.8	4000
		5	1.4	3.64	2600
		10	2.8	4.9	1750
		20	5.6	6.86	1225
		30	8.4	8.4	1000

Table A.14 Experimental data of shear rate (γ), shear stress (τ) and apparent viscosity (μa) for 30 % carob molasses concentrations at the different temperatures (25-60 °C)

C (%date)	T (°C)	Ω (rpm)	γ̇(1/s)	τx10^{-2} (mPa)	μa(mPa.s)
30%	25	2.5	0.7	5.6	8000
		5	1.4	8.56	6110
		10	2.8	13.44	4800
		20	5.6	19.04	3400
		30	8.4	25.2	3000
	30	2.5	0.7	5.32	7600
		5	1.4	7	5000
		10	2.8	9.52	3400
		20	5.6	15.51	2770
		30	8.4	21.42	2550
	40	2.5	0.7	5.18	7400
		5	1.4	6.44	4600
		10	2.8	9.1	3250
		20	5.6	13.02	2325
		30	8.4	16.64	2100
	50	2.5	0.7	4.34	6200
		5	1.4	5.46	3900
		10	2.8	7.84	2800
		20	5.6	11.2	2000
		30	8.4	14.28	1700
	60	2.5	0.7	3.64	5200
		5	1.4	5.18	3700
		10	2.8	7.42	2650
		20	5.6	10.08	1800
		30	8.4	11.76	1400

Table A.15 Experimental data of shear rate (γ), shear stress (τ) and apparent viscosity (μa) for 40 % carob molasses concentrations at the different temperatures (25-60 °C)

C (%carob)	T (°C)	Ω (rpm)	γ̇(1/s)	τx10^{-2} (mPa)	μa(mPa.s)
40%	25	2.5	0.7	9.17	13100
		5	1.4	13.72	9800
		10	2.8	19.88	7100
		20	5.6	29.68	5300
		30	8.4	35.28	4200
	30	2.5	0.7	8.4	12000
		5	1.4	13.3	9500
		10	2.8	19.6	7000
		20	5.6	28	5000
		30	8.4	33.6	4000
	40	2.5	0.7	7.7	11000
		5	1.4	11.06	7900
		10	2.8	15.96	5700
		20	5.6	22.4	4000
		30	8.4	32.76	3900
	50	2.5	0.7	7.07	10100
		5	1.4	9.94	7100
		10	2.8	14.28	5100
		20	5.6	20.16	3600
		30	8.4	26.88	3200
	60	2.5	0.7	6.93	9900
		5	1.4	9.8	7000
		10	2.8	13.72	4900
		20	5.6	19.88	3550
		30	8.4	26.25	3125

Table A.16 Experimental data of shear rate (γ), shear stress (τ) and apparent viscosity (μa) for 55 % carob molasses concentrations at the different temperatures (25-60 °C)

C (%carob)	T (°C)	Ω (rpm)	γ(1/s)	$\tau x10^{-2}$ (mPa)	μa(mPa.s)
55%	25	2.5	0.7	14.98	21400
		5	1.4	21	15000
		10	2.8	28	10000
		20	5.6	44.8	8000
		30	8.4	58.8	7000
	30	2.5	0.7	13.3	19000
		5	1.4	18.2	13000
		10	2.8	27.16	9700
		20	5.6	42	7500
		30	8.4	46.2	5500
	40	2.5	0.7	11.9	17000
		5	1.4	17.5	12500
		10	2.8	25.76	9200
		20	5.6	39.2	7000
		30	8.4	42	5000
	50	2.5	0.7	11.2	16000
		5	1.4	15.4	11000
		10	2.8	22.96	8200
		20	5.6	33.6	6000
		30	8.4	33.6	4000
	60	2.5	0.7	10.92	15600
		5	1.4	14.84	10600
		10	2.8	21.84	7800
		20	5.6	28.56	5100
		30	8.4	32.76	3900

Table A.17 Experimental data of shear rate (γ), shear stress (τ) and apparent viscosity (μa) for pure date molasses concentrations at the different temperatures (30-50 °C)

T (°C)	Ω (rpm)	γ̇(1/s)	τx10^{-2} (mPa)	μa(mPa.s)
30	1	0.93	1.02	1150
	2.5	2.33	1.95	860
	5	4.65	3.44	730
	10	9.3	6.32	690
	20	18.6	12	647.5
	30	27.9	17.44	625
40	1	0.93	1.44	1400
	2.5	2.33	3.8	760
	5	4.65	2.7	580
	10	9.3	4.93	525
	20	18.6	9.53	510
	30	27.9	15.21	541.7
50	1	0.93	0.84	850
	2.5	2.33	1.16	520
	5	4.65	2	430
	10	9.3	3.72	400
	20	18.6	6.93	370
	30	27.9	9.95	358.3

Table A.18 experimental data of shear rate (γ), shear stress (τ) and apparent viscosity (μa) for pure mulberry molasses concentrations at the different temperatures (25-60 °C)

T (°C)	Ω (rpm)	γ̇(1/s)	τx10^{-2} (mPa)	μa(mPa.s)
25	2.5	0.7	12.74	18000
	5	1.4	20.16	14400
	10	2.8	35.42	12650
	20	5.6	64.26	11475
	30	8.4	91.56	10900
30	2.5	0.7	8.54	12200
	5	1.4	12.04	8600
	10	2.8	18.76	6700
	20	5.6	31.92	5700
	30	8.4	45.08	5350
40	2.5	0.7	6.72	9600
	5	1.4	8.12	5800
	10	2.8	11.06	3950
	20	5.6	16.38	2925
	30	8.4	21.56	2567
50	2.5	0.7	6.16	8400
	5	1.4	6.44	4600
	10	2.8	7.84	2800
	20	5.6	10.22	1825
	30	8.4	12.6	1500
60	2.5	0.7	5.18	7400
	5	1.4	5.6	4000
	10	2.8	6.16	2200
	20	5.6	7.5	1350
	30	8.4	8.82	1050

Table A.19 Experimental data of shear rate (γ), shear stress (τ) and apparent viscosity (μa) for pure grape molasses concentrations at the different temperatures (30-50°C)

T (°C)	Ω (rpm)	γ̇(1/s)	τx10^{-2} (mPa)	μa(mPa.s)
30	10	2.8	0.14	50
	12	3.36	0.28	83.33
	20	5.6	0.84	150
	30	8.4	1.4	166.2
	50	14	2.52	180
40	20	5.6	0.14	25
	30	8.4	0.42	50
	50	14	0.98	70
	60	16.8	1.26	75
	100	28	2.24	80
50	50	14	0.28	20
	60	16.8	0.56	33.33
	100	28	0.84	30

Table A.20 Experimental data of shear rate (γ), shear stress (τ) and apparent viscosity (μa) for pure carob molasses concentrations at the different temperatures (25-60 °C)

T (°C)	Ω (rpm)	γ̇(1/s)	τx10^{-2} (mPa)	μa(mPa.s)
25	2.5	0.7	21.56	31000
	4	1.12	34.44	3075
	6	1.68	50.83	30250
	10	2.8	83.44	29800
	12	3.36	99.68	29667
30	2.5	0.7	9.24	13200
	6	1.68	19.04	11333
	10	2.8	31.22	11150
	20	5.6	61.32	10975
	30	8.4	91.56	10900
40	2.5	0.7	3.5	5000
	6	1.68	6.72	4000
	10	2.8	11.2	4000
	20	5.6	22.54	4025
	30	8.4	33.88	4033
50	2.5	0.7	1.54	2200
	6	1.68	4.9	2917
	10	2.8	7.14	2550
	20	5.6	12.88	2300
	30	8.4	17.64	2100
60	2.5	0.7	2.6	3800
	6	1.68	3.36	2000
	10	2.8	4.2	1500
	20	5.6	4.76	800
	30	8.4	9.1	1083

Table A. 21 Experimental data of shear rate (γ), shear stress (τ) and apparent viscosity (μa) for pure sesame paste concentrations at the different temperatures (25-60 °C)

T (°C)	Ω (rpm)	γ(1/s)	$\tau x10^{-2}$ (mPa)	μa(mPa.s)
25	10	2.8	8.4	3000
	20	5.6	10.5	1875
	30	8.4	12.6	1500
	50	14	16.52	11800
	100	28	26.18	935
30	10	2.8	7.84	2800
	20	5.6	9.66	1725
	30	8.4	11.34	1350
	50	14	14.7	1050
	100	28	22.4	800
40	10	2.8	7.56	2700
	20	5.6	8.96	1600
	30	8.4	10.36	1233
	50	14	13.3	950
	100	28	19.88	710
50	10	2.8	7	2500
	20	5.6	8.2	1475
	30	8.4	9.66	1150
	50	14	11.9	850
	100	28	17.5	625
60	10	2.8	6.72	2400
	20	5.6	7.98	1425
	30	8.4	9.24	1100
	50	14	10.92	780
	100	28	15.68	560

APPENDIX B

ANOVA results

Table B.1 ANOVA results for the flow behavior index under the effect of temperature and concentration

		C(%date)		
T (°C)	**20%**	**30%**	**40%**	**55%**
25	0.617	0.538	0.629	0.639
30	0.585	0.532	0.612	0.641
40	0.569	0.536	0.607	0.629
50	0.544	0.535	0.594	0.606
60	0.532	0.522	0.595	0.573

SUMMARY	Count	Sum	Average	Variance
Row1	4	2.423	0.60575	0.002121
Row2	4	2.37	0.5925	0.00215
Row3	4	2.341	0.58525	0.001692
Row4	4	2.279	0.56975	0.001258
Row5	4	2.222	0.5555	0.00118
Column 2	5	2.847	0.5694	0.001138
Column 3	5	2.663	0.5326	3.98E-05
Column 4	5	3.037	0.6074	0.000205
Column 5	5	3.088	0.6176	0.000815

ANOVA

Source of Variation	*SS*	*df*	*MS*	*F*	*P-value*	*F crit*
Rows	0.006147	4	0.001537	6.971799	0.003852	3.259167
Columns	0.022557	3	0.007519	34.10872	3.74E-06	3.490295
Error	0.002645	12	0.00022			
Total	0.03135	19				

Table B.2 ANOVA results for the flow behavior index under the effect of temperature and concentration

		C(%mulberry)		
T (°C)	**20%**	**30%**	**40%**	**55%**
25	0.659	0.698	0.699	0.69
30	0.691	0.69	0.683	0.682
40	0.69	0.69	0.68	0.676
50	0.689	0.679	0.679	0.674
60	0.683	0.671	0.67	0.661
SUMMARY	Count	Sum	Average	Variance
Row1	4	2.746	0.6865	0.000352
Row2	4	2.746	0.6865	2.17E-05
Row3	4	2.736	0.684	5.07E-05
Row4	4	2.721	0.68025	3.96E-05
Row5	4	2.685	0.67125	8.16E-05
Column 2	5	3.412	0.6824	0.000181
Column 3	5	3.428	0.6856	0.000112
Column 4	5	3.411	0.6822	0.000112
Column 5	5	3.383	0.6766	0.000115

ANOVA

Source of Variation	*SS*	*df*	*MS*	*F*	*P-value*	*F crit*
Rows	0.000651	4	0.000163	1.367304	0.302418	3.259167
Columns	0.00021	3	6.99E-05	0.587799	0.634544	3.490295
Error	0.001428	12	0.000119			
Total	0.002288	19				

Table B. 3 ANOVA results for the flow behavior index under the effect of temperature and concentration

C(%grape)				
T (°C)	**20%**	**30%**	**40%**	**55%**
25	0.604	0.525	0.512	0.496
30	0.579	0.508	0.462	0.46
40	0.546	0.456	0.62	0.461
50	0.515	0.418	0.382	0.389
60	0.511	0.374	0.331	0.336
SUMMARY	Count	Sum	Average	Variance
Row1	4	2.137	0.53425	0.002303
Row2	4	2.009	0.50225	0.00311
Row3	4	2.083	0.52075	0.006084
Row4	4	1.704	0.426	0.003763
Row5	4	1.552	0.388	0.007093
Column 2	5	2.755	0.551	0.001629
Column 3	5	2.281	0.4562	0.003908
Column 4	5	2.307	0.4614	0.012756
Column 5	5	2.142	0.4284	0.00418

ANOVA

Source of Variation	*SS*	*df*	*MS*	*F*	*P-value*	*F crit*
Rows	0.065254	4	0.016313	7.945567	0.00227	3.259167
Columns	0.042419	3	0.01414	6.886771	0.005968	3.490295
Error	0.024638	12	0.002053			
Total	0.13231	19				

Table B.4 ANOVA results for the flow behavior index under the effect of temperature and concentration

C(%carob)				
T (°C)	**20%**	**30%**	**40%**	**55%**
25	0.583	0.599	0.547	0.546
30	0.534	0.558	0.556	0.527
40	0.46	0.492	0.562	0.528
50	0.447	0.485	0.529	0.475
60	0.444	0.476	0.528	0.451
SUMMARY	Count	Sum	Average	Variance
Row1	4	2.275	0.56875	0.000703
Row2	4	2.175	0.54375	0.000243
Row3	4	2.042	0.5105	0.00195
Row4	4	1.936	0.484	0.001159
Row5	4	1.899	0.47475	0.001449
Column 2	5	2.468	0.4936	0.003846
Column 3	5	2.61	0.522	0.002903
Column 4	5	2.722	0.5444	0.000239
Column 5	5	2.527	0.5054	0.001627

ANOVA						
Source of Variation	*SS*	*df*	*MS*	*F*	*P-value*	*F crit*
Rows	0.025231	4	0.006308	8.200589	0.001991	3.259167
Columns	0.007281	3	0.002427	3.155239	0.064465	3.490295
Error	0.00923	12	0.000769			
Total	0.041743	19				

Table B.5 ANOVA results for the consistency coefficient under the effect of temperature and concentration

		C(%date)		
T (°C)	**20%**	**30%**	**40%**	**55%**
25	6626.9	8113.3	9719.3	10013
30	6166.3	7505.5	9468.6	9704
40	5315	6798.7	8712.6	9231.4
50	5013.1	6308.8	8014.5	8813.1
60	4365.1	5744.7	7664.6	8269.7
SUMMARY	Count	Sum	Average	Variance
Row1	4	34472.5	8618.125	2459363
Row2	4	32844.4	8211.1	2829712
Row3	4	30057.7	7514.425	3244453
Row4	4	28149.5	7037.375	2912161
Row5	4	26044.1	6511.025	3205307
Column 2	5	27486.4	5497.28	818279.2
Column 3	5	34471	6894.2	883264
Column 4	5	43579.6	8715.92	792643.3
Column 5	5	46031.2	9206.24	482731.5

ANOVA

Source of Variation	*SS*	*df*	*MS*	*F*	*P-value*	*F crit*
Rows	11669710	4	2917428	147.1207	4.38E-10	3.259167
Columns	43715025	3	14571675	734.8236	7.37E-14	3.490295
Error	237962	12	19830.17			
Total	55622697	19				

Table B.6 ANOVA results for the consistency coefficient under the effect of temperature and concentration

C(%mulberry)				
T (°C)	**20%**	**30%**	**40%**	**55%**
25	7714	8057.4	8597.7	10207
30	6868.1	7165.5	7769.1	9401
40	5753.2	6311.9	6981.9	8418.7
50	4809.9	5513.6	6168.7	7905.6
60	4461.1	4657.2	5792	7351.5
SUMMARY	Count	Sum	Average	Variance
Row1	4	34576.1	8644.025	1218037
Row2	4	31203.7	7800.925	1278393
Row3	4	27465.7	6866.425	1323220
Row4	4	24397.8	6099.45	1757711
Row5	4	22261.8	5565.45	1761935
Column 2	5	29606.3	5921.26	1876464
Column 3	5	31705.6	6341.12	1786612
Column 4	5	35309.4	7061.88	1318916
Column 5	5	43283.8	8656.76	1320439

ANOVA

Source of Variation	*SS*	*df*	*MS*	*F*	*P-value*	*F crit*
Rows	24923811	4	6230953	261.5174	1.48E-11	3.259167
Columns	21731978	3	7243993	304.0354	1.4E-11	3.490295
Error	285913.8	12	23826.15			
Total	46941703	19				

Table B. 7 ANOVA results for the consistency coefficient under the effect of temperature and concentration

	C(%grape)			
T (°C)	**20%**	**30%**	**40%**	**55%**
25	2084.5	2906.5	3254.4	4218.2
30	1647.4	2421.8	3033.4	4100.6
40	1300.1	2232.7	2782.3	3809.7
50	1113.7	2033.9	2582	3709.5
60	966.88	1876.5	2446.5	3496.6
SUMMARY	Count	Sum	Average	Variance
Row1	4	12463.6	3115.9	780627.3
Row2	4	11203.2	2800.8	1072518
Row3	4	10124.8	2531.2	1100774
Row4	4	9439.1	2359.775	1176680
Row5	4	8786.48	2196.62	1122375
Column 2	5	7112.58	1422.516	201688.2
Column 3	5	11471.4	2294.28	159301.2
Column 4	5	14098.6	2819.72	107952.5
Column 5	5	19334.6	3866.92	85799.02

ANOVA

Source of Variation	*SS*	*df*	*MS*	*F*	*P-value*	*F crit*
Rows	2126507	4	531626.7	68.99995	3.53E-08	3.259167
Columns	15666468	3	5222156	677.7849	1.19E-13	3.490295
Error	92456.87	12	7704.74			
Total	17885431	19				

Table B. 8 ANOVA results for the consistency coefficient under the effect of temperature and concentration

C(%carob)				
T (°C)	**20%**	**30%**	**40%**	**55%**
25	5714.8	7001.6	11290	17480
30	5123.2	6007.1	10671	15808
40	4515.9	5769.1	9176.6	14660
50	3762.7	4894.4	8390.3	13479
60	3194.4	4397	8213.7	12990
SUMMARY	Count	Sum	Average	Variance
Row1	4	41486.4	10371.6	28138498
Row2	4	37609.3	9402.325	24160224
Row3	4	34121.6	8530.4	20576853
Row4	4	30526.4	7631.6	19076121
Row5	4	28795.1	7198.775	19484441
Column 2	5	22311	4462.2	1026357
Column 3	5	28069.2	5613.84	1025733
Column 4	5	47741.6	9548.32	1888564
Column 5	5	74417	14883.4	3301107

ANOVA

Source of Variation	*SS*	*df*	*MS*	*F*	*P-value*	*F crit*
Rows	26738949	4	6684737	36.00247	1.35E-06	3.259167
Columns	3.32E+08	3	1.11E+08	596.1696	2.56E-13	3.490295
Error	2228093	12	185674.4			
Total	3.61E+08	19				

APPENDIX C

Regression statistics

Table C.1 Regression statistics for the linearized form of Eq.3.11 for date

	Ea/ R	b	n-1	ln K($\dot{\gamma}$,T,C)
Estimated values	960.9952	0.017028	-0.41826	5.225173
Standard errors (SE)	75.26185	0.000751	0.010763	0.241931
Coefficient of Determination (R^2)	0.957946			
Degrees of Freedom	99			
Regression sum of squares	20.63717			
Residual sum of squares	0.905977			

Table C.2 Regression statistics for the linearized form of Eq.3.12 for date

	Ea/ R	b	n-1	ln K($\dot{\gamma}$,T,C)
Estimated values	960.9952	0.606021	-0.41826	3.707243
Standard errors (SE)	64.15244	0.022231	0.009175	0.219362
Coefficient of Determination (R^2)	0.969445			
Degrees of Freedom	99			
Regression sum of squares	20.88489			
Residual sum of squares	0.658255			

Table C.3 Regression statistics for the linearized form of Eq.3.11 for mulberry

	Ea/ R	b	n-1	ln K($\dot{\gamma}$,T,C)
Estimated values	1320.318	0.011674	-0.31125	4.194863
Standard errors (SE)	45.92427	0.000458	0.006568	0.147625
Coefficient of Determination (R^2)	0.974849			
Degrees of Freedom	99			
Regression sum of squares	13.0747			
Residual sum of squares	0.337328			

Table C.4 Regression statistics for linearized form of Eq.3.12 for mulberry

	Ea/ R	b	n-1	ln K($\dot{\gamma}$,T,C)
Estimated values	1320.318	0.390498	-0.31125	3.242208
Standard errors (SE)	55.92499	0.01938	0.007998	0.191235
Coefficient of Determination (R^2)	0.962702			
Degrees of Freedom	99			
Regression sum of squares	12.91179			
Residual sum of squares	0.500241			

Table C.5 Regression statistics for the linearized form of Eq.3.11 for grape

	Ea/ R	b	n-1	ln K($\dot{\gamma}$,T,C)
Estimated values	1533.303	0.025254	-0.53582	1.982726
Standard errors (SE)	98.03838	0.000979	0.014021	0.315147
Coefficient of Determination (R^2)	0.961086			
Degrees of Freedom	99			
Regression sum of squares	37.9681			
Residual sum of squares	1.537304			

Table C.6 Regression statistics for the linearized form of Eq.3.12 for grape

	Ea/ R	b	n-1	ln K($\dot{\gamma}$,T,C)
Estimated values	1533.303	0.888077	-0.53582	-0.23076
Standard errors (SE)	88.69637	0.0230737	0.012685	0.303297
Coefficient of Determination (R^2)	0.968149			
Degrees of Freedom	99			
Regression sum of squares	38.24712			
Residual sum of squares	1.258285			

Table C.7 Regression statistics for the linearized form of Eq.3.11 for carob

	Ea/ R	b	n-1	ln K($\dot{\gamma}$,T,C)
Estimated values	1419.017	0.036663	-0.4837	3.086478
Standard errors (SE)	85.64691	0.000855	0.012248	0.275314
Coefficient of Determination (R^2)	0.974528			
Degrees of Freedom	99			
Regression sum of squares	44.88705			
Residual sum of squares	1.173251			

Table C.8 Regression statistics for linearized form of Eq.3.12 for carob

	Ea/ R	b	n-1	ln K($\dot{\gamma}$,T,C)
Estimated values	1419.017	1.261373	-0.4837	-0.02866
Standard errors (SE)	99.15877	0.034363	0.014181	0.339073
Coefficient of Determination (R^2)	0.965857			
Degrees of Freedom	99			
Regression sum of squares	44.48766			
Residual sum of squares	1.572641			